UNIVERSITÀ DEGLI STUDI DI PALERMO

Dottorato di Ricerca in Scienze Fisiche
Dipartimento di Fisica e Chimica - Emilio Segrè
Settore Scientifico Disciplinare FIS/03

RADIATION-MEDIATED PROCESSES IN EXTERNAL ENVIRONMENTS

IL DOTTORE
GIUSEPPE FISCELLI

IL COORDINATORE
PROF. GIOACCHINO MASSIMO PALMA

IL TUTOR
PROF. ROBERTO PASSANTE

CICLO - XXXII
ANNO CONSEGUIMENTO TITOLO - 2020

A Tiziana

Desidero ringraziare Roberto e Lucia, per avermi dato l'opportunità di lavorare nel loro gruppo e per essere stati un importante riferimento durante questi anni, non solo dal punto di vista professionale ma anche dal punto di vista umano.

Grazie ai miei genitori e a Tiziana.
Tutto questo è stato possibile anche grazie a voi.

Abstract

In this thesis, we present the results obtained during the PhD, concerning the radiation-mediated processes between atoms or molecules, such as the dispersion and the resonance interaction, the resonance energy transfer between atoms or molecules, in the presence of external environments, in the framework of quantum electrodynamics. The effect of external environments, or of non-equilibrium initial conditions, on radiation-mediated processes, and the possibility to manipulate and control such processes through external actions, has been widely investigated in recent literature from both a theoretical and experimental point of view. These investigations and research subjects have inspired the research work presented in this thesis.

Firstly, the resonance exchange of energy between two atoms placed inside a perfectly conductor cylindrical waveguide is considered. We find that the space dependence of the energy transfer rate and its magnitude are deeply modified if the atomic transition frequency is below the waveguide lower cut-off frequency; the possibility to change the energy transfer rate by changing the cylinder radius, is shown. In the same physical system, the resonance interaction energy between two entangled atoms is investigated. We find that the interaction is slightly modified if the atoms are in the near zone, becoming more and more suppressed approaching the intermediate zone, leading to a complete inhibition in the far-zone limit. In addition to the possibility to modify the interaction by changing the waveguide radius, we also show that the resonance force can change its character due to the waveguide, from repulsive to attractive, when the atoms have dipole moments orthogonal to the guide axis.

Next, a dynamical situation for the resonance interaction energy is considered. We investigate the time-dependent resonance interaction between two entangled atoms in the free space, starting from a nonequilibrium condition, during the dynamical atomic self-dressing process. We show that the interaction energy vanishes when the atoms are outside the light-cone of each other, in agreement with the relativistic causality, whereas it instantaneously settles to its static value after the causality time. We also analyse the time-dependent electric energy density in the space around the two correlated atoms, showing a suppression or an enhancement, if the system is prepared in the antisymmetric (subradiant) or symmetric (superradiant) state.

Finally, we consider the dispersion interaction (van der Waals and Casimir-Polder) between two ground-state hydrogen atoms, interacting with the electromagnetic field in the vacuum state, in the presence of external static electric fields. We show that the presence of the external field strongly modifies the dispersion force between the atoms both in the near and far zone, changing its space dependence, its magnitude and even its attractive/repulsive character. Our new find-

ings clearly show the possibility to control the interatomic dispersion interactions through external actions.

Contents

Introduction

The main topic of this PhD thesis concerns with the study of radiation-mediated processes between atoms or molecules in the presence of external environments, in the framework of quantum electrodynamics. Specifically, we have considered the following quantum radiative processes between neutral atoms, molecules or macroscopic bodies arising from their common interaction with the quantum electromagnetic field: the dispersion interaction (van der Waals and Casimir-Polder), the resonance interaction and the resonance energy transfer process. These processes have been investigated when the quantum emitters are in the presence of external environments and the field is in its *vacuum state*, in which every possible mode is occupied by zero photons. We have also studied the dynamical resonance interaction energy between two entangled atoms, starting from a nonequilibrium condition.

Called by Julian Schwinger *"one of the least intuitive consequences of quantum electrodynamics"*, Casimir dispersion forces are ubiquitous interactions between neutral atoms, molecules or among unpolarized and unmagnetized macroscopic bodies, mediated by the quantum electromagnetic field. They are deeply related to the existence of the vacuum field fluctuations of the electromagnetic field, and to the exchange of virtual photons between the atoms. In spite of their small intensity, the dispersion forces, such as the van der Waals interaction, the Casimir-Polder interaction and the Casimir interaction, are turned to be extremely important in many areas of science, from fundamental and solid-state physics, to quantum chemistry, biology and even in cosmology and in engineering. In fact, aside from its importance as a quantum fundamental interaction between any two neutral bodies, and more generally as a consequence of quantized fields, the Casimir force may take an increasingly practical importance. One reason was initially recognized by Feynman in 1959 in a talk on the physics involved in making micromachines: *there is the problem that materials stick together by the molecular (van der Waals) attraction.* In more recent years, their crucial role in the development of micro- and nano-electromechanical devices have been widely taken into account and investigated, and considerable efforts are now devoted to controlling these forces, also in relation to the problem of "stiction".

The resonance force is a quantum interaction between two atoms or molecules, one excited and the other in its ground-state, prepared in a symmetrical or anti-symmetrical entangled state. The main contribution to the resonance interaction is due to the exchange of a real photon between the two quantum emitters, and thus it is generally much larger than the van der Waals interaction between ground-state atoms, and comparable with the Casimir-Polder force between a ground-state atom and a macroscopic body. Despite its remarkable strength, this force has not been yet experimentally detected directly because several difficulties emerge, mainly that the atomic system must be prepared and maintained in an entangled state for a sufficiently long time. The spontaneous decay of the excited atom and all the perturbations due to the interactions with the environment, are the main factors that destroy the quantum correlation of the atomic state, making extremely difficult to detect such force.

Last but not the least, the resonance energy transfer between atoms, molecules or chromophores is one of the most simple and fundamental physical phenomenon in nature. It is the exchange of energy, typically electronic, between two quantum emitters, one excited (donor) and the other in its ground state (acceptor), interacting with the quantum electromagnetic field. The transfer of energy between a pair of entities such as atoms, molecules or even nano-structures plays an extremely important role in several areas of science: from fundamental physics, optics and photophysics, to quantum chemistry and especially in biophysics, with promising applications in nano-photonics, ranging from photovoltaics to bio-medical sensing. In the photosynthesis, in particular, the excitation energy is absorbed by pigments in the photosynthetic antennae and subsequently transferred to a reaction center by a series of hops between other chomophores units. In living organisms which perform photosynthesis, it has been found that the light-harvesting efficiency is indeed above 99%; although this process has been investigated extensively over many decades, there exist open questions regarding the underlying mechanisms leading to this remarkably high efficiency.

The common denominator of the radiation-mediated processes previously outlined is that they arise from the interaction between matter and the quantum electromagnetic field, even if the field is in the vacuum state. A fundamental and astonishing consequence of the field quantization is the existence of electromagnetic field fluctuations even in the vacuum state, where all possible modes are occupied by zero photons, and the system is at zero temperature. The *vacuum field fluctuations* are strictly related to *virtual photons*, each carries an energy equal to $\hbar\omega/2$, that cannot be converted to other forms of energy. In spite of this, the virtual photons can be seen as responsible for a range of physically observable effects, such as the Lamb shift of atomic energy levels in the free-space, the spontaneous decay of an excited atom, the Casimir effect, and the modification of the electron

magnetic moment. The interaction between virtual photons and the matter, such as atoms or molecules, leads also to observable radiation-mediated processes, such as the dispersion interaction between atoms or between atoms and macroscopic bodies, the resonance interaction between correlated atoms or molecules, as well as the resonance energy transfer between molecules, which are investigated in the thesis.

The normal modes of the quantum electromagnetic field strongly depend on the boundary conditions set by macroscopic bodies or, in general, by external environments. They dictate, for instance, if the wavevectors are continuous (as in the free space or in the presence of a single mirror) or discrete (as inside a cavity); in other words, the environment dictates the shape of the virtual and real photons that can exist. Therefore, since the presence of boundaries changes the density of states and the dispersion relation of the quantum field, it must also have an effect on the radiation-mediated processes considered. The dispersion and resonance interactions, as well as the resonance energy transfer, can be dramatically modified by means of an external environment, leading to deep changes of their strength and their dependence on the system's parameters. Structured environments, such as a cavity, a photonic crystal or a waveguide, can lead to an enhancement or a suppression of the dispersion and resonance interaction between atoms or molecules, modifying their dependence from the relevant parameters, e.g. the interatomic distance. They can even change the character of the dispersion force, turning them from attractive to repulsive and vice versa, as we find in this thesis. Likewise, the rate of the energy transfer process between quantum emitters can be controlled by means of external environments: it can be increased or suppressed, and it is even possible to activate the exchange of energy among the atoms by changing the structured environment or some system's parameters, e.g. the frequency of an oscillating mirror, nearby. The interest and ability to manipulate and control quantum interactions between atoms, has greatly increased during the last years. In fact, understanding how radiation-mediated processes can be modified and controlled through a macroscopic environment, offers not only the possibility to explore new fundamental aspects of the light-matter interaction, but also represents a fundamental goal in different fields of science, ranging from fundamental and atomic-molecular physics to chemistry and biology, and it could be important for the development of new technologies.

This thesis work is organized as follows. The first Chapter is devoted to an introduction to the radiation-mediated processes considered: the dispersion and the resonance interaction, and the resonance energy transfer between atoms. Such processes are considered both when the atoms are in the empty space and when they are in the presence of specific external environments: changes due to the presence of an external environment are widely discussed. Particular attention

will be given to the physical nature of these processes, strictly related to vacuum field fluctuations, and to the interaction between atoms/molecules and virtual photons.

In the second Chapter, the basic framework of the macroscopic quantum electrodynamics is outlined. One of the main advantage of this formalism is that it allows to approach and analyse quantum forces, due to the electromagnetic field, when quantum emitters are in the presence of a linear magneto-dielectric medium, whose geometrical and structural properties are totally included in the electromagnetic Green's tensor expression.

In the third Chapter, we present our original work on the resonance exchange of energy between two atoms or molecules when they are in the presence of a magneto-dielectric medium, in particular a cylindrical waveguide made of a perfect conductor. Firstly, an analytical expression for the energy transfer amplitude between two atoms near a generic linear medium is obtained, in terms of the Green's tensor; then, this expression is used to investigate the transfer of energy between the atoms when they are placed on the axis of a perfectly conducting cylindrical waveguide. The energy transfer process will be thoroughly analysed as a function of the relevant parameters of the system, such as the atomic distance, the waveguide radius and the atomic dipoles orientation, highlighting significant possibilities to manipulate the transfer of energy through external actions.

In the fourth Chapter, we present our original work on the resonance interaction energy between two correlated atoms in the presence of external environments or in a nonequilibrium condition. This Chapter is divided in two parts, where different aspects of the resonance interaction are investigated. In the first part, the time-dependent resonance interaction energy between two entangled atoms, starting from a nonequilibrium condition and interacting with the quantum vacuum, is analysed in great detail, during the self-dressing process of the system. We show how the interaction deeply changes when the atoms are inside or outside the light-cone of each other, and how its causal behaviour is closely related to the contribution of virtual photons. Also, we investigate in detail the time-dependent electric energy density around the atoms, showing a sort of a constructive or destructive interference depending if the atoms are prepared in the symmetric (superradiant) or antisymmetric (subradiant) entangled state. An experimental proposal to probe our findings is also suggested. The second part of the Chapter is devoted to investigate the effects of a structured environment on the resonance interaction energy between two entangled atoms. After obtaining the analytical expression for the resonance interaction, valid in the presence of a generic linear magneto-dielectric medium, the specific case of atoms inside a perfectly conducting cylindrical waveguide is considered; the interaction energy is analysed as a function of the interatomic distance and the waveguide radius, for atomic dipoles

both parallel and orthogonal to the guide axis. Our results clearly show the possibility to modify the magnitude and the distance dependence of the resonance interaction energy through the waveguide, even changing its character, turning it from repulsive to attractive.

In the last Chapter, we present our original results on the dispersion interaction between two hydrogen atoms, interacting with the quantum electromagnetic field in the vacuum state, in the presence of an external static electric field, both in the nonretarded and in the retarded Casimir-Polder regime. We consider in detail specific geometrical configurations of the atoms with respect to the external field, and/or the relative orientation of the fields acting on the two atoms. We find that the dispersion interaction changes its dependence from the interatomic distance, decreasing slower with the distance, compared to the case of unperturbed atoms. We show the possibility to totally control the magnitude and the character of the force, turning it from attractive to repulsive, or even make it vanishing, exploiting the external static fields. These results are also physically interpreted in terms of dipole moments induced by the external fields on the atoms. By a numerical estimate of the field-modified dispersion interaction, we show that at typical interatomic distances, such a control can be obtained for values of the external fields that can be currently achieved in the laboratory, and sufficiently weak that they can be taken into account perturbatively.

Chapter 1

Radiation-mediated processes

Quantum electrodynamics is one of the most accurate and successful theories so far known in physics used, in general, for calculating the interaction of the quantum electromagnetic field with particles, atoms and molecules. It also allows to calculate the interaction between atoms or molecules mediated by the electromagnetic radiation field. In applications so far made, its theoretical predictions are in excellent agreement with experimental results.

This Chapter provides all the basic information necessary for the radiation-mediated processes investigated in the thesis. It is organized as follows: the first Section is devoted to a brief introduction to the quantum electromagnetic field, paying particular attention to the existence of the zero-point field energy and vacuum field fluctuations. The matter-field interaction Hamiltonian and the radiation-mediated interactions, such as dispersion and resonance interactions, as well as the resonance energy transfer process, are introduced. These processes represent the core issues of our works. Central to all the investigations of the thesis is the study of such processes between atoms or molecules when they are in the presence of external environments, in the framework of quantum electrodynamics.

In Sections 1.2 and 1.3, a theoretical and experimental dissertation about dispersion forces between atoms or molecules is considered, respectively. We will consider in great detail the dispersion interactions, such as the van der Waals, the Casimir-Polder and the Casimir interactions, between quantum emitters (atoms, molecules or quantum dots) or macroscopic bodies, when they are placed in the free space, at zero temperature. In particular we shall highlight the case in which the radiation field is in its vacuum state, thus there are not real photon in any field mode, which means that the processes we consider arise from the interaction between matter and vacuum field fluctuations. Finally, some of the most relevant and pioneering experimental results regarding dispersion interactions are also discussed.

In Sec. 1.4, the resonance interaction between two correlated identical atoms

in the free space and interacting with the quantum vacuum, is introduced; the calculation of the vacuum resonance dipole-dipole interaction tensor is performed in detail and the results are discussed.

In Sec.1.5, the rate of the energy transfer between two quantum emitters, such as atoms, molecules or nano-structures, is considered. The main features of the Förster theory is outlined, and a unified theory of the resonance energy transfer is given, using the molecular quantum electrodynamics description. We also retrace the main steps of the calculation of the resonance energy transfer amplitude between two atoms, one excited and the other in its ground state, in the free space and interacting with the vacuum field.

In the last Section 1.6, the effects of external environments on radiation-mediated processes, for example the dispersion and the resonance interaction, as well as the resonance energy transfer process, are discussed. A striking feature of radiation-mediated processes is that they are significantly affected by the presence of external environments, which change the photon density of states and the dispersion relation of the radiation field. Structured environments, such as a cavity, a waveguide or a photonic crystal, as well as dynamical situations under non equilibrium conditions, strongly modify quantum interactions and the resonance exchange of energy between atoms or molecules. The amazing possibility to manipulate and control radiation-mediated processes through external environments, changing their magnitude, their behaviour, in particular their spatial dependence, and even the attractive or repulsive character of radiation-mediated forces, will be thoroughly investigated and represents the main goal of this thesis.

1.1 The quantum vacuum and the matter-field interaction

From Quantum Electrodynamics (QED) we know that the electromagnetic field in the free space can be seen as an infinity superposition of uncoupled quantum harmonic oscillators, one for each field mode of wavevector $\boldsymbol{k}$ and polarization λ of the radiation field [1–3]. The particles associated to the field quantization are bosons, called *photons*, and the electromagnetic field Hamiltonian in the free space and in the Coulomb gauge is given by the well-known expression

$$H_F = \sum_{\mathbf{k}\lambda} \hbar\omega_{\mathbf{k}} \left(a^\dagger_{\mathbf{k}\lambda} a_{\mathbf{k}\lambda} + \frac{1}{2} \right), \tag{1.1}$$

where $\omega_k = c|k|$ and the sum is performed over all possible wavevectors $\mathbf{k}$ and the two independent polarizations $\lambda = 1, 2$. $a^\dagger_{\mathbf{k}\lambda}$ and $a_{\mathbf{k}\lambda}$ are the familiar bosonic

creation and annihilation operators satisfying the following commutation rules

$$[a_{\mathbf{k}\lambda}, a^{\dagger}_{\mathbf{k}'\lambda'}] = \delta_{\lambda\lambda'}\delta_{\mathbf{k}\mathbf{k}'}, \tag{1.2}$$

$$[a_{\mathbf{k}\lambda}, a_{\mathbf{k}'\lambda'}] = [a^{\dagger}_{\mathbf{k}\lambda}, a^{\dagger}_{\mathbf{k}'\lambda'}] = 0, \tag{1.3}$$

which create or destruct photons in the field mode $(\mathbf{k}, \lambda)$. The quantum transverse electric field and the magnetic field operators in the Heisenberg picture and in the Coulomb gauge $\nabla \cdot \mathbf{A}(\mathbf{r}, t) = 0$ [3, 4], are given by

$$\mathbf{E}_{\perp}(\mathbf{r}, t) = i \sum_{\mathbf{k},\lambda} \sqrt{\frac{\hbar\omega_{\mathbf{k}}}{2\epsilon_0 V}} \hat{\mathbf{e}}_{\mathbf{k}\lambda} \left(a_{\mathbf{k}\lambda}(t) e^{i\mathbf{k}\cdot\mathbf{r}} - a^{\dagger}_{\mathbf{k}\lambda}(t) e^{-i\mathbf{k}\cdot\mathbf{r}} \right) \tag{1.4}$$

$$\mathbf{B}(\mathbf{r}, t) = i \sum_{\mathbf{k},\lambda} \sqrt{\frac{\hbar\omega_{\mathbf{k}}}{2\epsilon_0 c^2 V}} \left(a_{\mathbf{k}\lambda}(t) e^{i\mathbf{k}\cdot\mathbf{r}} - a^{\dagger}_{\mathbf{k}\lambda}(t) e^{-i\mathbf{k}\cdot\mathbf{r}} \right) \hat{\mathbf{k}} \times \hat{\mathbf{e}}_{\mathbf{k}\lambda}, \tag{1.5}$$

where $\hat{\mathbf{e}}_{\mathbf{k}\lambda}$ are polarization unit vectors, assumed real, V is the quantization volume, and since we are in the free space the dispersion relation is $\omega_k = ck$. One of the most fascinating consequence of the quantum theory of the electromagnetic field is the existence of the zero-point fluctuations [5]. When the electromagnetic field is in its ground state $|0\rangle$, where there are no photons in any field mode, the fields have quantum fluctuations around their average value zero, that is

$$\langle 0 | \, \mathbf{E}_{\perp}(\mathbf{r}, t) \, | 0 \rangle = 0, \quad \langle 0 | \, \mathbf{B}(\mathbf{r}, t) \, | 0 \rangle = 0, \tag{1.6}$$

$$\langle 0 | \, \mathbf{E}^2_{\perp}(\mathbf{r}, t) \, | 0 \rangle \neq 0, \quad \langle 0 | \, \mathbf{B}^2(\mathbf{r}, t) \, | 0 \rangle \neq 0. \tag{1.7}$$

Vacuum field fluctuations are directly related to the field energy density and, in the particular case for which the field is in the vacuum state, they are related to the zero-point energy given by

$$E_0 = \sum_{\mathbf{k}\lambda} \frac{\hbar\omega_{\mathbf{k}}}{2}. \tag{1.8}$$

The zero-point energy and the vacuum field fluctuations are a direct consequence of the non-commutativity, at equal time, of the transverse electric and magnetic field operators, given by

$$[E_{\perp m}(\mathbf{r}, t), B_n(\mathbf{r}', t)] = -4\pi i \, \hbar \, c \, \epsilon_{mnl} \frac{\partial}{\partial r_l} \delta(\mathbf{r} - \mathbf{r}'), \tag{1.9}$$

where ϵ_{mnl} is the totally antisymmetric symbol and the Einstein convention on repeated indices has been used [1, 5]. Owing to the commutation relation (1.9), electric and magnetic fields give rise to field fluctuations around their average value, that exist also in the vacuum state of the radiation field, and they are called

vacuum field fluctuations. The modern view of vacuum is then closely related to the zero-point energy and to the vacuum field fluctuations, that are ubiquitous [5].

In the zero-point energy expression (1.8), a sum over all allowed field modes is involved. The allowed modes and the dispersion relation depend on the presence of matter and boundary conditions; macroscopic magneto-dielectric or metallic bodies, atoms, molecules or matter in general, can significantly modify the dispersion relation and the density of states of the electromagnetic field. This means that also the zero-point energy, as well as vacuum fluctuations, depend on the presence of boundaries, and can be significantly affected by the external environments [1, 5–7]. Moreover, we wish to point out that, although the strength of these fluctuations diverges, their difference between two different configurations of the system is usually finite, and represent the origin of many physical phenomena of great interest in many areas of science, experimentally measured with high precision. One of the most famous effects, related to vacuum field fluctuations, is the Casimir force. It is a tiny force between two macroscopic neutral bodies in the vacuum space, theoretically predicted by Casimir in 1948 for the case of two parallel perfectly conducting plates [8]. Vacuum field fluctuations are also affected by the presence of atoms and molecules and are responsible for a range of physically observable effects of great importance, such as the Lamb shift of atomic energy levels, the spontaneous decay of an excited atom, the modification of the electron magnetic moment, as well as the van der Waals interaction between two atoms or molecules and the Casimir-Polder force among an atom and a metal or dielectric body [1, 6]. The number of research papers claiming some relation to the Casimir force and to vacuum field fluctuations is countless and the topics are very different, capturing the interests of scientists from cosmology to atomic physics, from chemistry to quantum field theory, and from biology to mathematics.

One of the most relevant triumph of the quantum electrodynamics theory is its application to the study of molecular and atomic interactions, including retardation effects [3, 6, 9]. In QED, the matter-radiation interaction Hamiltonian, in the Coulomb gauge and in the multipolar coupling scheme, can be written as [5, 9]

$$H_i = -\boldsymbol{\mu} \cdot \mathbf{E}(\mathbf{r}), \tag{1.10}$$

where we have used $\mathbf{E}(\mathbf{r})$ rather than $\mathbf{D}_\perp(\mathbf{r})$ because, outside of the atoms, the transverse displacement field coincides with the total (transverse plus longitudinal) electric field. $\boldsymbol{\mu}$ is the electric dipole moment operator of the atom, and the interaction Hamiltonian (1.10) was obtained within the dipole-dipole approximation: this means that the relevant wavelengths of the radiation field emitted or absorbed by the atom is very large compared to the atomic dimension: therefore it is possible to neglect the spatial variation of the electric field across atoms or molecules. The interaction Hamiltonian (1.10) takes into account both radiative and electrostatic contributions to intermolecular interactions, preserving the

causality [10]. This is the reason why the multipolar coupling scheme is much more convenient than the minimal coupling one, in order to calculate intermolecular radiation-mediated interactions, for example the dispersion and resonance interaction. Typical Feynman diagrams for quantum-electrodynamics interactions in the multipolar coupling scheme are shown in Fig. 1.1. The graph (i) shows a

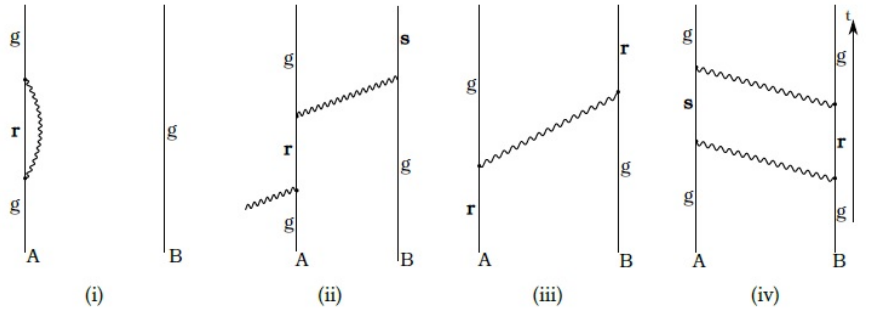

Figure 1.1: Feynman diagrams for radiation-mediated interactions of atoms or molecules in the multipolar coupling scheme [11].

typical Lamb shift interaction: the atom interacts with the radiation field, emitting and re-absorbing a virtual photon. Since the corresponding matrix element is independent of the atomic separation, and there is not a photon exchange of photons between the atoms, this process does not lead to an interatomic interaction, but only to an energy level shift. On the contrary, in diagrams (ii-iv) there is an exchange of photons between the atoms, leading to a force between them. We stress that in each Feynman diagram the energy is conserved only between the initial and final states of the interacting system, but energy conservation may be violated for intermediate states [11].

For the purpose of the thesis, we shall now focus our attention to the following radiation-mediated processes: the interatomic dispersion and resonance interactions, and the resonance exchange of energy between atoms or molecules.

1.2 Dispersion interactions

Dispersion interactions are quantum interactions between neutral atoms, molecules or quantum dots or even macroscopic unpolarised and unmagnetised bodies, due to their common interaction with the quantum electromagnetic field. In the last years, there has been a great interest for them in many areas of science, from both a theoretical and experimental point of view; they also play a fundamental role in many different fields of physics, as well as in chemistry, biology and cosmology. From an experimental and engineering point of view, the study and the control

of dispersion interactions is very important in micro- and nano- electromechanical systems (M.E.M.S. and N.E.M.S.) for which, owing to their small size and close distances, tiny dispersion forces becomes relevant [12].

Dispersion forces between neutral atoms or molecules were known even before the birth of quantum physics. From a classical point of view, can be explained in terms of atomic electric-dipole fluctuations: dipole fluctuations of one atom induce an electric dipole moment on the other atom, leading to an interaction between them. This interaction depends on the interatomic distance r as r^{-6}, corresponding to the van der Waals interaction. Early studies exploiting quantum perturbative calculations were performed by Eisenschits and London in 1930, confirming previous results obtained from van der Waals just in the short-range limit, so when the interatomic separation is much smaller than the relevant atomic transition wavelengths [13]. Nevertheless, a complete calculation of the interaction potential between two neutral atoms in their ground state, using quantum field theory, was first performed by Casimir and Polder in 1948 [14]. Taking into account retardation effects due to the finite speed of propagation of light, they found that the dispersion energy behaves as r^{-7} when the atoms are in the far zone (Casimir-Polder regime), that is when the interatomic distance is much larger than the atomic transition wavelength, and as r^{-6} when they are in the near zone limit (van der Waals regime). Therefore the van der Waals result is fully recovered in the short-range limit, and the dispersion interaction is essentially a radiationless interaction between fluctuating atomic dipoles, and the radiative contributions, due to the finite speed of propagation of light, can be neglected.

According to the microscopic versus macroscopic nature of the interacting systems, we may distinguish three types of dispersion forces [15], as shown in Fig. 1.2 : *van der Waals* forces are interactions between two microscopic neutral quantum emitters, such as atoms, molecules or quantum dots; the *Casimir-Polder* force is an interaction between an atom and a macroscopic body, such as for example the interaction between an atom and a plate or a sphere; finally the *Casimir effect* is a force acting between two macroscopic neutral, unpolarised and unmagnetised bodies, like the force between two parallel metallic plates predicted by Casimir in 1948 [8].
Afterwards, we will go through the calculations in more detail of the van der Waals interaction between two neutral atoms in the free space, the Casimir-Polder interaction between a ground-state atom and a perfectly conducting wall, and the Casimir force between two parallel perfectly conducting plates [16, 17].

1.2.1 Van der Waals interaction between two neutral atoms

Van der Waals (vdW) forces are long-range interactions between neutral atoms or molecules, mediated by the quantum electromagnetic field [12]. We assume

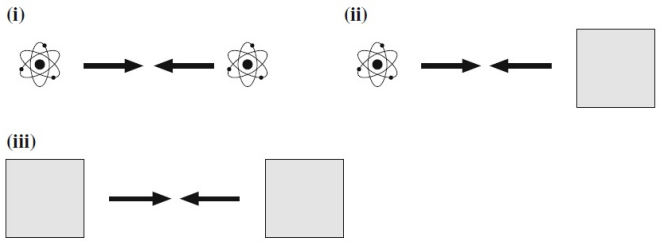

Figure 1.2: Different dispersion interactions: (i) van der Waals interaction; (ii) Casimir-Polder interaction; (iii) Casimir interaction [15].

that atoms do not have permanent electric dipole moments, and we will neglect contributions to the interaction due to higher-order electric multipole moments and magnetic multipoles. Van der Waals forces are tiny ubiquitous interaction: their small strength, e.g. with respect to the Coulomb interactions, is due to the fact that they are usually fourth-order interactions in the atom-field coupling. When the atoms are in their ground state the vdW force is always attractive and it is due to the exchange of a pair of virtual photons between the atoms. It can be repulsive if the atoms are in excited states: in this case real photons can contribute to the dispersion energy, leading to a change of the character of the interaction, from attractive to repulsive.

We consider two identical neutral atoms, labelled A and B, both in their electronic ground state, placed in the free space and interacting with the quantum electromagnetic field in its vacuum state [9, 11]. For simplicity, we model the atoms as two two-level systems. The Hamiltonian for the system in the multipolar coupling scheme, in the Coulomb gauge and within the dipole approximation, is

$$H = H_{at} + H_{rad} + H_i \tag{1.11}$$

where $H_{at} = H_A + H_B$ is the total atomic Hamiltonian of both atoms A and B, and H_{rad} is the radiation field Hamiltonian in the free space given by Eq. (1.1). H_i is the interaction Hamiltonian

$$H_i = -\boldsymbol{\mu}_A \cdot \mathbf{E}(\mathbf{r}_A) - \boldsymbol{\mu}_B \cdot \mathbf{E}(\mathbf{r}_B), \tag{1.12}$$

where we used $\mathbf{E}(\mathbf{r})$ instead of $\mathbf{D}_\perp(\mathbf{r})$ because, outside atoms and in the free space, the transverse displacement field coincides with the total (transverse plus longitudinal) electric field. $\boldsymbol{\mu}_\alpha$ is the electric dipole moment operator of the α-atom, placed in $\boldsymbol{r}_\alpha$, with $\alpha = A, B$. We wish to point out that the coupling Hamiltonian (1.12) takes into account the retardation effects due to the finite speed of light, and the electrostatic limit is recovered at short atomic distances, where retardation effects can be neglected. The unperturbed state of the system

is

$$|\psi_0\rangle = |E_0^A, E_0^B, 0\rangle\,, \tag{1.13}$$

where both atoms are in their ground state, with energy $E_0^{A(B)}$, and the radiation field is in the vacuum state $|0\rangle$. Since the initial state of the system coincides with the final state, the leading contributions to the dispersion interaction are at the fourth-order in the interaction Hamiltonian H_i, corresponding to two photons exchange between the atoms. Therefore, in the multipolar formalism, the dispersion interaction is viewed as arising from the exchange of two virtual photons between the atoms. By using fourth-order time-independent perturbation theory, the dispersion energy shift is given by

$$\begin{aligned}\Delta E = &- \sum_{I,II,III} \frac{\langle\psi_0|\, H_i\, |III\rangle\, \langle III|\, H_i\, |II\rangle\, \langle II|\, H_i\, |I\rangle\, \langle I|\, H_i\, |\psi_0\rangle}{(E_{III} - E_0)(E_{II} - E_0)(E_I - E_0)} \\ &+ \sum_{I,II} \frac{\langle\psi_0|\, H_i\, |II\rangle\, \langle II|\, H_i\, |\psi_0\rangle\, \langle\psi_0|\, H_i\, |I\rangle\, \langle I|\, H_i\, |\psi_0\rangle}{(E_I - E_0)^2(E_{II} - E_0)},\end{aligned} \tag{1.14}$$

where the second term in (1.14) is due to the normalization of the wavefunction. This term can be omitted since it does not yield a distance-dependent energy shift for nonpolar molecules [9, 11]. The sums, in expression (1.14), run over all possible intermediate states, with energies E_α (with $\alpha = I, II, III$), that link the unperturbed state $|\psi_0\rangle$ via the coupling Hamiltonian H_i (see Eq. 1.12). All possible intermediate states that can contribute to the energy shift (1.14) are illustrated in Fig. 1.3, using time-ordered diagrams. The states $|r\rangle$ and $|s\rangle$ are the excited states of the atom A and B, respectively. For example, in diagram (i) the various unperturbed states are

$$\begin{aligned}|\psi_0\rangle &= |E_0^A, E_0^B, 0\rangle\,, \\ |I\rangle &= |E_r^A, E_0^B, 1_{\mathbf{k}\lambda}\rangle\,, \\ |II\rangle &= |E_0^A, E_0^B, 1_{\mathbf{k}\lambda}, 1_{\mathbf{k}'\lambda'}\rangle\,, \\ |III\rangle &= |E_0^A, E_s^B, 1_{\mathbf{k}\lambda}\rangle\,,\end{aligned} \tag{1.15}$$

where the field state $|1_{\mathbf{k}\lambda}\rangle$ represent one photon in the field mode $(\mathbf{k}, \lambda)$. The

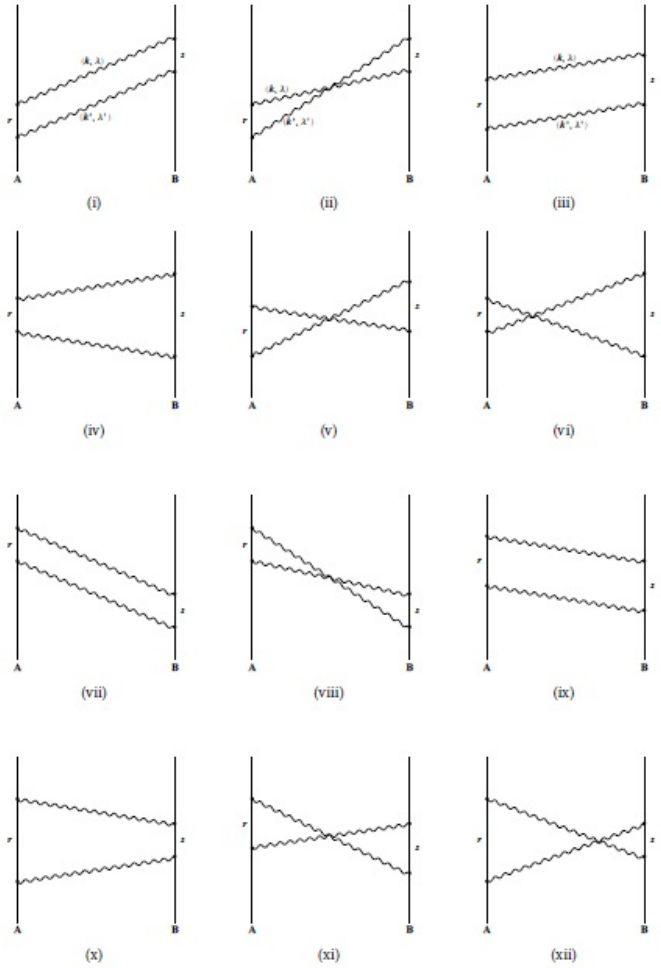

Figure 1.3: Twelve time-ordered diagrams used for the calculation of ground-state dispersion potential: they represent all the possible intermediate states that contribute to van der Waals dispersion interaction [11]

matrix elements related to the first diagram in Fig. 1.3 are

$$\langle\psi_0|\, H_i\, |III\rangle = -i\sqrt{\frac{\hbar ck}{2\epsilon_0 V}}(\hat{e}_{\mathbf{k}\lambda})_p(\mu_B^{0s})_p\; e^{i\mathbf{k}\cdot\mathbf{r}_B} \tag{1.16}$$

$$\langle III|\, H_i\, |II\rangle = -i\sqrt{\frac{\hbar ck'}{2\epsilon_0 V}}(\hat{e}_{\mathbf{k}'\lambda'})_l(\mu_B^{s0})_l\; e^{i\mathbf{k}'\cdot\mathbf{r}_B} \tag{1.17}$$

$$\langle II|\, H_i\, |I\rangle = i\sqrt{\frac{\hbar ck}{2\epsilon_0 V}}(\hat{e}_{\mathbf{k}\lambda})_i(\mu_A^{0r})_i\; e^{-i\mathbf{k}\cdot\mathbf{r}_A} \tag{1.18}$$

$$\langle I|\, H_i\, |\psi_0\rangle = i\sqrt{\frac{\hbar ck'}{2\epsilon_0 V}}(\hat{e}_{\mathbf{k}'\lambda'})_j(\mu_A^{r0})_j\; e^{-i\mathbf{k}'\cdot\mathbf{r}_A}, \tag{1.19}$$

where $(\mu_B^{0s})_p = \langle\psi_0|\,(\mu_B)_p\,|s\rangle$ is the matrix element between the ground and the excited state of the p-component of electric dipole moment of atom B. $\hat{e}_{\mathbf{k}\lambda}$ are polarization unit vectors with $\lambda = 1, 2$, assumed real. Therefore the total contribution from diagram (i) to the energy shift is

$$-\sum_{\mathbf{k},\mathbf{k}'}\sum_{\lambda,\lambda'}\sum_{r,s}\left(\frac{\hbar ck}{2\epsilon_0 V}\right)\left(\frac{\hbar ck'}{2\epsilon_0 V}\right)(\hat{e}_{\mathbf{k}\lambda})_i(\hat{e}_{\mathbf{k}'\lambda'})_j(\hat{e}_{\mathbf{k}\lambda})_l(\hat{e}_{\mathbf{k}'\lambda'})_p(\mu_A^{0r})_i(\mu_A^{r0})_j(\mu_B^{s0})_l(\mu_B^{0s})_p \times\frac{e^{i(\mathbf{k}+\mathbf{k}')\cdot\mathbf{r}}}{(E_{s0}+\hbar ck)(\hbar ck+\hbar ck')(E_{r0}+\hbar ck')}, \tag{1.20}$$

where $\mathbf{r} = \mathbf{r}_B - \mathbf{r}_A$ is the interatomic distance.
The contributions related to the other diagrams in Fig. 1.3 are evaluated in a similar manner. Therefore the total van der Waals energy shift is

$$\Delta E = -\sum_{\mathbf{k},\mathbf{k}'}\sum_{\lambda,\lambda'}\sum_{r,s}\left(\frac{\hbar ck}{2\epsilon_0 V}\right)\left(\frac{\hbar ck'}{2\epsilon_0 V}\right)(\hat{e}_{\mathbf{k}\lambda})_i(\hat{e}_{\mathbf{k}'\lambda'})_j(\hat{e}_{\mathbf{k}\lambda})_l(\hat{e}_{\mathbf{k}'\lambda'})_p (\mu_A^{0r})_i(\mu_A^{r0})_j(\mu_B^{s0})_l(\mu_B^{0s})_p e^{i(\mathbf{k}+\mathbf{k}')\cdot\mathbf{r}}\sum_{a=i}^{xii} D_a^{-1}, \tag{1.21}$$

where D_a are the energy denominators listed in Table 1.1.

Table 1.1: Energy denominators D_a

Graph	Denominator
(i)	$(E_{s0}+\hbar ck)(\hbar ck+\hbar ck')(E_{r0}+\hbar ck')$
(ii)	$(E_{s0}+\hbar ck')(\hbar ck+\hbar ck')(E_{r0}+\hbar ck')$
(iii)	$(E_{s0}+\hbar ck)(E_{s0}+E_{r0})(E_{r0}+\hbar ck')$
(iv)	$(E_{s0}+\hbar ck)(E_{s0}+E_{r0})(E_{s0}+\hbar ck')$
(v)	$(E_{s0}+\hbar ck')(E_{s0}+E_{r0}+\hbar ck+\hbar ck')(E_{r0}+\hbar ck')$
(vi)	$(E_{s0}+\hbar ck')(E_{s0}+E_{r0}+\hbar ck+\hbar ck')(E_{r0}+\hbar ck)$
(vii)	$(E_{r0}+\hbar ck)(\hbar ck+\hbar ck')(E_{s0}+\hbar ck')$
(viii)	$(E_{r0}+\hbar ck)(\hbar ck+\hbar ck')(E_{s0}+\hbar ck)$
(ix)	$(E_{r0}+\hbar ck)(E_{s0}+E_{r0})(E_{s0}+\hbar ck')$
(x)	$(E_{r0}+\hbar ck)(E_{s0}+E_{r0})(E_{r0}+\hbar ck')$
(xi)	$(E_{r0}+\hbar ck)(E_{s0}+E_{r0}+\hbar ck+\hbar ck')(E_{s0}+\hbar ck)$
(xii)	$(E_{r0}+\hbar ck)(E_{s0}+E_{r0}+\hbar ck+\hbar ck')(E_{r0}+\hbar ck')$

The sum over polarizations can be carried out by using the relation

$$\sum_{\lambda=1,2}(\hat{e}_{\mathbf{k}\lambda})_i(\hat{e}_{\mathbf{k}\lambda})_j = (\delta_{ij} - \hat{k}_i\hat{k}_j), \tag{1.22}$$

since $\hat{e}_{\mathbf{k}1}$, $\hat{e}_{\mathbf{k}2}$ and $\mathbf{k}$ form a set of mutually perpendicular unit vectors. The energy denominators from the twelve diagrams may be summed and written as

$$\sum_{a=i}^{xii} D_a^{-1} = \frac{4(k_{r0}+k_{s0}+k)}{\hbar^3 c^3 (k_{r0}+k_{s0})(k_{r0}+k)(k_{s0}+k)} \left(\frac{1}{k+k'} - \frac{1}{k-k'} \right), \tag{1.23}$$

where k_{r0} and k_{s0} are the wavevectors associated to the atomic transition between ground and excited state of atom A and B, respectively. Using the relation (1.22), (1.23) and taking the continuum limit over the radiation field modes

$$\frac{1}{V} \sum_{\mathbf{k}} \Rightarrow \int \frac{d^3\mathbf{k}}{(2\pi)^3}, \tag{1.24}$$

the total energy shift (1.21) becomes

$$\Delta E = -\frac{1}{\epsilon_0^2 \hbar c} \sum_{r,s} \frac{(\mu_A^{0r})_i (\mu_A^{r0})_j (\mu_B^{s0})_l (\mu_B^{0s})_p}{(k_{r0}+k_{s0})} \int\int \frac{d^3\mathbf{k}}{(2\pi)^3} \frac{d^3\mathbf{k}'}{(2\pi)^3} kk' (\delta_{ip} - \hat{k}_i \hat{k}_p)(\delta_{jl} - \hat{k}'_j \hat{k}'_l)$$
$$\times \frac{(k_{r0}+k_{s0}+k)}{(k_{r0}+k)(k_{s0}+k)} \left(\frac{1}{k+k'} - \frac{1}{k-k'} \right) e^{i(\mathbf{k}+\mathbf{k}')\cdot\mathbf{r}}. \tag{1.25}$$

The angular integration can be performed using the convenient relation

$$\frac{1}{4\pi} \int (\delta_{ij} - \hat{k}_i \hat{k}_j) e^{i\mathbf{k}\cdot\mathbf{r}} d\Omega = \mathrm{Im} F_{ij}(kr), \tag{1.26}$$

where $F_{ij}(kr)$ is defined as

$$F_{ij}(kr) = \left[(\delta_{ij} - \hat{r}_i \hat{r}_j) \frac{1}{kr} + (\delta_{ij} - 3\hat{r}_i \hat{r}_j) \left(\frac{i}{k^2 r^2} - \frac{1}{k^3 r^3} \right) \right] e^{ikr}. \tag{1.27}$$

Therefore, we obtain

$$\Delta E = -\frac{1}{4\pi^4 \epsilon_0^2 \hbar c} \sum_{r,s} \frac{(\mu_A^{0r})_i (\mu_A^{r0})_j (\mu_B^{s0})_l (\mu_B^{0s})_p}{(k_{r0}+k_{s0})} \int_0^\infty \int_0^\infty dk\, dk'\, \mathrm{Im}[F_{ip}(kr)]\, \mathrm{Im}[F_{jl}(k'r)]$$
$$\times k^3 k'^3 \frac{(k_{r0}+k_{s0}+k)}{(k_{r0}+k)(k_{s0}+k)} \left(\frac{1}{k+k'} - \frac{1}{k-k'} \right). \tag{1.28}$$

Since $\mathrm{Im}[F_{jl}(k'r)]$ is an even function of k', the limits of the k'-integral in (1.28) can be extended to $-\infty$ to $+\infty$. Taking the principal value at the pole $k = -k'$ we get

$$\int_{-\infty}^{\infty} \frac{k'^3}{k+k'}\, \mathrm{Im}[F_{jl}(k'r)]\, dk' = \pi k^3\, \mathrm{Re}[F_{jl}(kr)], \tag{1.29}$$

so the expression (1.28) can be written as

$$\Delta E = -\frac{1}{4\pi^3\epsilon_0^2\hbar c}\sum_{r,s}\frac{(\mu_A^{0r})_i(\mu_A^{r0})_j(\mu_B^{s0})_l(\mu_B^{0s})_p}{(k_{r0}+k_{s0})} \times \int_0^\infty \mathrm{Im}[F_{ip}(kr)]\ \mathrm{Re}[F_{jl}(kr)]\ k^6\frac{(k_{r0}+k_{s0}+k)}{(k_{r0}+k)(k_{s0}+k)}dk. \tag{1.30}$$

Multiplying the real and imaginary part of the tensor field $F_{ij}(kr)$ in Eq. (1.30), assuming freely rotating molecules, such that

$$\langle(\mu_A^{0r})_i(\mu_A^{r0})_j\rangle\langle(\mu_B^{s0})_l(\mu_B^{0s})_p\rangle = \frac{1}{9}\delta_{ij}\delta_{pl}\ |\boldsymbol{\mu}_A^{0r}|^2\ |\boldsymbol{\mu}_B^{0s}|^2, \tag{1.31}$$

and the changing integration variable $k = iu$, after some algebraic calculations, the familiar van der Waals (or sometimes called Casimir-Polder) potential for isotropic systems is obtained

$$\Delta E = -\frac{1}{36\pi^3\epsilon_0^2\hbar c}\sum_{r,s}|\boldsymbol{\mu}_A^{0r}|^2|\boldsymbol{\mu}_B^{0s}|^2\int_0^\infty\frac{k_{r0}k_{s0}}{(k_{r0}^2+u^2)(k_{s0}^2+u^2)} \times\left[\frac{1}{u^2r^2}+\frac{2}{u^3r^3}+\frac{5}{u^4r^4}+\frac{6}{u^5r^5}+\frac{3}{u^6r^6}\right]e^{-2ur}u^6du, \tag{1.32}$$

which holds for all interatomic distances r beyond the wavefunction overlap region [9, 11].

Les us now consider the asymptotic behaviour of the Casimir-Polder potential (1.32) in the limits of large and small interatomic separation. In the near zone, $rk_0 \ll 1$, which means that the interatomic separation is much smaller than the characteristic atomic transition wavelength, $e^{-2ur} \approx 1$ and the dominant term in the square brackets is the one proportional to r^{-6}. Exploiting the integral relation

$$2\int_0^\infty\frac{ab}{(a^2+u^2)(b^2+u^2)}du = \frac{\pi}{a+b}, \qquad a,b>0, \tag{1.33}$$

the Casimir-Polder potential in the near zone becomes

$$\Delta E_{nz} = -\frac{1}{24\pi^2\epsilon_0^2r^6}\sum_{r,s}\frac{|\boldsymbol{\mu}_A^{0r}|^2|\boldsymbol{\mu}_B^{0s}|^2}{E_{r0}+E_{s0}}, \tag{1.34}$$

which is the same result obtained by London in 1930 for the dispersion energy, with the familiar r^{-6} spatial dependence. As mentioned before, the dispersion interaction in the near zone can be viewed essentially as an electrostatic interaction between two induced, fluctuating, electric-dipole moments, that occurs instantaneously, and thus behaves as r^{-6}.

On the other hand, for large interatomic separations, $rk_0 \gg 1$, in the energy denominators of (1.32) u^2 can be ignored with respect to k_{r0}^2 and k_{s0}^2. Thus, performing the u-integral, the Casimir-Polder potential in the far zone is

$$\Delta E_{fz} = -\frac{23\hbar c}{64\pi^3\epsilon_0^2}\frac{\alpha_A\alpha_B}{r^7}, \tag{1.35}$$

in which the static polarizabilities of the atom A and B appear, given by

$$\alpha_A = \frac{2}{3}\sum_r \frac{|\boldsymbol{\mu}_A^{0r}|^2}{E_{r0}} \quad , \quad \alpha_B = \frac{2}{3}\sum_s \frac{|\boldsymbol{\mu}_B^{0s}|^2}{E_{s0}}. \tag{1.36}$$

As already mentioned, at large interatomic separation the dispersion potential changes its space dependence from r^{-6} to r^{-7}; thus it decreases with the distance faster than the electrostatic London potential. This result is due to the fact that, in the far zone limit, the dispersion interaction between two atoms is a radiative process, that takes into account retardation effects due to the finite propagation speed of the electromagnetic radiation.

As previously mentioned, being fourth-order interaction in the atom-field coupling, van der Waals interactions are very small with respect to the Coulomb interaction. A numerical estimation of the vdW dispersion force between two hydrogen atoms in the ground-state and in the free space can be easily obtained : considering atoms placed at a distance of $r \backsimeq 1\mu$m and including only contributions involving the $n = 2$ states of the hydrogen atoms, the van der Waals force is about $F_{vdW} \sim 8 \cdot 10^{-39}$N.

1.2.2 The atom-surface Casimir-Polder interaction

Dispersion forces between a polarizable system, such as an atom or a molecule, and a surface, are known as Casimir-Polder interactions. They have been recently studied in many physical situations: dielectric and metal surfaces, vacuum state of the field or at a finite temperature, as well as in dynamical situations, under non equilibrium conditions [18–24]. In this section we consider only the simple case of the Casimir-Polder interaction between a ground-state atom and a perfectly conducting wall, with the radiation field in its vacuum state.
We consider a ground state two-level atom placed at $z = r$ in front of an infinite perfectly conducting mirror placed in the origin, at $z = 0$, as shown in Fig. 1.4.
The bulk mirror, treated classically as a boundary condition of the electromagnetic field, modifies the density of states of the radiation field and the vacuum field fluctuations, that now, in consequence of the presence of the mirror, depend on the atom-mirror distance r. The interaction between the atom and the space-dependent vacuum field fluctuations leads to the atom-surface Casimir-Polder

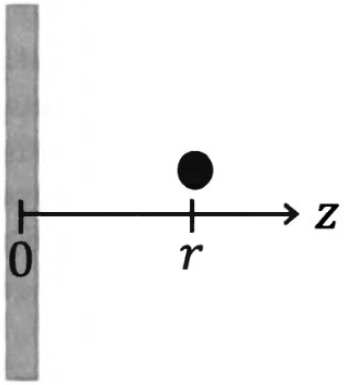

Figure 1.4: A two-level ground-state atom placed at a distance r from an infinite mirror plate, made of a perfect conductor, that extends over the xy plane at $z = 0$ [18].

force. In order to obtain the situation of an atom in front of a perfectly conducting wall, we first assume that the atom, in its ground state $|g\rangle$, is placed inside a cuboid cavity made of an empty box with perfectly conducting walls of size L; we consider the case for which the atom is near one of the walls of the cavity, say the one placed in $z = 0$, but sufficiently far away from the others walls so that their effect may be ignored. The normal modes for the electromagnetic field inside the cuboid cavity of volume $V = L^3$ enclosed by perfectly conducting walls are [18, 25]

$$\boldsymbol{u}_{\boldsymbol{n}\lambda}(\boldsymbol{r}) = \sqrt{\frac{8}{V}} \begin{bmatrix} \cos(\frac{\pi n_x}{L}x)\sin(\frac{\pi n_y}{L}y)\sin(\frac{\pi n_z}{L}z) \\ \sin(\frac{\pi n_x}{L}x)\cos(\frac{\pi n_y}{L}y)\sin(\frac{\pi n_z}{L}z) \\ \sin(\frac{\pi n_x}{L}x)\sin(\frac{\pi n_y}{L}y)\cos(\frac{\pi n_z}{L}z) \end{bmatrix}, \tag{1.37}$$

where the wavevector components take discrete values

$$\boldsymbol{k} = \frac{\pi}{L}(n_x, n_y, n_z) \quad \text{with } \boldsymbol{n} = (n_x, n_y, n_z) \in \mathbb{N}^3. \tag{1.38}$$

Within the dipole approximation and in the multipolar coupling scheme, the interaction Hamiltonian can be written as

$$H_i = -\boldsymbol{\mu} \cdot \mathbf{E}(\mathbf{r}), \tag{1.39}$$

where $\boldsymbol{\mu}$ is the electric atomic dipole moment operator and

$$\mathbf{E}(\mathbf{r}) = \sum_{\mathbf{k},\lambda} i\sqrt{\frac{\hbar\omega_{\mathbf{k}}}{2\epsilon_0 V}} \left(a_{\mathbf{k}\lambda} - a^{\dagger}_{\mathbf{k}\lambda}\right) \boldsymbol{u}_{\boldsymbol{n}\lambda}(\boldsymbol{r}) \tag{1.40}$$

is the electric field operator written in terms of the normal field modes inside the cavity, that takes into account the boundary conditions on the perfectly conducting walls. For a two-level atom, the dipole moment operator $\boldsymbol{\mu}$ can be conveniently written in terms of pseudospin operators $S_+ = |e\rangle\langle g|$ and $S_- = |g\rangle\langle e|$, as

$$\boldsymbol{\mu} = \boldsymbol{\mu}^{eg}(S_+ + S_-) \,, \tag{1.41}$$

where $\boldsymbol{\mu}^{eg} = \langle e|\,\boldsymbol{\mu}\,|g\rangle$ is the dipole matrix element (assumed real) between the excited $|e\rangle$ and ground $|g\rangle$ atomic states. Therefore the interaction Hamiltonian (1.39) becomes

$$H_i = -i\sum_{\boldsymbol{k},\lambda}\sqrt{\frac{\hbar\omega_{\mathbf{k}}}{2\epsilon_0 V}}\left(\boldsymbol{u}_{\boldsymbol{n}\lambda}(\boldsymbol{r})\cdot\boldsymbol{\mu}^{eg}\right)\left(a_{\mathbf{k}\lambda} - a^{\dagger}_{\mathbf{k}\lambda}\right)(S_+ + S_-) \tag{1.42}$$

that takes into account the absorption and emission of both virtual and real photons from the dipole. Since we assume that the system is in its unperturbed ground state $|g,0\rangle$, with the radiation field in the vacuum state and the atom in its ground state, only virtual absorption and emission processes can occur.
The energy shift of the system can be calculated using the second-order time-independent perturbation theory [1, 18],

$$\Delta E = \sum_I \frac{\langle g,0|\,H_i\,|I\rangle\,\langle I|\,H_i\,|g,0\rangle}{E_0 - E_I}, \tag{1.43}$$

where E_0 and E_I are energies of the ground and intermediate states, respectively. The intermediate states that can contribute to the energy shift (1.43) are $|I\rangle = |e,1_{\boldsymbol{k}\lambda}\rangle$, shown in Fig. 1.5, where one (virtual) photon is emitted in the $(\boldsymbol{k},\lambda)$ field mode and the atom is in its excited state $|e\rangle$.

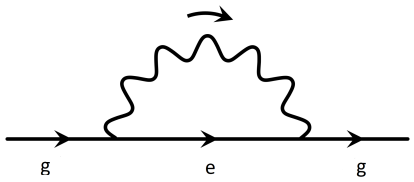

Figure 1.5: Self-energy diagram for the atom-surface interaction; since the vacuum field fluctuations are space-dependent, the atom-field self-interaction leads to a space-dependent interaction energy, and thus to a force between the atom and the surface.

From Eq. (1.43), using the interaction Hamiltonian (1.42), we obtain

$$\Delta E = -\frac{1}{2\epsilon_0 V}\sum_{\boldsymbol{k},\lambda}\frac{\omega_{\boldsymbol{k}}}{\omega_0+\omega_{\boldsymbol{k}}}|(\boldsymbol{u}_{\boldsymbol{n}\lambda}(\boldsymbol{r})\cdot\boldsymbol{\mu}^{eg})|^2 \tag{1.44}$$

where $\omega_0 = (E_e - E_g)/\hbar$ is the atomic transition frequency.

In order to perform the sum over the polarizations we use the general relation [25]

$$\sum_{\lambda}(u_{\boldsymbol{n}\lambda}(\boldsymbol{r}))_i(u_{\boldsymbol{n}\lambda}(\boldsymbol{r'}))_j = (\delta_{ij}-\hat{k}_i\hat{k}_j)e^{i\boldsymbol{k}\cdot(\boldsymbol{r}-\boldsymbol{r'})} - \sigma_{il}(\delta_{lj}-\hat{k}_l\hat{k}_j)e^{i\boldsymbol{k}\cdot(\boldsymbol{r}-\sigma\boldsymbol{r'})}\ , \tag{1.45}$$

where σ is the reflection matrix given by

$$\sigma = \begin{pmatrix} 1 & 0 & 0 \\ 0 & 1 & 0 \\ 0 & 0 & -1 \end{pmatrix}. \tag{1.46}$$

Here $\boldsymbol{r}$ and $\boldsymbol{r'}$ are generic positions inside the cuboid cavity, assumed near one wall but far away from the others. Thus, taking into account only space-dependent contributions given by the second term of Eq. (1.45) and taking the continuum limit, we obtain

$$\begin{aligned}\Delta E &= \frac{1}{2\epsilon_0}\mu_i^{eg}\mu_j^{ge}\sigma_{il}\int\frac{dk^3}{(2\pi)^3}\frac{k}{k_0+k}(\delta_{lj}-\hat{k}_l\hat{k}_j)e^{i\boldsymbol{k}\cdot(\boldsymbol{r}-\sigma\boldsymbol{r})} \\ &= -\frac{1}{2\epsilon_0}\tilde{\mu}_i^{eg}\mu_j^{ge}\int\frac{dk^3}{(2\pi)^3}\frac{k}{k_0+k}(\delta_{ij}-\hat{k}_i\hat{k}_j)e^{i\boldsymbol{k}\cdot\boldsymbol{q}} \\ &= \frac{1}{4\pi^2\epsilon_0}\tilde{\mu}_i^{eg}\mu_j^{ge}(\delta_{ij}\nabla^2-\nabla_i\nabla_j)\left[\frac{f(k_0q)}{q}\right]\end{aligned} \tag{1.47}$$

where $\tilde{\boldsymbol{\mu}} = -\sigma\boldsymbol{\mu}$ is the image atomic dipole operator beyond the mirror, and the gradients are taken with respect to $\boldsymbol{q} = (\boldsymbol{r}-\sigma\boldsymbol{r})$ [25]. We stress that $q = |\boldsymbol{q}| = 2r$, where r is the shortest distance to the wall $z = 0$, and the direction of $\boldsymbol{q}$ is orthogonal to the wall. Applying the differential operators, the energy shift (1.47) becomes

$$\begin{aligned}\Delta E = \frac{\tilde{\mu}_i^{eg}\mu_j^{ge}}{32\pi^2\epsilon_0 r^3}\Big\{&(\delta_{ij}-3\hat{r}_i\hat{r}_j)\Big[f(2k_0r)+2k_0r\ g(2k_0r)\Big] \\ &+(\delta_{ij}-\hat{r}_i\hat{r}_j)\Big[2k_0r-(2k_0r)^2f(2k_0r)\Big]\Big\},\end{aligned} \tag{1.48}$$

where

$$f(x) = \mathrm{Ci}(x)\sin x - \mathrm{si}(x)\cos x\ , \tag{1.49}$$

$$g(x) = -\mathrm{Ci}(x)\cos x - \mathrm{si}(x)\sin x \tag{1.50}$$

are the auxiliary functions in terms of the cosine and sine integral functions $\mathrm{Ci}(x)$ and $\mathrm{si}(x) = \mathrm{Si}(x) - \frac{\pi}{2}$, [26–28]. Eq. (1.48) is the Casimir-Polder potential of one atom placed in front of a perfectly conducting wall.

In the short-range limit $k_0 r \ll 1$, when the atom-wall distance is much smaller than the atomic transition wavelength, $f(x) \to \pi/2$ and $g(x) \to \log(x)$ when $x \to 0$, and therefore the Casimir-Polder potential (1.48) becomes

$$\Delta E_{nz} \simeq \frac{\tilde{\mu}_i^{eg} \mu_j^{ge}}{64\pi\epsilon_0 r^3}(\delta_{ij} - 3\hat{r}_i\hat{r}_j), \tag{1.51}$$

showing that the near zone (nonretarded) Casimir-Polder potential scales as r^{-3}. On the other hand, in the far-zone limit $k_0 r \gg 1$, the asymptotic expansion for auxiliary functions are

$$f(x) \sim \frac{1}{x}\left(1 - \frac{2!}{x^2} + \frac{4!}{x^4} - \frac{6!}{x^6} + \dots\right) \tag{1.52}$$

$$g(x) \sim \frac{1}{x^2}\left(1 - \frac{3!}{x^2} + \frac{5!}{x^4} - \frac{7!}{x^6} + \dots\right). \tag{1.53}$$

and therefore the Casimir-Polder interaction is

$$\Delta E_{fz} \simeq \frac{\tilde{\mu}_i^{eg} \mu_j^{ge}}{16\pi^2\epsilon_0 k_0 r^4}(\delta_{ij} - 2\hat{r}_i\hat{r}_j). \tag{1.54}$$

The last result can be written in terms of the static polarizability of the atom,

$$\alpha = \frac{2}{3}\sum_r \frac{|\boldsymbol{\mu}^{gr}|^2}{E_{gr}} \tag{1.55}$$

where the sum is performed on the generic atomic excited states, obtaining

$$\Delta E_{fz} = -\frac{3\hbar c\alpha}{32\pi^2\epsilon_0 r^4}, \tag{1.56}$$

scaling as r^{-4} with the distance.

These results show that for short atom-surface distance ($k_0 r \ll 1$), the attractive interaction between the atom and the wall behaves as r^{-3}, and it is essentially instantaneous, since retardation effects can be neglected; in fact, the same result can be obtained by considering the electrostatic interaction of the atom with its image on the other side of the wall. On the other hand, in the long-range limit ($k_0 r \gg 1$), owing to retardation effects, the atom-wall Casimir-Polder potential behaves as r^{-4}, rather than r^{-3}. In both cases the atom-wall force is attractive if the

atom is in its ground state, and in the quasi-static hypothesis, it can be obtained by taking the derivative of ΔE with respect to r, changed by sign [1, 15, 18, 25].

A numerical estimate of the atom-surface force can be done considering, for example, a ground-state hydrogen atom placed at $r \simeq 1$ μm from a plane mirror: in this case, considering contributions only involving the $n = 2$ state of the hydrogen atom, the Casimir-Polder force is about $F_{CP} \sim 2 \cdot 10^{-27}$N.

1.2.3 The Casimir effect

With the expression *"Casimir forces"* we generally refer to dispersion interactions between two neutral, unpolarized and unmagnetized macroscopic bodies, mediated by quantum electromagnetic field. These forces are associated with topological constraints on the radiation field, because the boundary conditions given by any macroscopic body strongly modifies the density of states, and thus its zero-point energy and vacuum field fluctuations [15]. Since the value of this energy depends on the shape and position of the macroscopic objects, a force arises between them, that is the Casimir force. The existence of this force is a pure quantum effect, arising from the change of the vacuum field fluctuations, and cannot be predicted by classical electrodynamics. Although the Casimir force is generally a weak interaction, it is of great interest for both theoretical and experimental reasons: in fact, it is an ubiquitous force, that becomes more and more relevant when the size of the physical system is getting smaller and smaller. For these reasons, it plays a fundamental role in many areas of science, from fundamental and cosmological physics, to chemistry, biology and even engineering, with its application in the development of micro- and nano- electromechanical systems (M.E.M.S and N.E.M.S). The first and most famous prediction of the Casimir effect was obtained by Casimir in 1948, who found that between two neutral, parallel and perfectly conducting plates, separated by a distance L at zero temperature, there is an attractive force per unit area given by [8]

$$F = -\frac{\pi^2 \hbar c}{240 L^4}. \tag{1.57}$$

A generalization of the Casimir effect was obtained by Lifshitz, considering the interaction force between two dielectric half-spaces separated by a vacuum region of width d, for finite (equilibrium) temperatures [29]. Later, other Casimir forces between objects with different shapes and made of different materials, such as plate-sphere or sphere-sphere, have been calculated [30–32]

We now retrace the main steps of the original calculation of Casimir, in its original configuration of two parallel, neutral, metallic plates separated by a distance L, in the vacuum space, as shown in Fig. 1.6.

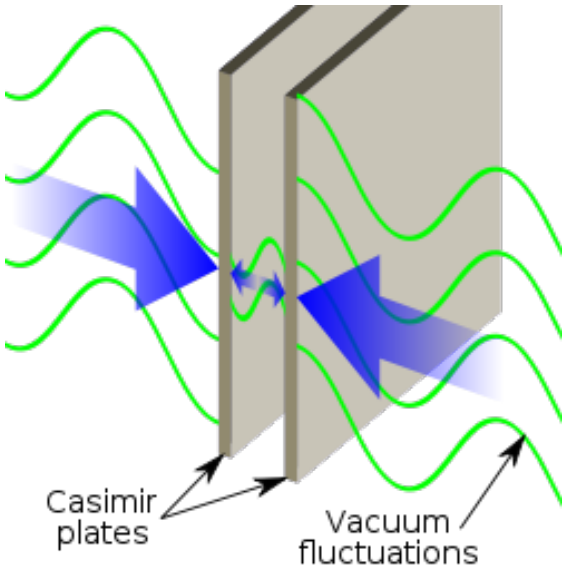

Figure 1.6: The Casimir effect: two parallel metal slabs in the vacuum space, of area $A = L_x L_y$, at distance L.

In order calculate the Casimir force between the plates, we initially assume the vacuum field modes are enclosed in a cuboid cavity of dimensions (L_x, L_y, L), where the area of the plates is $A = L_x L_y$ and L is the distance between them [1, 17]. To reproduce the physical system of just two metal parallel plates at distance L, we then take $L_x, L_y \gg L$. The normal modes of the electromagnetic field inside a cuboid cavity are given by (1.37), with dispersion relation given by

$$\omega_{\boldsymbol{k}} = c\sqrt{\left(\frac{n_x\pi}{L_x}\right)^2 + \left(\frac{n_y\pi}{L_y}\right)^2 + \left(\frac{n_z\pi}{L}\right)^2}, \quad \text{with} \quad (n_x, n_y, n_z) \in \mathbb{N}. \tag{1.58}$$

The zero-point field energy can be written as

$$E_0(L) = \frac{\hbar c}{2} \sum_{n_x n_y n_z \lambda}^{+\infty} \sqrt{\left(\frac{n_x\pi}{L_x}\right)^2 + \left(\frac{n_y\pi}{L_y}\right)^2 + \left(\frac{n_z\pi}{L}\right)^2}, \tag{1.59}$$

where the summation is performed over all frequencies and polarizations. Since $L_x, L_y \gg L$, the electromagnetic field has a continuum spectrum of modes along

the x and y direction, so

$$\begin{aligned} E_0(L) =& \frac{\hbar c L_x L_y}{2\pi^2} \int_0^{+\infty} dk_x \int_0^{+\infty} dk_y \sum_{n_z\lambda}^{+\infty} \sqrt{k_x^2 + k_y^2 + \left(\frac{n_z\pi}{L}\right)^2} \\ =& \frac{\hbar c A}{2\pi} \int_0^{+\infty} dk_\parallel k_\parallel \sum_{n_z=0}^{+\infty}{}' \sqrt{k_\parallel^2 + \left(\frac{n_z\pi}{L}\right)^2}, \end{aligned} \tag{1.60}$$

where, in the last row, we introduce the polar coordinates in the $k_x k_y$ plane, for which $\int_0^{+\infty} dk_x \int_0^{+\infty} dk_y = \pi/2 \int_0^{+\infty} dk_\parallel k_\parallel$. We have also performed the sum over polarizations, which is trivial because the energy of the modes is polarization-independent, so a factor 2 appears for each $n_z = 1, 2, 3...$ except for $n_z = 0$, for which only one polarization exists. The primed sum in Eq. (1.60) takes into account this fact.

We wish to point out that the Casimir energy (1.60) diverges, and in particular contains two different divergences of vacuum QED: the ultra-violet divergence and the self energy divergence [18]. The former arises because virtual photons of arbitrarily large energies has been taken into account for the zero-point energy. Since real metal plates becomes transparent for high-frequency, virtual photons that exceed the plasma frequency of the metal ω_p cease to interact with the plates and therefore cannot contribute to the Casimir energy (distance dependent) anymore. To consider this high-frequency transparency, we introduce a cut-off function $e^{-\lambda_p\sqrt{k_\parallel^2+k_z^2}}$, which exponentially suppresses the contribution from virtual photons with wavelength larger than the plasma wavelength $\lambda_p = 2\pi c/\omega_p$.
On the other hand, in order to deal with the self-energy divergence of expression (1.60), we have to renormalise the Casimir energy as

$$\Delta E_0(L) = E_0(L) - E_0(L \to +\infty) \tag{1.61}$$

where $E_0(L \to +\infty)$ is the Casimir self-energy calculated in the limit $L \to +\infty$, that is when the distance between the plates becomes very large; in such a limiting case, the sum over the field modes, also along the z-direction, approaches a quasi-continuous spectrum. This energy can be written as

$$E_0(L \to +\infty) = \frac{\hbar c A L}{2\pi^2} \int_0^{+\infty} dk_\parallel k_\parallel \int_0^{+\infty} dk_z e^{-\lambda_p\sqrt{k_\parallel^2+k_z^2}} \sqrt{k_\parallel^2 + k_z^2}. \tag{1.62}$$

Therefore the equation (1.61) is the Casimir energy expression, no more divergent, given by the difference between the vacuum field energy with and without the

plates. Performing the calculations, we obtain

$$\Delta E_0(L) = \frac{\hbar c A}{2\pi} \int_0^{+\infty} dk_\parallel k_\parallel \left[{\sum_{n_z=0}^{+\infty}}' e^{-\lambda_p \sqrt{k_\parallel^2 + (\frac{n_z \pi}{L})^2}} \sqrt{k_\parallel^2 + \left(\frac{n_z \pi}{L}\right)^2} \right. \tag{1.63}$$

$$\left. - \frac{L}{\pi} \int_0^{+\infty} dk_z e^{-\lambda_p \sqrt{k_\parallel^2 + k_z^2}} \sqrt{k_\parallel^2 + k_z^2} \right], \tag{1.64}$$

and using the Euler-Maclaurin formula

$${\sum_{n_z=0}^{+\infty}}' f(n) - \int_0^{+\infty} dx f(x) = \frac{1}{12} f'(0) + \frac{1}{720} f'''(0) + ... \tag{1.65}$$

the familiar Casimir energy expression is obtained

$$\Delta E_0(L) = -\frac{\hbar c \pi^2 A}{720 L^3}, \tag{1.66}$$

that, in the quasi-static regime, yields to the well-known attractive effect (1.57) between two parallel metal plates predicted by Casimir in 1948, scaling with the distance as L^{-3} for the energy, and thus as L^{-4} for the force. We stress that the Casimir force (1.57) is a very tiny force: in fact, for example, considering plates with area $A = 1$ cm^2, separated by a distance $L = 10^{-6}$ m, the force between them is about $F \sim 10^{-7}$ N . Although this is a very small force, it become relevant when the size of the system becomes smaller and smaller, as for example, in the micro- and nano- electromechanical systems. Also, it has been measured with high precision, how we will discuss in the next section.

1.3 Dispersion forces: experiments

Dispersion interactions, such as the van der Waals, the Casimir-Polder and the Casimir force, discussed in the previous sections, have been theoretically predicted and experimentally proved with high precision, although they are quite tiny interactions and therefore very difficult to detect. In following, we present some of the main ideas for measuring dispersion forces.

One of the first significant experiments about the Casimir force was carried out by Sparnaay in 1958, performed in the original configuration of two metal parallel plates proposed by Casimir in 1948 [33]. This experiment did not confirm the existence of this interaction, owing to large experimental errors, but highlighted the main experimental difficulties to take a significant measurement of the force between the plates. The first problem was that the material of the plates had to

be as pure and smooth as possible, to ensure good conductibility and to avoid any contact between the slabs during the experiment; keep plates perfectly parallel to each other involved considerable experimental complications, which increase with the size of the slabs. Due to these main experimental issues, the Sparnaay's experiment did not confirm the theoretical predictions of Casimir but, as he said, neither did contradict them.
In order to overcome the plates parallelism's problem, some experiments, for example that of van Blockland e Overbeek (in 1978) [34], have been performed detecting the Casimir force between a sphere and a slab, theoretically given by

$$F = -\frac{\hbar c \pi^3 R}{360 d^3}, \tag{1.67}$$

valid when $d \ll R$, where R is the sphere radius and d is the sphere-slab distance. In this framework a relevant experimental work was performed by Lamoreaux in 1997 [35], that measured the Casimir force between two quartz lenses covered with copper, one spherical and the other flat, separated by a distance between $0,6$ μ m and 6 μm. He exploited an electromechanical system based on a torsion pendulum: the lens is attached to one pendulum arm and the other arm was connected to a planar capacitor. The Casimir force between the lenses change the capacitance of the planar capacitor and he was able to measure it, achieving an accuracy of the order of $5 - 10\%$.
In the 1990s, the modern technology, such as the atomic force microscope (AFM), has been used to investigate and detect the Casimir force. In 1998, Mohideen and Roy [36] measured the Casimir force between a polystyrene sphere with diameter of $0,3$ mm, covered with a small layer of gold and aluminium, and a sapphire plates. The sphere was attached to the AFM cantilever and placed at $0,1$ μm from the sapphire plate, as shown in Fig. 1.7. The Casimir force between the sphere

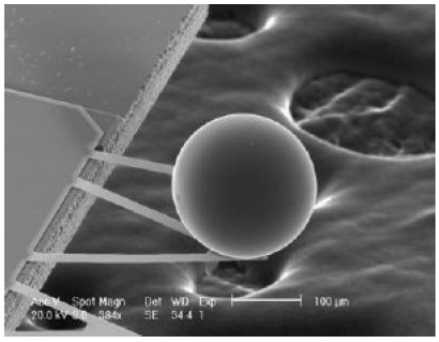

Figure 1.7: Polystyrene sphere attached to the AFM cantilever near the sapphire plate [36].

and the sapphire plate leads to a cantilever deflection that was measured from

the reflection of a laser beam on a photodiodes matrix; through this experimental setup, shown in Fig. 1.8, an accuracy of 1% was achieved. Only in 2002 it was

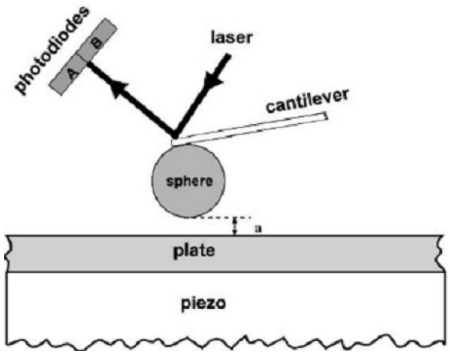

Figure 1.8: Experimental setup used in [36] to measure the sphere-plate Casimir force through AFM.

possible to check experimentally the Casimir effect in its original configuration proposed by Casimir himself in 1948, of two perfectly conducting parallel plates. The experiment, performed by Bressi *et al* [37], measured the Casimir force between parallel metallic plates with an accuracy of 15% in a distance range of the slabs of $0.5 - 3$ μm.

Regarding van der Waals and Casimir-Polder forces, the experimental situation becomes even more difficult since microscopic interacting objects are involved. In fact the control of position, velocity, forces acting on the atoms, is very hard to obtain, and making a direct measurement of these interactions is extremely difficult. However indirect manifestations of these forces can be found in the measurement of macroscopic quantities, as for example suggested by van der Waals himself when he studied the modifications of the equation of state of a gas owing to the van der Waals interaction between molecules [38]. More accurate measurements of the van der Waals forces can be performed exploiting scattering experiments. These experiments can be torn into two main groups: in the former case the scattering of an atomic beam passing through a stationary gas which serves as target is investigated. In this situation, the van der Waals interactions with the atoms of the gas deflect the atomic beam and then an attenuation of the beam is detected [39–41]. In the other case, experiments involving two distinct beams which intersect can be performed: owing to the vdW potential, atoms were scattering in various directions and, detecting the number of atoms as a function of the scattering angle, it was possible to infer the vdW potential [42, 43].

Casimir-Polder interactions can be experimentally measured in a similar way. When an atomic beam is directed along a macroscopic body, the Casimir-Polder force attracts the atoms towards the body, leading to a deflection from their original

path, as shown in Fig. 1.9. The Casimir-Polder potential can be then inferred by

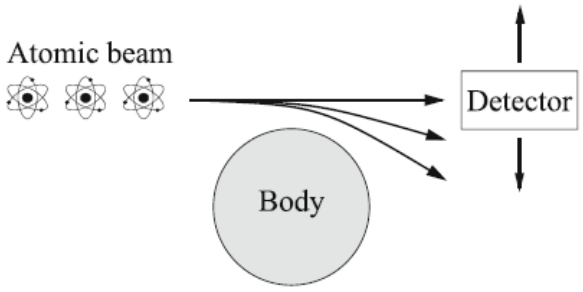

Figure 1.9: Classical scattering method to measure Casimir-Polder potential [15] .

measuring the deflection angle of the atoms. This idea was first developed for ground-state atoms interacting with a metallic or dielectric cylinder [44–46].

1.4 Resonance interaction between two entangled atoms in the free space

The resonance interaction, or resonant dipole-dipole interaction (RDDI), is an interaction between two atoms, molecules or any quantum emitters, one excited and the other in its ground state, prepared in a symmetric or antisymmetric entangled state, mediated by the quantum electromagnetic field [11]. In this section we consider the resonance interaction between two identical two-levels atoms, A and B, interacting with the quantum vacuum, when they are in the free space: the atomic ground state $|g\rangle$ (with energy E_g) and the atomic excited state $|e\rangle$ (with energy E_e) are connected by an electric dipole transition. The physical system is prepared in a symmetric or antisymmetric entangled state

$$|\psi\rangle = \frac{1}{\sqrt{2}}(|g_A, e_B, 0\rangle \pm |e_A, g_B, 0\rangle) \tag{1.68}$$

where $|0\rangle$ is the vacuum state of the radiation field; the excitation is thus delocalized between the atoms. As previously done for the dispersion interaction calculation (see Sec. (1.2)), we consider the matter-field interaction Hamiltonian in the multipolar coupling scheme and within the dipole approximation

$$H_i = -\boldsymbol{\mu}_A \cdot \mathbf{E}(\mathbf{r_A}) - \boldsymbol{\mu}_B \cdot \mathbf{E}(\mathbf{r_B}). \tag{1.69}$$

Since the system is prepared in the unperturbed state (1.68), the resonance interaction ΔE between the atoms is a second-order interaction in the atom-field

coupling, that can be calculated using the second-order time-independent perturbation theory

$$\Delta E = \sum_I \frac{\langle\psi|\, H_i\, |I\rangle\, \langle I|\, H_i\, |\psi\rangle}{E_\psi - E_I}, \tag{1.70}$$

where $|I\rangle$ are all the possible intermediate states that can contribute to the total energy shift with energy E_I. They are in the former

$$|I_1\rangle = |g_A, g_B, 1_{\mathbf{k}'\lambda'}\rangle \;\; ; \quad |I_2\rangle = |e_A, e_B, 1_{\mathbf{k}'\lambda'}\rangle\,, \tag{1.71}$$

which represent both atoms in their ground state with one photon in the field mode $(\mathbf{k}', \lambda')$, and both atoms in their excited states with one photon in the field mode $(\mathbf{k}', \lambda')$.

The intermediate states (1.71) are depicted in the Feynman diagrams in Fig. 1.10.

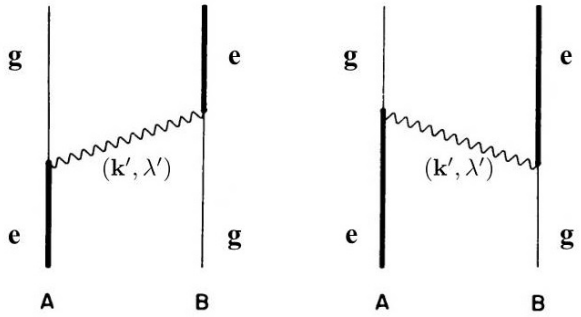

Figure 1.10: Feynman diagrams for the resonance interaction between two atoms in the multipolar coupling method [11]

We now calculate the matrix element for the intermediate state $|I_1\rangle$:

$$\begin{aligned}
\langle\psi|\, H_i\, |I_1\rangle &= \frac{1}{\sqrt{2}} \sum_{\mathbf{k}'\lambda'} \Big(\langle g_A, e_B, 0| + \langle e_A, g_B, 0| \Big) H_i\, |g_A, g_B, 1_{\mathbf{k}'\lambda'}\rangle \\
&= -\frac{1}{\sqrt{2}} \sum_{\mathbf{k}'\lambda'} \Big[\langle e_B|\, \boldsymbol{\mu}_B\, |g_B\rangle \cdot \langle 0|\, \mathbf{E}(\mathbf{r}_B)\, |1_{\mathbf{k}'\lambda'}\rangle + \langle e_A|\, \boldsymbol{\mu}_A\, |g_A\rangle \cdot \langle 0|\, \mathbf{E}(\mathbf{r}_A)\, |1_{\mathbf{k}'\lambda'}\rangle \Big] \\
&= -i \sum_{\mathbf{k}'\lambda'} \sum_{\mathbf{k}\lambda} \left(\frac{\hbar\omega_{\mathbf{k}}}{4\epsilon_0 V} \right)^{1/2} (\hat{e}_{\mathbf{k}'\lambda'})_i\, \delta_{\mathbf{k}\mathbf{k}'} \delta_{\lambda\lambda'} \Big[\mu_{Bi}^{eg}\, e^{i\mathbf{k}\cdot\mathbf{r}_B} + \mu_{Ai}^{eg}\, e^{i\mathbf{k}\cdot\mathbf{r}_A} \Big] \\
&= -i \sum_{\mathbf{k}\lambda} \left(\frac{\hbar\omega_{\mathbf{k}}}{4\epsilon_0 V} \right)^{1/2} (\hat{e}_{\mathbf{k}\lambda})_i \Big[\mu_{Bi}^{eg}\, e^{i\mathbf{k}\cdot\mathbf{r}_B} + \mu_{Ai}^{eg}\, e^{i\mathbf{k}\cdot\mathbf{r}_A} \Big],
\end{aligned} \tag{1.72}$$

where the Einstein notation for repeated indices has been used. Similarly

$$\langle I_1|\, H_i\, |\psi\rangle = i \sum_{\mathbf{k}\lambda} \left(\frac{\hbar\omega_{\mathbf{k}}}{4\epsilon_0 V}\right)^{1/2} (\hat{e}^*_{\mathbf{k}\lambda})_j \Big[\mu^{ge}_{Bj}\; e^{-i\mathbf{k}\cdot\mathbf{r}_B} + \mu^{ge}_{Aj}\; e^{-i\mathbf{k}\cdot\mathbf{r}_A}\Big]. \tag{1.73}$$

Therefore, taking into account only the distance-dependent contribution to ΔE,

$$\frac{\langle\psi|\, H_i\, |I_1\rangle\, \langle I_1|\, H_i\, |\psi\rangle}{E_\psi - E_{I_1}} = \sum_{\mathbf{k}\lambda} \left(\frac{\hbar\omega_{\mathbf{k}}}{4\epsilon_0 V}\right) \mu^{eg}_{Ai}\; \mu^{ge}_{Bj}\; (\hat{e}_{\mathbf{k}\lambda})_i\; (\hat{e}^*_{\mathbf{k}\lambda})_j \left[e^{i\mathbf{k}\cdot\mathbf{r}} + e^{-i\mathbf{k}\cdot\mathbf{r}}\right] \left(\frac{1}{\hbar\omega_0 - \hbar\omega}\right), \tag{1.74}$$

where $\boldsymbol{r} = \boldsymbol{r}_B - \boldsymbol{r}_A$ is the interatomic distance and $\omega_0 = ck_0$ is the atomic transition frequency. In a similar way, we calculate the contribution related to the intermediate states $|I_2\rangle$, and obtain the total energy shift as

$$\begin{aligned}
\Delta E &= \sum_{\mathbf{k}\lambda} \left(\frac{\hbar\omega_{\mathbf{k}}}{4\epsilon_0 V}\right) \mu^{eg}_{Ai}\; \mu^{ge}_{Bj}\; (\hat{e}_{\mathbf{k}\lambda})_i\; (\hat{e}^*_{\mathbf{k}\lambda})_j \left[\frac{e^{i\mathbf{k}\cdot\mathbf{r}} + e^{-i\mathbf{k}\cdot\mathbf{r}}}{\hbar\omega_0 - \hbar\omega} - \frac{e^{i\mathbf{k}\cdot\mathbf{r}} + e^{-i\mathbf{k}\cdot\mathbf{r}}}{\hbar\omega_0 + \hbar\omega}\right] \\
&= \sum_{\mathbf{k}} \left(\frac{1}{2\epsilon_0 V}\right) \mu^{eg}_{Ai}\; \mu^{ge}_{Bj}\; (\delta_{ij} - \hat{k}_i\hat{k}_j) \frac{k^2}{k_0^2 - k^2} \left[e^{i\mathbf{k}\cdot\mathbf{r}} + e^{-i\mathbf{k}\cdot\mathbf{r}}\right] \\
&= \frac{\mu^{eg}_{Ai}\; \mu^{ge}_{Bj}}{16\pi^3\epsilon_0} \int_0^\infty dk \int d\Omega\; \frac{k^4}{k_0^2 - k^2} (\delta_{ij} - \hat{k}_i\hat{k}_j) \left[e^{i\mathbf{k}\cdot\mathbf{r}} + e^{-i\mathbf{k}\cdot\mathbf{r}}\right],
\end{aligned} \tag{1.75}$$

where, in the second and third row, we have performed the sum over polarization (1.22) and taken the continuum limit $V \longrightarrow +\infty$. Exploiting the relation

$$\tau_{ij} = \frac{1}{4\pi} \int d\Omega\; (\delta_{ij} - \hat{k}_i\hat{k}_j) e^{\pm i\mathbf{k}\cdot\mathbf{r}} = \left[(\delta_{ij} - \hat{r}_i\hat{r}_j)\frac{\sin kr}{kr} + (\delta_{ij} - 3\hat{r}_i\hat{r}_j)\left(\frac{\cos kr}{k^2r^2} - \frac{\sin kr}{k^3r^3}\right)\right], \tag{1.76}$$

the energy shift becomes

$$\Delta E = \frac{\mu^{eg}_{Ai}\; \mu^{ge}_{Bj}}{2\pi^2\epsilon_0} \int_0^\infty dk \frac{k^4}{k_0^2 - k^2}\; \tau_{ij}(kr), \tag{1.77}$$

where $\tau_{ij}(kr)$ is the expression in the square brackets in Eq. (1.76). To perform the divergent integral in (1.77), we introduce a convergence factor $e^{-\gamma|k|}$, and then we take the limit $\gamma \to 0^+$. In this way the integral converges and, using the residue theorem, the resonance energy shift becomes

$$\Delta E = \mu^{eg}_{Ai}\; \mu^{ge}_{Bj}\; V_{ij}(k_0, \mathbf{r}), \tag{1.78}$$

where

$$V_{ij}(k_0, \mathbf{r}) = \frac{1}{4\pi\epsilon_0 r^3}\left[(\delta_{ij} - 3\hat{r}_i\hat{r}_j)(\cos k_0 r + k_0 r \sin k_0 r) - (\delta_{ij} - \hat{r}_i\hat{r}_j)k_0^2 r^2 \cos k_0 r\right], \tag{1.79}$$

is the retarded interaction potential. Eq. (1.78) represent the resonance interaction energy between two entangled atoms when they are in the free space with the radiation field in the vacuum state.

When the atoms are in the near zone, i.e. when the interatomic distance is much smaller than the atomic transition wavelength ($k_0 r \ll 1$), the resonance interaction behaves as r^{-3}; essentially, in this range, the interaction can be seen as an electrostatic interaction between two electric atomic dipoles. On the other hand, in the far zone limit ($k_0 r \gg 1$), the interaction is mainly a radiative process owing to the exchange of a real photon between atoms; in this range the resonance interaction behaves as r^{-1}, thus having a very long range behaviour, and it is spatially oscillating. It is important to point out that, because there is a contribution of a real photon and it is a second-order effect in the atom-field coupling, the resonance interaction is several orders of magnitude larger than dispersion interactions between two atoms, which is fourth-order interaction in the atom-field coupling. In fact, a numerical estimate of the resonance force between two correlated hydrogen atoms in the free space (taking into account contribution involving only the $n = 2$ states of the hydrogen atoms), placed at a distance of $r \simeq 1\mu$m, leads to a force of $F_R \sim 3 \cdot 10^{-19}$ N, whereas the van der Waals force is about $F_{vdW} \sim 8 \cdot 10^{-39}$ N.

Although the resonance force is much larger than van der Waals interaction between ground-state atoms and comparable to atom-surface Casimir-Polder force, it has not been yet experimentally detected directly. The main experimental difficulty is that the system must be prepared and maintained in a correlated state for a sufficiently long time, in order to measure the resonance interaction force between the atoms. But the entangled state is a very fragile state since, owing to the spontaneous emission of excited atoms or perturbations due to any interaction with the environment, can decay in a factorized state, destroying its correlation. When the system is in a factorized state, the resonance force becomes a fourth-order interaction in the atom-field coupling, essentially a van der Waals interaction between two atoms, one excited and the other in its ground state, much weaker than the resonance interaction and widely investigated in the literature [15, 47–49].

1.5 Resonance energy transfer between two atoms in the free space

From the point of view of molecular quantum electrodynamics, one of the simplest intermolecular interaction, at least conceptually, is the resonant exchange of energy between two quantum emitters, which may be atoms, molecules, chromophores and others [9, 11, 50–52]. This process corresponds to the resonant transfer of excitation, typically electronic, from a species D, which is initially excited and called "donor", to a species A, which is in the ground state, called "acceptor"; owing to the exchange of energy, the donor D decays to the ground state and the acceptor A becomes excited, as shown in Fig. 1.11, in which a HOMO-LUMO (Highest Occupied Molecular Orbital and Lowest Unoccupied Molecular Orbital) scheme has been used to depict this process.

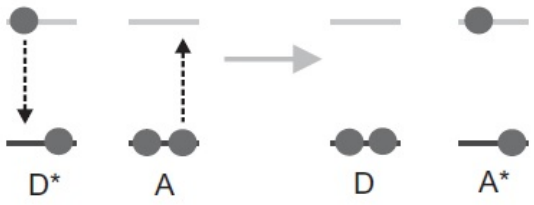

Figure 1.11: Excitation energy transfer between a donor molecule D and an acceptor molecule A. A HOMO-LUMO scheme has been used for both molecules. D is initially in its excited state, in which one electron has been promoted from the HOMO to the LUMO. In the final state, D is in its ground state and A is excited [53].

The resonance energy transfer (RET) between any two quantum emitters, mediated by the quantum electromagnetic field, can be represented by the following non-chemical equation

$$D^* + A \longrightarrow D + A^*,$$

where the asterisk denotes the localization of excitation energy. Due to its fundamental nature, the resonance energy transfer has great relevance in many areas of physics, as well as in chemistry and biology, where coherent energy transfer between chromophores is supposed to be related to the very high efficiency in light-harvesting observed in the photosynthesis process [50–52, 54].

The actual type of energy transfer process between two or more molecules is mainly determined by two time scales [53]: the intramolecular vibrational relaxation time τ_r, and the transfer time τ_t. The intramolecular relaxation time is the time needed to the nuclear vibrations of each molecule to return to thermal

equilibrium after that the electronic transition takes place. On the other hand, the transfer time is the time that the energy needs to move from one molecule to another, neglecting any additional perturbations. It is defined as the inverse of the characteristic interaction energy between two molecules. Depending on the relation between these two time scales, different regimes of the RET can be considered, as shown in Fig. 1.12, where the regimes have been drawn versus the intramolecular and intermolecular interaction strengths.

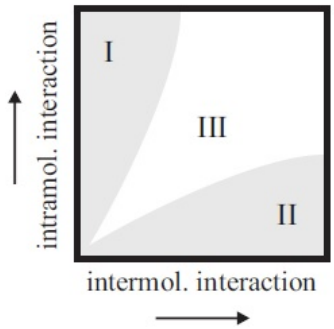

Figure 1.12: Schematic representation of different RET regimes. The strength of intermolecular and intramolecular interactions increase, respectively, along the horizontal axis and the vertical axis. Förster incoherent transfer, for which $\tau_r \ll \tau_t$, is typical for region I whereas coherent transfer, $\tau_r \gg \tau_t$, is given in the region II. The white region III is an intermediate region for which $\tau_r \sim \tau_t$ [53].

If $\tau_r \gg \tau_t$, the excitation energy can move almost freely from molecule to molecule and can be considered as delocalized between them. The exciton travels coherently through the molecules aggregate as a quantum mechanical wave packet. In this case, the intermolecular interactions are much larger with respect to the intramolecular interactions, and can not be treated as a perturbation of the system; this is the so-called strong-coupling regime, indicated by the grey-region II in Fig. 1.12. On the other hand, if $\tau_r \ll \tau_t$, the intermolecular interactions are small with respect to the intramolecular interactions and therefore the RET can be treated perturbatively [55]. In this case, owing to the strong intramolecular interactions, it is impossible to construct a wave function involving different molecules and thus the transfer of energy is incoherent, just characterized by the probability $P_m(t)$ for the excitation energy to be on the molecule m at time t. This is the weak-coupling regime, indicated by the grey-region I in Fig. 1.12. Clearly, there are regions between the coherent and the incoherent RET type, for which $\tau_r \sim \tau_t$. In this case the motion of energy between molecules is called partially coherent, and is represented by the white-region III in Fig. 1.12.
We now consider in detail the resonance exchange of energy between two quantum emitters in the case for which the intermolecular interactions are much smaller with respect to the intramolecular interactions, so that the resonance energy transfer can be treated as a perturbation of the system. In this case, the energy transfer rate between two molecules A and B, can be obtained using the Förster theory. Within the dipole-dipole approximation, so assuming that the molecular dimensions are much smaller than the intermolecular separations, the energy transfer

rate is given by the Förster equation [53]

$$K_{RET} = \frac{1}{\tau_A}\left(\frac{R_F}{r}\right)^6, \tag{1.80}$$

where τ_A is the mean lifetime for the donor atom A and R_F is the Förster radius, defined as the distance for which the transfer rate is equal to the radiative decay rate of the donor. The Förster equation shows that the energy transfer rate between two molecules behaves as r^{-6} in the weak coupling regime, where r is the intermolecular distance. It is important to underline that this equation remains valid for intermolecular separations large enough to avoid any superposition of electronic molecular orbitals (allowing to neglect exchange interactions) and much smaller than the relevant molecular transition wavelength, which means $r \ll \lambda_0$. The second hypothesis, $r \ll \lambda_0$, means that the energy transfer rate in the Förster equation (1.80) is due only to the Coulomb electrostatic interaction between molecules; in this short-range limit the transfer rate does not involve the exchange of a real photon, so there is not a radiative contribution to the interaction between the molecules, neglecting retardation effects [55]. For an intermolecular distance equal or larger than the molecular transition wavelength, the equation (1.80) is no longer valid because radiative contributions, arising from the exchange of a real photon, become relevant. A full quantum electrodynamic approach allows to investigate the resonance energy transfer process for all intermolecular distance, taking into account both radiative and radiationless contributions [56–59].

We will now outline the well-known quantum calculation for the resonance energy transfer rate for the simple system of two atoms in the vacuum space, and in the weak coupling regime [59, 60]. We consider the resonance energy transfer between two identical two-level atoms, labelled A and B, where the donor atom A is initially excited and the acceptor atom B is in the ground state, and the radiation field is in its vacuum state. The atom A can decay and emit a real or virtual photon, which can be absorbed by atom B. Excitation is thus transferred from donor to acceptor through the electromagnetic field [56–58, 61]. The Hamiltonian of the system is

$$H = H_0 + H_i, \tag{1.81}$$

where

$$H_0 = H_A + H_B + H_F, \tag{1.82}$$

is the unperturbed Hamiltonian, sum of the atomic Hamiltonians (H_A and H_B) and the radiation free-field Hamiltonian (H_F). H_i is the interaction Hamiltonian that, in the multipolar coupling scheme and within the dipole approximation, can be written as

$$H_i = -\boldsymbol{\mu}_A \cdot \mathbf{E}(\mathbf{r}_A) - \boldsymbol{\mu}_B \cdot \mathbf{E}(\mathbf{r}_B). \tag{1.83}$$

where $\boldsymbol{\mu}_\alpha$ is the electric dipole moment operator of atom α placed at $\mathbf{r}_\alpha$, with $\alpha = A, B$. Exploiting the second-order time-dependent perturbation theory, according to the generalized Fermi golden rule [50, 62], the energy transfer rate between two atoms in the vacuum space can be written as

$$W_{i\to f} = \frac{2\pi}{\hbar} |\langle\psi_i| T |\psi_f\rangle|^2 \delta(E_f - E_i), \tag{1.84}$$

where $|\psi_i\rangle = |e_A, g_B, 0\rangle$ and $|\psi_f\rangle = |g_A, e_B, 0\rangle$ are respectively the initial and the final state of the system, with energy E_i and E_f. $|\ g_{A(B)}\rangle$ and $|\ e_{A(B)}\rangle$ are respectively the ground and excited atomic states, and $|\ 0\rangle$ represents the photon vacuum state. For simplicity we consider identical atoms, with transition frequency $\omega_0 = ck_0$, placed at a distance $\boldsymbol{r} = \boldsymbol{r}_A - \boldsymbol{r}_B$ from each other. T is the second-order transition operator,

$$T = H_i + H_i \frac{1}{E_i - H_0 \pm i\eta} H_i, \qquad \eta \longrightarrow 0 \tag{1.85}$$

where H_0 and H_i are the unperturbed and interaction Hamiltonians, respectively, and $E_i = E_f$ is the energy of the initial and final states. The second-order contribution of the transition operator T leads to a resonance exchange of energy between the atoms, changing both atomic quantum states without alteration of the state of the radiation field. For this reason, the resonance energy transfer amplitude is given by

$$M = \langle\psi_i| T |\psi_f\rangle = \sum_I \frac{\langle\psi_i| H_i |I\rangle \langle I| H_i |\psi_f\rangle}{E_i - E_I \pm i\eta}, \qquad \eta \longrightarrow 0 \tag{1.86}$$

where $|I\rangle$ are the intermediate states, with energy E_I, that can contribute to the energy transfer process. These states are $|e_A, g_B, 1_{\boldsymbol{k}\lambda}\rangle$ and $|g_A, e_B, 1_{\boldsymbol{k}\lambda}\rangle$, and are the same found in the resonance interaction energy in Sec. (1.4), represented by Feynman diagrams in Fig. 1.10. Therefore, with similar calculations to those done for the resonance interaction in Sec. (1.4), we can easily calculate the resonance energy transfer amplitude as

$$M = \sum_{\mathbf{k}\lambda} \left(\frac{\hbar\omega_{\mathbf{k}}}{2\epsilon_0 V}\right) \mu_{Ai}^{eg}\, \mu_{Bj}^{ge} (\hat{e}_{\mathbf{k}\lambda})_i (\hat{e}^*_{\mathbf{k}\lambda})_j \left[\frac{e^{i\mathbf{k}\cdot\mathbf{r}}}{\hbar\omega_0 - \hbar\omega \pm i\eta} - \frac{e^{-i\mathbf{k}\cdot\mathbf{r}}}{\hbar\omega_0 + \hbar\omega \pm i\eta}\right] \tag{1.87}$$

$$= \left(\frac{1}{16\pi^3\epsilon_0}\right) \mu_{Ai}^{eg}\, \mu_{Bj}^{ge} \int_0^\infty k(\delta_{ij} - \hat{k}_i\hat{k}_j) \left[\frac{e^{i\mathbf{k}\cdot\mathbf{r}}}{k_0 - k \pm i\eta} - \frac{e^{-i\mathbf{k}\cdot\mathbf{r}}}{k_0 + k \pm i\eta}\right] d^3k, \tag{1.88}$$

and using the relation

$$\frac{1}{4\pi} \int d\Omega (\delta_{ij} - \hat{k}_i\hat{k}_j) e^{\pm i\mathbf{k}\cdot\mathbf{r}} = \frac{1}{k^3}(-\nabla^2\delta_{ij} + \nabla_i\nabla_j)\frac{\sin kr}{r}, \tag{1.89}$$

we get

$$M = \left(\frac{1}{4\pi^2\epsilon_0}\right)\mu_{Ai}^{eg}\,\mu_{Bj}^{ge}(-\nabla^2\delta_{ij}+\nabla_i\nabla_j)\int_0^\infty\left[\frac{1}{k_0-k\pm i\eta}-\frac{1}{k_0+k\pm i\eta}\right]\frac{\sin kr}{r}dk, \tag{1.90}$$

where the Einstein convention for repeated indices has been used. We point out that the sum over polarizations relation (see Eq. (1.22)) and the limit to continuous has been applied to obtain the equation (1.90). Performing the wavevector integral through residue theorem, the energy transfer amplitude can be written as

$$M = \mu_{Ai}^{eg}\,\mu_{Bj}^{ge}\,V_{ij}^{\pm}(k_0,\boldsymbol{r}), \tag{1.91}$$

where $V_{ij}^{\pm}(k_0,\boldsymbol{r})$ is the complex retarded resonant dipole-dipole coupling tensor defined by

$$\begin{aligned} V_{ij}^{\pm}(k_0,\boldsymbol{r}) &= -\frac{1}{4\pi\epsilon_0}(-\nabla^2\delta_{ij}+\nabla_i\nabla_j)\frac{e^{\pm i\mathbf{k}_0\cdot\mathbf{r}}}{r} \\ &= \frac{1}{4\pi\epsilon_0 r^3}\left[(\delta_{ij}-3\hat{r}_i\hat{r}_j)(1\pm ik_0r)-(\delta_{ij}-\hat{r}_i\hat{r}_j)k_0^2r^2\right]e^{\mp i\mathbf{k}_0\cdot\mathbf{r}}, \end{aligned} \tag{1.92}$$

where the second row is being obtained after application of the differential operators [59]. Both choices of signs appearing in the coupling tensor (1.92) are permitted, since M is just the probability amplitude for the RET and has no effect on the transfer rate. In fact, the energy transfer rate K_{RET} between the pair molecules $A-B$ is obtained by taking the modulus square of the matrix element (1.91), and using the Fermi golden rule (1.84), leading to

$$K_{RET} = \frac{2\pi\rho_f}{\hbar}\mu_{Ai}^{eg}\,\mu_{Bj}^{ge}\,\mu_{Ai'}^{eg}\,\mu_{Bj'}^{ge}\,V_{ij}^{\pm}(k,\boldsymbol{r})\,(V_{i'j'}^{\pm}(k,\boldsymbol{r}))^*, \tag{1.93}$$

where ρ_f is the density of the final states of the acceptor. This result holds for any orientations of the electric dipole moments. Thus, considering random orientations of the atomic dipole moments, Eq. (1.93) yields a monotonic distance dependence of the energy transfer rate [63], proportional to

$$\mid M^{(\pm)}\mid^2 = \frac{2\mid\boldsymbol{\mu}_A\mid^2\mid\boldsymbol{\mu}_B\mid^2}{9(4\pi\epsilon_0 r^3)^2}\left(3+k_0^2r^2+k_0^4r^4\right). \tag{1.94}$$

This result is valid for all interatomic distances r beyond wavefunction overlap, and has a complicated distance dependence, in contrast to the semi-classical Förster theory that predicts only a r^{-6} dependence. Indeed, Eq. (1.94) obtained with the QED formalism, underscores the unification of the radiationless and radiative energy transfer mechanisms, containing three different distance dependencies:

r^{-2}, r^{-4} and r^{-6}, related to three distinct regimes, that is the long-, intermediate- and short-range, respectively [59]. In the near zone, when $k_0 r \ll 1$, that is for interatomic distance much smaller than the atomic transition wavelength, the first term of Eq.(1.94) is dominant, leading to

$$\mid M^{(\pm)} \mid^2_{nz} = \frac{\mid \boldsymbol{\mu}_A \mid^2 \mid \boldsymbol{\mu}_B \mid^2}{24\pi^2 \epsilon_0^2 r^6}, \tag{1.95}$$

yielding the familiar r^{-6} Förster-type dependence. As expected, in the short-range limit, we find that the resonance energy transfer rate can be viewed as the radiationless exchange of excitation between the atoms, arising from an electrostatic dipolar coupling in which the interaction between the pair is instantaneous [9]. On the other hand, when $k_0 r \gg 1$, corresponding to the far zone limit, the main contribution is given by the last term of Eq. (1.94), yielding

$$\mid M^{(\pm)} \mid^2_{fz} = \frac{\mid \boldsymbol{\mu}_A \mid^2 \mid \boldsymbol{\mu}_B \mid^2 k_0^2}{72\pi^2 \epsilon_0^2 r^2}, \tag{1.96}$$

which exhibits an r^{-2} scaling with the distance. In the long-range limit the transfer of energy is a radiative process, where the dominant contribution is due to the exchange of a real photon between the two atoms. Therefore the exchange of energy between the pair in this range can be viewed as a result of two separate events: a spontaneous emission by the donor (excited) atom A, followed by the absorption of the real photon by the (ground-state) acceptor atom B. We also stress that the virtual photon contributions to the transfer of energy is still present but clearly play a minor role compared to the real photon contribution.

1.6 Effects of external environments on radiation-mediated processes

Since the pioneering work of Purcell, it is known that radiative processes of any quantum emitter(s), for example the spontaneous emission of one or more atoms, are affected by the environment [64]. The presence of matter, such as atoms or molecules, and dynamical or static external environments, such as macroscopic objects like fixed or moving metallic/dielectric plates as well as cavities, waveguides or photonic crystals (shown in Fig. 1.13), significantly modify radiation-mediated processes. In fact, the density of states and the dispersion relation of the radiation field is deeply changed by the external environments, and this involves changes of the radiation-mediated processes between quantum emitters.
Dispersion and resonance interactions, as well as the resonance energy transfer process, can thus be modified and controlled through external environments [25, 65–

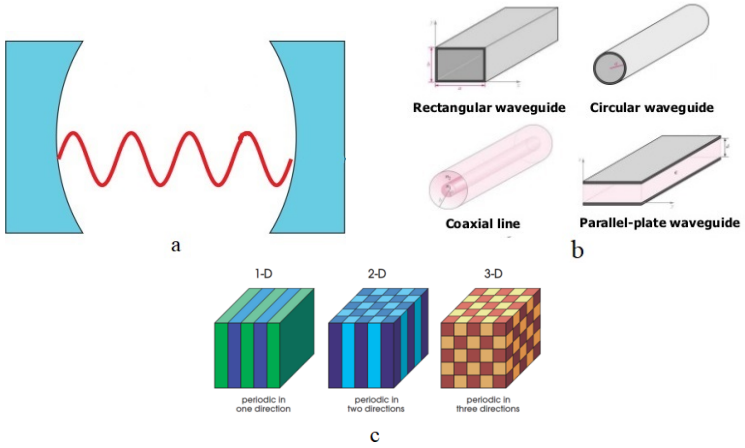

Figure 1.13: Some examples of static structured environments: a) A cavity; b) waveguides with different geometries; c) one- two and three-dimensional photonic crystals.

69], as well as from the presence of neighbouring atoms [70–72], or due to a uniformly accelerated motion of the atoms [73, 74]. These effects have attracted great attention in many different areas of science, ranging from fundamental and atomic-molecular physics to chemistry, biology and engineering, because it offers the possibility of controlling dispersion and resonance interactions and the exchange of energy between quantum emitters, with regard to potential applications.

Being dominant at nanoscale separations, dispersion forces have a significant role in the interaction with nanostructured materials [75], biological processes [76, 77] and in applications in micro- and nano-technologies, for example micro-electromechanical devices [78, 79].

On the other hand, the control of one of the most basic processes in nature, such as the exchange of energy between atoms, molecules or even nanostructures is one of the major challenges of quantum electrodynamics and quantum chemistry. It plays an important role in the photodynamics of multichromophoric assemblies, and it mediates the storage and migration of energy in photosynthetic systems [80, 81]. In recent years, many investigations have been concerned with artificial light harvesting antenna devices [82–88] and nanoemitters, especially spasers [89]. Moreover, the resonance energy transfer process between quantum dots has become important in bio-inspired applications [90, 91], such as nanosensors [92–97] and photodynamic therapy [98, 99].

Through external environments, it is possible to enhance or inhibit a radiative process and even change its qualitative behaviour (for example the distance-dependence) with respect to the free space case. Moreover, regarding dispersion and resonance interaction between quantum emitters, even the attractive or re-

pulsive character of the force can be controlled through external actions, as we will discuss in detail later on. Furthermore, in recent years, many investigations have concerned with radiative processes in a time-dependent environment under non-equilibrium conditions: new remarkable and interesting effects arise when the boundary conditions on the radiation field, or some relevant parameters of the system, change adiabatically or non-adiabatically in time. [100–102]. This also yields further and new possibilities for controlling radiation-mediated interactions between atoms, as well as the energy transfer process with respect to the static case [103, 104]. Dynamical situations can be obtained if the overall system is in a non-equilibrium condition, for example when the atoms or molecules are in excited states or are coupled to thermal baths at different temperatures [105, 106]. Non-equilibrium conditions can be also obtained when the boundary conditions on the electromagnetic field, or other important parameters of the system, are time-dependent [101, 107–109]. Examples are quantum emitters are placed inside a dynamical external environment for which its geometry and/or configuration is time-dependent, such as a cavity with a moving wall or a time-modulated photonic crystal. Here below are some recent works where the effect of statical and dynamical external environments on the resonance and the dispersion interactions, and the resonance energy transfer process, has been investigated. The effect of a structured environment, in particular a photonic crystal, on the resonance force between two entangled atoms has been investigated [110–114], showing the possibility to enhance or suppress the interaction, and even changing its distance dependence. In [115], the resonance interaction between two entangled atoms placed inside a photonic crystal has been studied. The dispersion relation for the electromagnetic field inside a 3-D isotropic photonic crystal is given by

$$\omega_k = \frac{c}{4na} \arccos\left[\frac{4n\cos(kL) + (1-n)^2}{(1+n)^2}\right], \tag{1.97}$$

and showed in Fig. 1.14, where L is the lattice constant and $2a$ is the thickness of the dielectric layers of refractive index n, assumed real and frequency-independent, with vacuum space between them. The atoms, one excited and the other in its

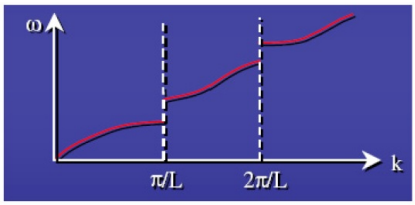

Figure 1.14: Dispersion relation for the electromagnetic field inside a 3-D isotropic photonic crystal, for which the frequency gap are placed at $k = \frac{m\pi}{L}$, with $m \in \mathbb{Z}$.

ground state, are prepared in a symmetric entangled state and the atomic transition frequency is assumed to be near the edge of the photonic band-gap and outside of it. In this case the resonance force can be enhanced of about three orders of magnitude with respect that one in the free space,

$$| \frac{F_{PC}}{F_{vac}} | \simeq 10^3, \tag{1.98}$$

whereas the spatial-dependence remains unchanged. On the other hand, if the atomic transition frequency is inside the photonic band-gap, the resonance interaction not only is suppressed with respect to the free space one, but also its spatial behaviour is modified; when the atoms are in the far zone regime, it scales as r^{-2} rather than r^{-1}, where r is the interatomic distance.

In [116], the dispersion interaction between two atoms inside a perfectly conducting rectangular waveguide has been investigated. The waveguide, showed in Fig. 1.15, determines a lower cut-off frequency $\omega_c \sim \frac{c\pi}{a}$, where a is the height of the rectangular waveguide. Assuming that the atomic transition frequency is be-

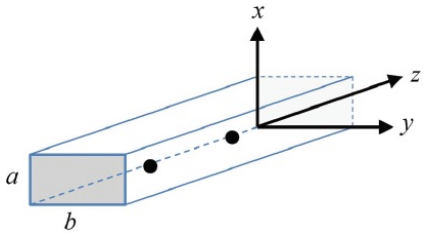

Figure 1.15: Two atoms inside a perfectly conducting rectangular waveguide [116].

low the waveguide's lower cut-off frequency, the dispersion interaction between the atoms decay exponentially with the interatomic distance r, if r is much larger than the atomic transition wavelength (far-zone regime, $r \gg \lambda$); on the other hand, in the near zone range $r \ll \lambda$, the interaction is the same as that in the free space.

In [117] the intermolecular energy transfer in the presence of multislab planar structures and microspheres is studied. In particular when the two molecules are near a planar interface, the enhancement (inhibition) of energy transfer is accompanied by inhibition (enhancement) of donor decay; moreover, a change of the typical spatial-dependence in the free space is obtained.

Regarding radiation-mediated processes in time-dependent environments, the dynamical Casimir-Polder interaction between an atom and a reflecting plate, after a non-adiabatic change of some physical parameter of the system, have been investigated [49, 118–121], as well as the time-dependent Casimir-Polder interactions between two or more atoms, during their self-dressing process [70, 122]. In [121], for example, the dynamical Casimir-Polder force between an excited atom

and a perfectly conducting plate, is investigated. The non-equilibrium configuration of the system shows new relevant features compared to the equilibrium case of a ground-state atom, due to the presence of an atom-field resonance. In fact, the time-dependent Casimir-Polder interaction exhibits oscillations in time and space, changing from attractive to repulsive, contrarily to the static case, where the force is always attractive. Moreover, around and after the round-trip time $t = \frac{2d}{c}$ (d being the atom-wall separation), the dynamical force is much stronger (some orders of magnitude) than that obtained for a ground-state atom.

The interest of studying systems under non-equilibrium conditions is both theoretical and experimental. In many realistic physical situations, systems are in a non-equilibrium condition, for example the temperatures of the interacting objects can be different from the environment's temperature or from each other, or the objects involved can be in relative motion. On the other hand, it is also a fundamental issue to investigate whether and how non-equilibrium initial conditions can influence the dynamics of a given system, or modify radiation-mediated (resonance or dispersion) interactions between atoms/molecules during their dynamic evolution. Another relevant conceptual issue is investigating how the new equilibrium condition is approached by the system.

The possibility to manipulate and control radiation-mediated interactions and the resonance energy transfer through external environments is the fundamental goal of this PhD thesis. In the next chapters we will investigate the resonance and dispersion interaction, as well as the resonance energy transfer process, both in a static and dynamical situation, pointing out the possibility to activate or inhibit such processes as well as to control their strength, their space-dependence, and even the qualitative character of quantum forces.

Chapter 2

Macroscopic quantum electrodynamics

In this Chapter, the theory of macroscopic quantum electrodynamic is outlined, which represents one of the basic theory for the analysis of radiation-mediated processes in external environments considered in the thesis. This technique will be the basis for part of the original work of this thesis, that will be presented in the following chapters. Starting from classical electrodynamics in free-space and in the presence of magneto-dielectric media, we discuss the main steps to construct a consistent theory of the quantised electromagnetic field in the presence of generic dispersive and dissipative media, in terms of the electromagnetic Green's tensor. This theory will allow to investigate radiation-mediated interactions and resonance energy transfer process between quantum emitters, that are the main topics of this thesis, in the presence of an arbitrary linear magneto-dielectric medium, studying whether and how they can be modified and manipulated through external environments. The advantage of this formalism is that it contains no assumptions about the state of the medium or the field, beyond the fact that the macroscopic Maxwell equations are valid.

This Chapter is organized as follows: in Section 2.1 we first review the basic concepts of macroscopic classical electrodynamics, starting with the simplest case of radiation field in the free space, and going on with the more general case in which a magneto-dielectric medium is present. In Section 2.2 the quantization of the electromagnetic field in the presence of generic macroscopic dispersive and dissipative bodies, based on the Green's tensor, is outlined.

2.1 Classical electrodynamics in material media

Classical electrodynamics is described by the well-known classical Maxwell equations for the electromagnetic field which, in the absence of charges and currents, are

$$\begin{aligned} \nabla \cdot \mathbf{E} &= 0, \\ \nabla \cdot \mathbf{B} &= 0, \\ \nabla \times \mathbf{E} &= -\frac{\partial \mathbf{B}}{\partial t}, \\ \nabla \times \mathbf{B} &= \frac{1}{c^2}\frac{\partial \mathbf{E}}{\partial t}, \end{aligned} \tag{2.1}$$

where $\mathbf{E}$ and $\mathbf{B}$ are the electric and magnetic field in the free space, functions of position and time [123]. They are related to the vector potential $\mathbf{A}$ and to the scalar potential ϕ according to the following relations

$$\begin{aligned} \mathbf{E} &= -\frac{\partial \mathbf{A}}{\partial t} - \nabla\phi, \\ \mathbf{B} &= \nabla \times \mathbf{A}, \end{aligned} \tag{2.2}$$

that, employing the Coulomb gauge imposed by the condition

$$\nabla \cdot \mathbf{A} = 0, \tag{2.3}$$

satisfy the Laplace equation

$$\nabla^2 \phi = 0, \tag{2.4}$$

and the Helmholtz equation

$$\nabla^2 \mathbf{A} - \frac{1}{c^2}\frac{\partial^2 \mathbf{A}}{\partial t^2} = 0. \tag{2.5}$$

The presence of magneto-dielectric media, usually given by one or more macroscopic bodies, significantly modify the electromagnetic field and therefore Maxwell equations (2.1). A generic medium can be viewed as an ensemble of a very large number of charged particles, mutually interacting. Since the number of particles is extremely large, a microscopic description of the system in term of particles interacting with the radiation field is practically impossible. Fortunately, in most cases, an effective, macroscopic description of the overall effect of these particles on the electromagnetic field can be done [15].

Les us now consider the situation in which just the bound charges contained in the magneto-dielectric medium are present, without any other free charges. The

Maxwell equations take the form

$$\begin{aligned} \nabla \cdot \mathbf{E} &= \frac{\rho_{in}}{\epsilon_0}, \\ \nabla \cdot \mathbf{B} &= 0, \\ \nabla \times \mathbf{E} &= -\frac{\partial \mathbf{B}}{\partial t}, \\ \nabla \times \mathbf{B} &= \frac{1}{c^2}\frac{\partial \mathbf{E}}{\partial t} + \mu_0 \boldsymbol{j}_{in}, \end{aligned} \tag{2.6}$$

where ρ_{in} and $\boldsymbol{j}_{in}$ are, respectively, the internal charge and current density associated to the bounded particles inside the medium, satisfying the continuity equation

$$\nabla \cdot \boldsymbol{j}_{in} + \frac{\partial \rho_{in}}{\partial t} = 0. \tag{2.7}$$

Defining the polarization $\boldsymbol{P}$ and the magnetization $\boldsymbol{M}$ of the medium according to

$$\nabla \cdot \boldsymbol{P} = -\rho_{in} \tag{2.8}$$

$$\boldsymbol{j}_{in} = \frac{\partial \boldsymbol{P}}{\partial t} + \nabla \times \boldsymbol{M}, \tag{2.9}$$

we can write down the Gauss and Ampere laws in their well-known form

$$\begin{aligned} \nabla \cdot \mathbf{D} &= 0, \\ \nabla \times \mathbf{H} &= \frac{\partial \mathbf{D}}{\partial t}, \end{aligned} \tag{2.10}$$

where the electric displacement field $\mathbf{D} = \epsilon_0 \boldsymbol{E} + \boldsymbol{P}$ and the magnetic excitation $\boldsymbol{H} = \boldsymbol{B}/\mu_0 - \boldsymbol{M}$ have been introduced. Assuming that the external radiation field can be regarded as a weak perturbation to the equilibrium position of the charged particles of the medium and thus its response to the external field is linear and causal, polarization and magnetization are given by the Langevin equations

$$\boldsymbol{P}(\boldsymbol{r}, t) = \epsilon_0 \int_{-\infty}^{+\infty} d\tau \int d^3 r' \boldsymbol{\chi}(\boldsymbol{r}, \boldsymbol{r}', t) \cdot \boldsymbol{E}(\boldsymbol{r}', t - \tau) + \boldsymbol{P}_N(\boldsymbol{r}, t), \tag{2.11}$$

$$\boldsymbol{M}(\boldsymbol{r}, t) = \frac{1}{\mu_0} \int_{-\infty}^{+\infty} d\tau \int d^3 r' \boldsymbol{\zeta}(\boldsymbol{r}, \boldsymbol{r}', t) \cdot \boldsymbol{B}(\boldsymbol{r}', t - \tau) + \boldsymbol{M}_N(\boldsymbol{r}, t), \tag{2.12}$$

which show a reactive and a random term. The first reactive terms of the medium response in (2.11) and (2.12), is linear to the external radiation field, where $\boldsymbol{\chi}$

and $\boldsymbol{\zeta}$ are the retarded electric and magnetic susceptibility tensor of the medium, respectively. In order to preserve the causality

$$\boldsymbol{\chi}(\boldsymbol{r},\boldsymbol{r}',t)=\mathbf{0}, \qquad \boldsymbol{\zeta}(\boldsymbol{r},\boldsymbol{r}',t)=\mathbf{0}, \quad \text{for } |\boldsymbol{r}-\boldsymbol{r}'|>ct. \tag{2.13}$$

The random parts are given by the noise polarization $\boldsymbol{P}_N(\boldsymbol{r},t)$ and noise magnetization $\boldsymbol{M}_N(\boldsymbol{r},t)$, which account for the fluctuations in the medium, related to the noise charge density and to the noise current density by the following relations

$$\nabla\cdot\boldsymbol{P}_N=-\rho_N \tag{2.14}$$

$$\boldsymbol{j}_N=\frac{\partial\boldsymbol{P}_N}{\partial t}+\nabla\times\boldsymbol{M}_N. \tag{2.15}$$

Assuming that the medium response is local and isotropic, which means that

$$\boldsymbol{\chi}(\boldsymbol{r},\boldsymbol{r}',t)=\chi(\boldsymbol{r},t-t')\delta(\boldsymbol{r}-\boldsymbol{r}')\boldsymbol{I}, \tag{2.16}$$

$$\boldsymbol{\zeta}(\boldsymbol{r},\boldsymbol{r}',t)=\zeta(\boldsymbol{r},t-t')\delta(\boldsymbol{r}-\boldsymbol{r}')\boldsymbol{I}, \tag{2.17}$$

the polarization and magnetization expressions become

$$\boldsymbol{P}(\boldsymbol{r},t)=\epsilon_0\int_{-\infty}^{+\infty}d\tau\;\chi(\boldsymbol{r},t)\boldsymbol{E}(\boldsymbol{r},t-\tau)+\boldsymbol{P}_N(\boldsymbol{r},t), \tag{2.18}$$

$$\boldsymbol{M}(\boldsymbol{r},t)=\frac{1}{\mu_0}\int_{-\infty}^{+\infty}d\tau\;\zeta(\boldsymbol{r},t)\boldsymbol{B}(\boldsymbol{r},t-\tau)+\boldsymbol{M}_N(\boldsymbol{r},t). \tag{2.19}$$

Working in the Fourier space, and introducing the Fourier transform of a generic function f as,

$$\hat{f}(\omega)=\frac{1}{2\pi}\int_{-\infty}^{+\infty}dt f(t)e^{i\omega t}, \tag{2.20}$$

and exploiting the convolution theorem, Eqs. (2.18) and (2.19) in the Fourier space can be written in the simpler form

$$\hat{\boldsymbol{P}}(\boldsymbol{r},\omega)=\epsilon_0\;\chi(\boldsymbol{r},\omega)\hat{\boldsymbol{E}}(\boldsymbol{r},\omega)+\hat{\boldsymbol{P}}_N(\boldsymbol{r},\omega), \tag{2.21}$$

$$\hat{\boldsymbol{M}}(\boldsymbol{r},\omega)=\frac{\zeta(\boldsymbol{r},\omega)}{\mu_0}\hat{\boldsymbol{B}}(\boldsymbol{r},\omega)+\hat{\boldsymbol{M}}_N(\boldsymbol{r},\omega), \tag{2.22}$$

where

$$\chi(\boldsymbol{r},\omega)=\int_{-\infty}^{+\infty}d\tau\chi(\boldsymbol{r},\tau)e^{i\omega\tau}, \tag{2.23}$$

$$\zeta(\boldsymbol{r},\omega)=\int_{-\infty}^{+\infty}d\tau\zeta(\boldsymbol{r},\tau)e^{i\omega\tau}. \tag{2.24}$$

According to the classical statistical fluctuation-dissipation theorem, the fluctuation spectrum of the noise fields is related to the imaginary part of the response function, and in our case we have

$$\langle \Delta \boldsymbol{P}_N(\boldsymbol{r},\omega)\Delta \boldsymbol{P}_N^*(\boldsymbol{r}',\omega')\rangle_{cl} = \frac{k_B T}{\pi\omega}\epsilon_0 \,\mathrm{Im}\chi(\boldsymbol{r},\omega)\;\delta(\boldsymbol{r}-\boldsymbol{r}')\delta(\omega-\omega'), \tag{2.25}$$

$$\langle \Delta \boldsymbol{M}_N(\boldsymbol{r},\omega)\Delta \boldsymbol{M}_N^*(\boldsymbol{r}',\omega')\rangle_{cl} = \frac{k_B T}{\pi\omega}\;\frac{\mathrm{Im}\zeta(\boldsymbol{r},\omega)}{\mu_0}\;\delta(\boldsymbol{r}-\boldsymbol{r}')\delta(\omega-\omega'). \tag{2.26}$$

These equations reveal the strict connection between fluctuations and absorption, owing to the imaginary part of the response function: fluctuations are inevitably present in any absorbing system at non-zero temperature.
Introducing the electric permittivity and the magnetic permeability of the medium as

$$\epsilon(\boldsymbol{r},\omega) = 1+\chi(\boldsymbol{r},\omega) \tag{2.27}$$

$$\mu(\boldsymbol{r},\omega) = \frac{1}{1-\zeta(\boldsymbol{r},\omega)}, \tag{2.28}$$

the Maxwell equations, in Fourier space, can be written as

$$\begin{aligned} \nabla\cdot\hat{\mathbf{D}} &= 0 \\ \nabla\cdot\hat{\mathbf{B}} &= 0, \\ \nabla\times\hat{\mathbf{E}} &= i\omega\hat{\mathbf{B}}, \\ \nabla\times\hat{\mathbf{H}} &= -i\omega\hat{\mathbf{D}}, \end{aligned} \tag{2.29}$$

where

$$\hat{\mathbf{D}} = \epsilon_0\epsilon\hat{\boldsymbol{E}} + \hat{\boldsymbol{P}}_N, \qquad \hat{\boldsymbol{H}} = \frac{\hat{\boldsymbol{B}}}{\mu_0\mu} - \hat{\boldsymbol{M}}_N. \tag{2.30}$$

In order to construct a solution for the Maxwell equations, despite to the free-space case where a wave equation for the vector potential $\mathbf{A}$ is obtained, it is here more convenient to formulate a dynamical equation for the electric field $\mathbf{E}$. We find that the electric field satisfies an inhomogeneous Helmholtz equation

$$\left[\nabla\times\frac{1}{\mu}\nabla\times - \frac{\omega^2}{c^2}\epsilon\right]\hat{\mathbf{E}}(\boldsymbol{r},\omega) = i\mu_0\omega\hat{\mathbf{j}}_N(\boldsymbol{r},\omega), \tag{2.31}$$

with the source term being given by the noise current density [15]. A formal solution of this equation can be written as

$$\hat{\mathbf{E}}(\boldsymbol{r},\omega) = i\omega\mu_0\int d^3r'\boldsymbol{G}(\boldsymbol{r},\boldsymbol{r}',\omega)\cdot\hat{\boldsymbol{j}}_N(\mathbf{r}',\omega), \tag{2.32}$$

where $\boldsymbol{G}(\boldsymbol{r},\boldsymbol{r}',\omega)$ is the electromagnetic Green's tensor [15, 124–126], solution of the Helmholtz equation

$$\left[\nabla\times\frac{1}{\mu}\nabla\times-\frac{\omega^2}{c^2}\epsilon\right]\mathbf{G}(\mathbf{r},\mathbf{r}',\omega)=\delta(\boldsymbol{r}-\boldsymbol{r}'), \tag{2.33}$$

with the boundary condition that

$$\mathbf{G}(\mathbf{r},\mathbf{r}',\omega)\to\mathbf{0}\quad\text{for}\quad|\mathbf{r}-\mathbf{r}'|\to\infty. \tag{2.34}$$

Furthermore it can be shown that $\mathbf{G}(\mathbf{r},\mathbf{r}',\omega)$ satisfies the Schwarz reflection principle

$$\boldsymbol{G}^*(\boldsymbol{r},\boldsymbol{r}',\omega)=\boldsymbol{G}(\boldsymbol{r},\boldsymbol{r}',-\omega^*), \tag{2.35}$$

the Onsager reciprocity relation

$$\boldsymbol{G}^T(\boldsymbol{r},\boldsymbol{r}',\omega)=\boldsymbol{G}(\boldsymbol{r}',\boldsymbol{r},-\omega^*), \tag{2.36}$$

and the integral relation [127, 128]

$$\int d^3s\Bigg\{-\frac{\operatorname{Im}\mu(\mathbf{s},\omega)}{|\mu(\mathbf{s},\omega)|^2}\Big[\nabla_{\mathbf{s}}\times\mathbf{G}(\mathbf{s},\mathbf{r},\omega)\Big]^T\cdot\Big[\nabla_{\mathbf{s}}\times\mathbf{G}^*(\mathbf{s},\mathbf{r}',\omega)\Big] +\frac{\omega^2}{c^2}\operatorname{Im}\epsilon(\mathbf{s},\omega)\;\mathbf{G}(\mathbf{r},\mathbf{s},\omega)\cdot\mathbf{G}^*(\mathbf{s},\mathbf{r}',\omega)\Bigg\}=\operatorname{Im}\mathbf{G}(\mathbf{r},\mathbf{r}',\omega). \tag{2.37}$$

From the electric field expression (2.32), the explicit expression for the magnetic field $\boldsymbol{B}$ in terms of the Green's tensor can be obtained

$$\hat{\mathbf{B}}(\boldsymbol{r},\omega)=\mu_0\int d^3r'\;\nabla\times\boldsymbol{G}(\boldsymbol{r},\boldsymbol{r}',\omega)\cdot\hat{\boldsymbol{j}}_N(\mathbf{r}',\omega). \tag{2.38}$$

Upon expressing the noise current density in terms of noise polarization and magnetization via (2.15), the electromagnetic field expressions can be written in the alternative form

$$\hat{\mathbf{E}}(\boldsymbol{r},\omega)=-\frac{1}{\epsilon_0}\int d^3r'\boldsymbol{G}_{ee}(\boldsymbol{r},\boldsymbol{r}',\omega)\cdot\hat{\boldsymbol{P}}_N(\mathbf{r}',\omega)-Z_0\int d^3r'\boldsymbol{G}_{em}(\boldsymbol{r},\boldsymbol{r}',\omega)\cdot\hat{\boldsymbol{M}}_N(\mathbf{r}',\omega), \tag{2.39}$$

$$\hat{\mathbf{B}}(\boldsymbol{r},\omega)=-Z_0\int d^3r'\boldsymbol{G}_{me}(\boldsymbol{r},\boldsymbol{r}',\omega)\cdot\hat{\boldsymbol{P}}_N(\mathbf{r}',\omega)-\mu_0\int d^3r'\boldsymbol{G}_{mm}(\boldsymbol{r},\boldsymbol{r}',\omega)\cdot\hat{\boldsymbol{M}}_N(\mathbf{r}',\omega), \tag{2.40}$$

where the vacuum impedance $Z_0 = \sqrt{\mu_0/\epsilon_0}$ has been introduced. Here we have introduced the tensors

$$\boldsymbol{G}_{ee}(\boldsymbol{r},\boldsymbol{r}',\omega) = \frac{i\omega}{c}\boldsymbol{G}(\boldsymbol{r},\boldsymbol{r}',\omega)\frac{i\omega}{c}, \tag{2.41}$$

$$\boldsymbol{G}_{em}(\boldsymbol{r},\boldsymbol{r}',\omega) = \frac{i\omega}{c}\boldsymbol{G}(\boldsymbol{r},\boldsymbol{r}',\omega)\times\nabla, \tag{2.42}$$

$$\boldsymbol{G}_{me}(\boldsymbol{r},\boldsymbol{r}',\omega) = \nabla\times\boldsymbol{G}(\boldsymbol{r},\boldsymbol{r}',\omega)\frac{i\omega}{c}, \tag{2.43}$$

$$\boldsymbol{G}_{mm}(\boldsymbol{r},\boldsymbol{r}',\omega) = \nabla\times\boldsymbol{G}(\boldsymbol{r},\boldsymbol{r}',\omega)\times\nabla, \tag{2.44}$$

where $\boldsymbol{G}_{\lambda\lambda'}$ relates the induced electric and magnetic field (for $\lambda = e, m$) to their two possible polarization and magnetization sources (for $\lambda' = e, m$).
The development of the classical electrodynamics in terms of the Green's tensor is a very useful way to investigate and calculate the electromagnetic field, in particular when macroscopic media are present in the system. In fact, all the magneto-dielectric properties of the media are included in the Green's tensor expression; thus, the formal solutions given in Eqs. (2.32) and (2.38) for the electric and magnetic field, represent the radiation field in the presence of a generic macroscopic medium, due only to the noise charge and the noise current density, in the absence of free charges and currents. Therefore the goal of this approach is that through these equations, knowing the Green tensor expression, we can investigate the electromagnetic field in presence of any arbitrary magneto-dielectric media.

2.2 Quantum electrodynamics in linear media

The canonical quantization scheme, used to quantise the radiation field in the free space, cannot be applied to quantise the electromagnetic field in the presence of generic magneto-dielectric media. In fact, if we naively extend the plane-wave expansion for the electromagnetic field in the presence of dielectrics, we should replace the plane-wave solution of the Helmholtz equation $e^{i\boldsymbol{k}\cdot\boldsymbol{r}}$ with $e^{in\boldsymbol{k}\cdot\boldsymbol{r}}$, where $n \equiv n(\omega)$ is the refractive index of the medium, which is a complex function of frequency $n(\omega) = \eta(\omega) + i\kappa(\omega)$, that satisfies the Kramers-Kronig dispersion relations

$$\eta(\omega) = \frac{1}{\pi}P\int_{-\infty}^{+\infty} d\omega' \frac{\kappa(\omega')}{\omega'-\omega}, \qquad \kappa(\omega) = -\frac{1}{\pi}P\int_{-\infty}^{+\infty} d\omega' \frac{\eta(\omega')}{\omega'-\omega}. \tag{2.45}$$

Owing to the inevitable imaginary part of the refractive index, the plane waves inside the medium are damped, which implies that they do not form a complete set of orthonormal functions, needed to perform a Fourier decomposition of the

electromagnetic field. Therefore the canonical quantization procedure in presence of media leads to a failure; in fact imposing the bosonic commutation rules for the amplitude operators $a_{\boldsymbol{k},\lambda}$ and $a^{\dagger}_{\boldsymbol{k},\lambda}$, the commutation relations for the electric field operator $\boldsymbol{E}(\boldsymbol{r})$ and the magnetic field operator $\boldsymbol{B}(\boldsymbol{r})$ are no longer being fulfilled; on the other hand, if we postulate the correctness of commutation relations between the fields, the amplitude operators cannot represent annihilation and creation operators of photonic modes [15]. The failure of this quantization scheme is related to the fact that the electromagnetic field is coupled to the dielectric matter, and can no longer be treated as in the free space, taking into account the presence of media by means of the refractive index $n(\omega)$ only [128].

For these reasons, we shall necessarily consider the electromagnetic field interacting with an absorbing dielectric matter, that can be microscopically depicted as an atomic system coupled to a reservoir that is responsible for absorption. Historically the first attempt of quantising the electromagnetic field in absorbing dielectric media is due to Huttner and Barnett [129, 130]. They consider the radiation field interacting with an homogeneous and isotropic bulk dielectric, in which an harmonic oscillator, representing the medium polarization, is linearly coupled to a continuum of harmonic oscillators, standing for the reservoir.

In order to develop a macroscopic quantum theory for the electromagnetic field in presence of dielectric media, we require that the equations of motion for the electromagnetic field must be the same as the classical ones, therefore electric and magnetic field operators must obey Maxwell equations in Fourier space (2.29) with the constitutive relations (2.30). The electric and magnetic field must also fulfil the correct commutation relations, and the quantum fluctuations of both noise fields and radiation fields should satisfy the fluctuation-dissipation theorem.

Since the noise polarization and magnetization fields are now operators, we must specify their commutation relations. Their expressions shall be such that quantum averages of noise polarization and noise magnetization vanish, and their fluctuation spectrum fulfils the fluctuation-dissipation theorem. Expressions for noise polarization and magnetization operators are

$$\boldsymbol{P}_N(\boldsymbol{r},\omega) = i\sqrt{\frac{\hbar\epsilon_0}{\pi}\mathrm{Im}\epsilon(\boldsymbol{r},\omega)}\;\boldsymbol{f}_e(\boldsymbol{r},\omega), \tag{2.46}$$

$$\boldsymbol{M}_N(\boldsymbol{r},\omega) = \sqrt{\frac{\hbar}{\pi\mu_0}\frac{\mathrm{Im}\mu(\boldsymbol{r},\omega)}{|\mu(\boldsymbol{r},\omega)|^2}}\;\boldsymbol{f}_m(\boldsymbol{r},\omega), \tag{2.47}$$

where $\boldsymbol{f}^{\dagger}_{\lambda}(\boldsymbol{r},\omega)$ and $\boldsymbol{f}_{\lambda}(\boldsymbol{r},\omega)$ are creation and annihilation bosonic matter-assisted operators, respectively, where the subscript $\lambda = (e,m)$ refers to the electric and magnetic parts. They represent the combined system of the electromagnetic field and the magneto-dielectric medium, and describe the collective polariton-like

bosonic excitation of the body-field system. They satisfy the following bosonic commutation relations

$$\Big[f_{\lambda i}(\mathbf{r},\omega), f^{\dagger}_{\lambda' i'}(\mathbf{r}',\omega')\Big] = \delta_{\lambda\lambda'}\ \delta_{ii'}\ \delta(\mathbf{r}-\mathbf{r}')\delta(\omega-\omega'),$$
$$\Big[f_{\lambda i}(\mathbf{r},\omega), f_{\lambda' i'}(\mathbf{r}',\omega')\Big] = \Big[f^{\dagger}_{\lambda i}(\mathbf{r},\omega), f^{\dagger}_{\lambda' i'}(\mathbf{r}',\omega')\Big] = 0, \tag{2.48}$$

and the ground state of the system is defined as

$$\boldsymbol{f}_{\lambda}(\boldsymbol{r},\omega)\,|0\rangle = \mathbf{0} \quad \forall\ \ \lambda,\boldsymbol{r},\omega. \tag{2.49}$$

The complete Hilbert space of the matter-field system is given by Fock states obtained by repeated applications of the creation operator $\boldsymbol{f}^{\dagger}_{\lambda}(\boldsymbol{r},\omega)$ on the ground state, from which the general n-quantum Fock state is

$$|\mathbf{1}_{\lambda_1}(\boldsymbol{r}_1,\omega_1)\ldots\mathbf{1}_{\lambda_n}(\boldsymbol{r}_n,\omega_n)\rangle = \frac{1}{\sqrt{n!}}\boldsymbol{f}^{\dagger}_{\lambda_n}(\boldsymbol{r}_n,\omega_n)\cdots\boldsymbol{f}^{\dagger}_{\lambda_1}(\boldsymbol{r}_1,\omega_1)\,|0\rangle\,. \tag{2.50}$$

Here, $|\mathbf{1}_{\lambda}(\boldsymbol{r},\omega)\rangle$ is the one medium-assisted photon state of the combined system of radiation field and macroscopic medium. From the above definition of the ground state, it immediately follows that the creation and annihilation operators have a vanishing average on the ground state,

$$\langle \boldsymbol{f}^{\dagger}_{\lambda}(\boldsymbol{r},\omega)\rangle = \langle 0|\,\boldsymbol{f}^{\dagger}_{\lambda}(\boldsymbol{r},\omega)\,|0\rangle = \mathbf{0}, \tag{2.51}$$
$$\langle \boldsymbol{f}_{\lambda}(\boldsymbol{r},\omega)\rangle = \langle 0|\,\boldsymbol{f}_{\lambda}(\boldsymbol{r},\omega)\,|0\rangle = \mathbf{0} \tag{2.52}$$

and exploiting the bosonic commutation relations, the following results are obtained

$$\langle \boldsymbol{f}_{\lambda}(\boldsymbol{r},\omega)\boldsymbol{f}_{\lambda'}(\boldsymbol{r}',\omega')\rangle = \mathbf{0}, \tag{2.53}$$
$$\langle \boldsymbol{f}^{\dagger}_{\lambda}(\boldsymbol{r},\omega)\boldsymbol{f}^{\dagger}_{\lambda'}(\boldsymbol{r}',\omega')\rangle = \mathbf{0}, \tag{2.54}$$
$$\langle \boldsymbol{f}^{\dagger}_{\lambda}(\boldsymbol{r},\omega)\boldsymbol{f}_{\lambda'}(\boldsymbol{r}',\omega')\rangle = \mathbf{0}, \tag{2.55}$$
$$\langle \boldsymbol{f}_{\lambda}(\boldsymbol{r},\omega)\boldsymbol{f}^{\dagger}_{\lambda'}(\boldsymbol{r}',\omega')\rangle = \delta_{\lambda\lambda'}\boldsymbol{\delta}(\mathbf{r}-\mathbf{r}')\delta(\omega-\omega'). \tag{2.56}$$

The above relations imply that the noise polarization and magnetization, given by expressions (2.46) and (2.47), have zero ground-state average

$$\langle \boldsymbol{P}_N\rangle = \mathbf{0}, \qquad \langle \boldsymbol{M}_N\rangle = \mathbf{0}, \tag{2.57}$$

and satisfy the fluctuation-dissipation theorem,

$$\langle S[\Delta\boldsymbol{P}_N(\boldsymbol{r},\omega)\Delta\boldsymbol{P}^{\dagger}_N(\boldsymbol{r}',\omega')]\rangle = \frac{\hbar\epsilon_0}{2\pi}\,\mathrm{Im}\chi(\boldsymbol{r},\omega)\boldsymbol{\delta}(\mathbf{r}-\mathbf{r}')\delta(\omega-\omega'), \tag{2.58}$$
$$\langle S[\Delta\boldsymbol{M}_N(\boldsymbol{r},\omega)\Delta\boldsymbol{M}^{\dagger}_N(\boldsymbol{r}',\omega')]\rangle = \frac{\hbar}{2\pi\mu_0}\,\mathrm{Im}\zeta(\boldsymbol{r},\omega)\boldsymbol{\delta}(\mathbf{r}-\mathbf{r}')\delta(\omega-\omega'), \tag{2.59}$$

as previously requested. Here $S[\boldsymbol{ab}] = \frac{1}{2}(\boldsymbol{ab} + \boldsymbol{ba})$ is a symmetrized operator product.
Having introduced the fundamental dynamical variables of the system and their commutation relations, the electromagnetic field quantization can be performed by expressing field operators in terms of $\boldsymbol{f}^{\dagger}_{\lambda}(\boldsymbol{r},\omega)$ and $\boldsymbol{f}_{\lambda}(\boldsymbol{r},\omega)$. Similarly to the classical case, an Helmholtz equation for the electric field operator can be obtained,

$$\left[\nabla \times \frac{1}{\mu}\nabla \times -\frac{\omega^2}{c^2}\epsilon\right]\mathbf{E} = i\mu_0\omega\boldsymbol{j}_N, \tag{2.60}$$

which can be formally solved by means of the Green's tensor,

$$\mathbf{E}(\boldsymbol{r},\omega) = i\omega\mu_0 \int d^3r' \boldsymbol{G}(\boldsymbol{r},\boldsymbol{r}',\omega)\cdot\boldsymbol{j}_N(\mathbf{r}',\omega). \tag{2.61}$$

Exploiting the noise current expression $\boldsymbol{j}_N(\mathbf{r}',\omega) = -i\omega\boldsymbol{P}_N(\boldsymbol{r},\omega) + \nabla\times\boldsymbol{M}_N(\boldsymbol{r},\omega)$, together with Eqs. (2.46) and (2.47), we obtain the electric field expression in terms of the Green's tensor and the bosonic field-matter operators

$$\begin{aligned}\mathbf{E}(\boldsymbol{r}) &= \int_0^{+\infty} d\omega \boldsymbol{E}(\boldsymbol{r},\omega) + H.c. \\ &= \int_0^{+\infty} d\omega \sum_{\lambda=e,m}\int d^3r'\, \boldsymbol{G}_{\lambda}(\boldsymbol{r},\boldsymbol{r}',\omega)\cdot\boldsymbol{f}_{\lambda}(\boldsymbol{r}',\omega) + H.c.\end{aligned} \tag{2.62}$$

where

$$\boldsymbol{G}_e(\boldsymbol{r},\boldsymbol{r}',\omega) = i\frac{\omega^2}{c^2}\sqrt{\frac{\hbar}{\pi\epsilon_0}\mathrm{Im}\,\epsilon(\boldsymbol{r}',\omega)}\;\boldsymbol{G}(\boldsymbol{r},\boldsymbol{r}',\omega), \tag{2.63}$$

$$\boldsymbol{G}_m(\boldsymbol{r},\boldsymbol{r}',\omega) = i\frac{\omega}{c}\sqrt{\frac{\hbar}{\pi\epsilon_0}\frac{\mathrm{Im}\,\mu(\boldsymbol{r}',\omega)}{|\mu(\mathbf{r}',\omega)|^2}}\;[\nabla'\times\boldsymbol{G}(\boldsymbol{r},\boldsymbol{r}',\omega)]^T, \tag{2.64}$$

are respectively the electric and magnetic Green's tensor components. By means of Eqs. (2.63) and (2.64), the integral relation (2.37) can be written in the more compact form,

$$\sum_{\lambda=e,m}\int d^3s\; \boldsymbol{G}_{\lambda}(\boldsymbol{r},\boldsymbol{s},\omega)\cdot\boldsymbol{G}^{*T}_{\lambda}(\boldsymbol{r}',\boldsymbol{s},\omega) = \frac{\hbar\mu_0}{\pi}\,\omega^2\,\mathrm{Im}\,\boldsymbol{G}_{\lambda}(\boldsymbol{r},\boldsymbol{r}',\omega). \tag{2.65}$$

Using Eq. (2.62) together with Maxwell equations in the frequency space, the expression of the magnetic field $\boldsymbol{B}$ in terms of dynamical variables of the system

can be written as

$$\begin{aligned}\mathbf{B}(\boldsymbol{r}) &= \int_0^{+\infty} d\omega\ \boldsymbol{B}(\boldsymbol{r},\omega) + H.c. \\ &= \int_0^{+\infty} \frac{d\omega}{i\omega} \sum_{\lambda=e,m} \int d^3r'\ \nabla \times \boldsymbol{G}_\lambda(\boldsymbol{r},\boldsymbol{r}',\omega) \cdot \boldsymbol{f}_\lambda(\boldsymbol{r}',\omega) + H.c. \end{aligned} \tag{2.66}$$

Exploiting the bosonic commutation relations for $\boldsymbol{f}_\lambda^\dagger(\boldsymbol{r},\omega)$ and $\boldsymbol{f}_\lambda(\boldsymbol{r},\omega)$, may be shown that the new expressions for the electric and magnetic field in terms of field-matter operators, (2.62) and (2.66), obey the equal-time commutation relations

$$\Big[\mathbf{E}(\boldsymbol{r}),\mathbf{E}(\boldsymbol{r}')\Big] = \Big[\mathbf{B}(\boldsymbol{r}),\mathbf{B}(\boldsymbol{r}')\Big] = \mathbf{0}, \tag{2.67}$$

$$\Big[\mathbf{E}(\boldsymbol{r}),\mathbf{B}(\boldsymbol{r}')\Big] = \frac{i\hbar}{\epsilon_0}\ \nabla \times \boldsymbol{\delta}(\boldsymbol{r}-\boldsymbol{r}'), \tag{2.68}$$

as requested [125, 127, 128, 131]. They also satisfy the fluctuation-dissipation theorem since the ground-state fluctuation spectrum of the electric field is [15, 125, 127]

$$\langle S[\Delta\boldsymbol{E}(\boldsymbol{r},\omega)\Delta\boldsymbol{E}^\dagger(\boldsymbol{r}',\omega')]\rangle = \frac{\hbar\mu_0\omega^2}{2\pi}\ \mathrm{Im}\,\boldsymbol{G}_\lambda(\boldsymbol{r},\boldsymbol{r}',\omega)\delta(\omega-\omega'), \tag{2.69}$$

where the integral relation (2.65) has been used. Finally, in order to complete the quantization scheme we need to specify the Hamiltonian of the system in terms of bosonic field-matter operators, which has the following expression

$$H_F = \sum_{\lambda=e,m} \int d^3r \int_0^{+\infty} d\omega\ \hbar\omega\ \boldsymbol{f}_\lambda^\dagger(\boldsymbol{r},\omega)\cdot\boldsymbol{f}_\lambda(\boldsymbol{r},\omega). \tag{2.70}$$

In conclusion, the expressions for the quantum electromagnetic field and the radiation field Hamiltonian in terms of the new bosonic field-matter operators $\boldsymbol{f}_\lambda^\dagger(\boldsymbol{r},\omega)$ and $\boldsymbol{f}_\lambda(\boldsymbol{r},\omega)$ have been obtained, which represent the medium-assisted quantum electromagnetic field [15]. These expressions can be very useful to investigate the radiation field in presence of an arbitrary bulk dielectric medium, since all the information and physical properties of the medium, its material or its geometry for example, are included in the classical Green tensor expression.

To summarize, the macroscopic QED theory outlined in the present Chapter fulfils three fundamental requirements: it is compatible with the classical macroscopic electrodynamics, fulfilling Maxwell equations; the quantum fluctuations of both noise and electromagnetic fields obeys the fluctuation-dissipation theorem and, finally, the radiation field satisfies the correct commutation relations.

Finally, we conclude this section with a few remarks about the validity and physical interpretation of the macroscopic QED theory [15]. This theory describes the quantum electromagnetic field in the presence of an arbitrary linear, causal magneto-dielectric medium, characterized, respectively, by its permittivity and permeability $\epsilon(\boldsymbol{r},\omega)$ and $\mu(\boldsymbol{r},\omega)$. The validity of this quantization scheme is strictly related to the assumption that all the space is filled with an absorbing medium, so that $\mathrm{Im}\epsilon(\boldsymbol{r},\omega) > 0$ and $\mathrm{Im}\mu(\boldsymbol{r},\omega) > 0$ hold everywhere. This condition is fundamental to guarantee the convergence of the spatial integrals presented, for example, in expressions (2.62) and (2.66). In fact, the free-space QED case, for which $\mathrm{Im}\epsilon(\boldsymbol{r},\omega) = 0$ and $\mathrm{Im}\mu(\boldsymbol{r},\omega) = 0$, can be obtained from this theory by performing the limits $\mathrm{Im}\epsilon(\boldsymbol{r},\omega) \to 0$ and $\mathrm{Im}\mu(\boldsymbol{r},\omega) \to 0$, after taking the expectation values and having calculated all space integrals.

Chapter 3

Resonance energy transfer between two atoms in external environments

The resonance energy transfer between two quantum emitters, such as atoms, molecules, chromophores or macromolecular assemblies, is the exchange of electronic excitation between them mediated by the quantum electromagnetic field [60]. The transport of electronic energy from one atom or molecule to another has significant importance to a number of diverse areas of science, from atomic-molecular physics to chemistry and biology, above all in biochemical and solid-state system [50]. It is also supposed that this process is strictly related to the very high efficiency in light-harvesting observed in photosynthetic systems [51, 52], accounting for energy hopping between chlorophyll molecules in the photosynthetic-unit [132, 133]. More recently the resonance energy transfer between carbon nanotubes [134–137] and quantum dots [138–140] has been also investigated .

When two molecules are in presence of external environments, the radiation field can be significantly modified with respect to that in the free space and therefore the intermolecular energy transfer can be deeply modified accordingly [117]. This latter effect has attracted much attention, because it offers the possibility to manipulate and control the exchange of energy between quantum emitters through external environments, with regard to promising potential applications [141], e.g., in high-efficiency light-harvesting systems, photovoltaic [142, 143], optical networks and bio-medical sensing [93, 144]. The possibility of controlling the energy transfer between nanostructured emitters through a reflecting plate or exploiting laser external fields has been also investigated [145–147]. Many other calculations of the energy transfer rate have been performed in order to include the effect of bulk materials [148], microspheres [149] and planar microcavities [150, 151].

In this Chapter we present our original work on the resonance exchange of

energy between two identical atoms, or any other quantum emitters (for example quantum dots), placed on the axis of a cylindrical waveguide made of a perfect conductor [152]. Our purpose is to investigate whether and how the transfer of energy between two atoms can be manipulated and controlled through a cylindrical waveguide.

Firstly, we will obtain an analytical expression of the energy transfer amplitude, in terms of the electromagnetic Green's tensor, when the atoms are in the presence of a generic linear, dispersive and dissipative magneto-dielectric medium. Then we use the specific Green's tensor of the cylindrical waveguide, whose analytic expression is known, to evaluate numerically the energy transfer amplitude inside the waveguide in terms of the relevant parameters of the system: the distance between the atoms and the radius of the waveguide, relative to the atomic transition wavelength. We shall consider both cases of atomic dipoles parallel and orthogonal to the guide axis. We explicitly show that the presence of a lower cut-off frequency inside the waveguide deeply changes the energy transfer amplitude between the atoms when they are in the far radiative zone. On the other hand, we find that the influence of the waveguide when the atoms are in the radiationless near zone, although present, is much less important. We also show the possibility to strongly modify the transfer of energy between the atoms by varying the waveguide radius, allowing a control of the energy transfer process by means of a macroscopic parameter of the system. A transparent physical interpretation of these results is given.

This Chapter is organized as follows: in Sec. 3.1 we first obtain the intermolecular energy transfer amplitude in the presence of an arbitrary dispersing and absorbing magneto-dielectric medium. To achieve this purpose the macroscopic QED and the Green tensor formalism, outlined in Chapter 2, is used. In Sec. 3.2 we apply the generic RET expression in terms of the Green's tensor to the case of atoms placed inside a perfectly conducting cylindrical waveguide. The energy transfer process is analysed in detail as a function of the waveguide radius, the interatomic distance and the atomic dipoles orientation. We shall point out the possibility to modify and control such process through the macroscopic parameters of the environment. Finally, Sec. 3.3 summarizes our findings and conclusive remarks.

3.1 Resonance energy transfer in the presence of magneto-dielectric media

In this section we consider the resonance energy transfer between two atoms when an arbitrary magneto-dielectric medium is present nearby. In order to achieve

this purpose, we generalise the quantum approach to the resonance energy transfer, outlined in Chapter 1, using the macroscopic quantum electrodynamics formalism and the Green's tensor (introduced in Chapter 2), that includes all properties of the macroscopic environment around the system [15, 117, 153].

Les us consider two two-level identical atoms, labelled A and B, placed in a generic linear magneto-dielectric medium; we assume that the atom A (donor) is in its excited state, while the atom B (acceptor) is in its ground state, and the whole system is embedded inside an arbitrary dissipative and dispersive medium. The radiation field is in its vacuum state, thus every possible mode has zero photons. The Hamiltonian of the system can be expressed as

$$H = H_a + H_f + H_i, \tag{3.1}$$

where H_a and H_f are respectively the unperturbed atomic and field Hamiltonians, in the presence of the medium, given by

$$H_a = \sum_{n=e,g} E_n^A \left|n_A\right\rangle \left\langle n_A\right| + \sum_{n=e,g} E_n^B \left|n_B\right\rangle \left\langle n_B\right|, \tag{3.2}$$

$$H_f = \sum_{\lambda=e,m} \int d^3r \int_0^\infty d\omega\, \hbar\omega\, \mathbf{f}_\lambda^\dagger(\mathbf{r},\omega)\cdot\mathbf{f}_\lambda(\mathbf{r},\omega), \tag{3.3}$$

where $|n_{A(B)}\rangle$ are eigenstates of the atomic Hamiltonian of atom A(B), $|e\rangle$ and $|g\rangle$ being in particular the atomic excited and ground state, with energy E_e and E_g, respectively. Owing to the presence of the medium, the free-field Hamiltonian (3.3) is written in terms of the bosonic matter-assisted field operators $\mathbf{f}_\lambda(\mathbf{r},\omega)$ and $\mathbf{f}_\lambda^\dagger(\mathbf{r},\omega)$ introduced in Chapter 2. We recall that they represent the medium-assisted electromagnetic field, and satisfy the following bosonic commutation relations

$$\begin{aligned}\Big[f_{\lambda i}(\mathbf{r},\omega), f^\dagger_{\lambda' i'}(\mathbf{r}',\omega')\Big] &= \delta_{\lambda\lambda'}\delta_{ii'}\delta(\mathbf{r}-\mathbf{r}')\delta(\omega-\omega'),\\ \Big[f_{\lambda i}(\mathbf{r},\omega), f_{\lambda' i'}(\mathbf{r}',\omega')\Big] &= 0,\end{aligned} \tag{3.4}$$

where the subscript $\lambda = e, m$ refers to the electric and magnetic parts. H_i is the interaction Hamiltonian written in the multipolar coupling scheme and within the dipole approximation

$$H_i = -\boldsymbol{\mu}_A\cdot\mathbf{E}(\mathbf{r}_A) - \boldsymbol{\mu}_B\cdot\mathbf{E}(\mathbf{r}_B) \tag{3.5}$$

where $\mathbf{r}_{A(B)}$ is the position of the atom A (B) and $\boldsymbol{\mu}_{A(B)}$ is its atomic electric dipole moment operator. $\mathbf{E}(\mathbf{r})$ is the medium-assisted electric field operator evaluated at the atomic position $\mathbf{r} = \mathbf{r}_{A(B)}$, expressed in terms of the Green's tensor as

$$\begin{aligned}\mathbf{E}(\mathbf{r}) &= \int_0^\infty d\omega'\, \mathbf{E}(\mathbf{r},\omega') + H.c.\\ &= \sum_{\lambda'=e,m} \int d^3r' \int_0^\infty d\omega'\, \mathbf{G}_{\lambda'}(\mathbf{r},\mathbf{r}',\omega')\cdot\mathbf{f}_{\lambda'}(\mathbf{r}',\omega') + H.c.,\end{aligned} \tag{3.6}$$

where

$$\mathbf{G}_e(\mathbf{r},\mathbf{r}',\omega') = i\frac{\omega'^2}{c^2}\sqrt{\frac{\hbar}{\pi\epsilon_0}\mathrm{Im}\,\epsilon(\mathbf{r}',\omega')}\;\mathbf{G}(\mathbf{r},\mathbf{r}',\omega') \tag{3.7}$$

$$\mathbf{G}_m(\mathbf{r},\mathbf{r}',\omega') = i\frac{\omega'}{c}\sqrt{\frac{\hbar}{\pi\epsilon_0}\frac{\mathrm{Im}\,\mu(\boldsymbol{r}',\omega')}{|\mu(\mathbf{r}',\omega')|^2}}\;[\nabla'\times\mathbf{G}(\mathbf{r},\mathbf{r}',\omega')]^T \tag{3.8}$$

are respectively the electric and magnetic Green's tensor components. They satisfy the following integral relation

$$\sum_{\lambda'=e,m}\int d^3s\mathbf{G}_{\lambda'}(\mathbf{r},\mathbf{s},\omega')\cdot\mathbf{G}^{*T}_{\lambda'}(\mathbf{r}',\mathbf{s},\omega') = \frac{\hbar\mu_0}{\pi}\omega'^2\mathrm{Im}\mathbf{G}_{\lambda}(\mathbf{r},\mathbf{r}',\omega'). \tag{3.9}$$

In order to develop our calculation, it is more convenient to write explicitly equations (3.6) and (3.9) in terms of their components

$$E_i(\mathbf{r}) = \sum_{\lambda'=e,m}\int d^3r'\int_0^\infty d\omega'\sum_l\Big[G_{\lambda' il}(\mathbf{r},\mathbf{r}',\omega')f_{\lambda' l}(\mathbf{r}',\omega') + G^*_{\lambda' il}(\mathbf{r},\mathbf{r}',\omega')f^\dagger_{\lambda' l}(\mathbf{r}',\omega')\Big], \tag{3.10}$$

$$\sum_{\lambda'=e,m}\int d^3s\sum_\beta G_{\lambda' i\beta}(\mathbf{r},\mathbf{s},\omega')\;G^*_{\lambda' j\beta}(\mathbf{r}',\mathbf{s},\omega') = \frac{\hbar\omega'^2}{\pi\epsilon_0 c^2}\;\mathrm{Im}G_{ij}(\mathbf{r},\mathbf{r}',\omega'). \tag{3.11}$$

where the Einstein notation for repeated indices has been used. As done for the free-space case, the energy transfer rate between two atoms embedded in a generic magneto-dielectric medium is given by the generalized Fermi golden rule [50, 62]

$$W_{i\to f} = \frac{2\pi}{\hbar}|\left\langle\psi_i\right|T\left|\psi_f\right\rangle|^2\delta(E_f-E_i), \tag{3.12}$$

where $|\psi_i\rangle = |e_A,g_B,0\rangle$ and $|\psi_f\rangle = |g_A,e_B,0\rangle$ are respectively the initial and the final state of the system, with energy E_i and E_f, and the radiation field is in the vacuum state. T is the transition operator at the second-order in the interaction Hamiltonian

$$T = H_i + H_i\frac{1}{E_i - H_0 \pm i\eta}H_i, \tag{3.13}$$

where H_0 and H_i are the unperturbed and interaction Hamiltonians, respectively, and $E_i = E_f = \hbar\omega_0$ is the energy of the initial and final state. $\omega_0 = ck_0$ is the transition frequency of both atoms, assumed identical. The second-order energy transfer amplitude can thus be written as

$$M = \left\langle\psi_i\right|T\left|\psi_f\right\rangle = \sum_I\frac{\left\langle\psi_i\right|H_i\left|I\right\rangle\left\langle I\right|H_i\left|\psi_f\right\rangle}{E_i - E_I \pm i\eta}, \tag{3.14}$$

where $|I\rangle$ are the intermediate states, with energy E_I, that can contribute to the energy transfer process and $\eta \to 0^+$. Taking into account Eq. (3.5), only two intermediate states contribute to the energy transfer amplitude (3.14),

$$\begin{aligned} |I\rangle_1 &= |g_A, g_B, \mathbf{1}_\lambda(\mathbf{r},\omega)\rangle\,, \\ |I\rangle_2 &= |e_A, e_B, \mathbf{1}_\lambda(\mathbf{r},\omega)\rangle\,, \end{aligned} \tag{3.15}$$

shown in Fig. 3.1, where $\mathbf{1}_\lambda(\mathbf{r},\omega)$ is a medium-assisted excitation of the radiation field.

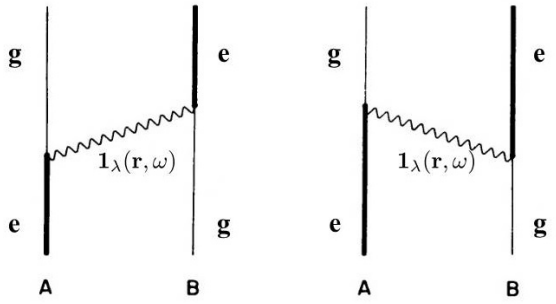

Figure 3.1: Feynman diagrams for the resonance energy transfer between two atoms in the multipolar method.

The sum over the intermediate states can be written as a sum over $\lambda = e, m$, the magnetic and electric part, and an integral over space and over frequency, leading to

$$M = \sum_{\lambda=e,m} \int d^3r \int_0^{+\infty} d\omega \left[\frac{\langle e_A, g_B, 0|\, H_i\, |g_A, g_B, \mathbf{1}_\lambda(\mathbf{r},\omega)\rangle \langle g_A, g_B, \mathbf{1}_\lambda(\mathbf{r},\omega)|\, H_i\, |g_A, e_B, 0\rangle}{\hbar\omega_0 - \hbar\omega \pm i\eta} \right.$$
$$\left. - \frac{\langle e_A, g_B, 0|\, H_i\, |e_A, e_B, \mathbf{1}_\lambda(\mathbf{r},\omega)\rangle \langle e_A, e_B, \mathbf{1}_\lambda(\mathbf{r},\omega)|\, H_i\, |g_A, e_B, 0\rangle}{\hbar\omega_0 + \hbar\omega \pm i\eta} \right]. \tag{3.16}$$

Calculating the matrix elements, for the first term in Eq. (3.16), we obtain

$$\begin{aligned} &\langle e_A, g_B, 0|\, H_i\, |g_A, g_B, \mathbf{1}_\lambda(\mathbf{r},\omega)\rangle = -\langle e_A, g_B, 0|\, \boldsymbol{\mu}_A \cdot \mathbf{E}(\mathbf{r}_A)\, |g_A, g_B, \mathbf{1}_\lambda(\mathbf{r},\omega)\rangle = \\ &\sum_i \langle e_A, g_B, 0|\, \mu_{Ai}\, E_i(\mathbf{r}_A)\, |g_A, g_B\rangle\, |\mathbf{1}_\lambda(\mathbf{r},\omega)\rangle = \\ &\sum_i \sum_{\lambda' l} \int d^3r' \int_0^\infty d\omega' \langle e_A, g_B, 0|\, \mu_{Ai}\, G_{\lambda' il}(\mathbf{r}_A, \mathbf{r}', \omega') f_{\lambda' l}(\mathbf{r}', \omega)\, |g_A, g_B\rangle\, |\mathbf{1}_\lambda(\mathbf{r},\omega)\rangle = \\ &\sum_{ij} \langle e_A, g_B|\, \mu_{Ai}\, G_{\lambda ij}(\mathbf{r}_A, \mathbf{r}, \omega)\, |g_A, g_B\rangle = \sum_{ij} \mu_{Ai}^{eg}\, G_{\lambda ij}(\mathbf{r}_A, \mathbf{r}, \omega), \end{aligned} \tag{3.17}$$

where in the last row we have used the commutation relations for the bosonic operators $\mathbf{f}_\lambda(\mathbf{r},\omega)$ and $\mathbf{f}^\dagger_\lambda(\mathbf{r},\omega)$. Here, $\mu^{eg}_{Ai} = \langle e_A| \mu_{Ai} |g_B\rangle$ is the matrix element of the i-component of the dipole moment operator of the atom A between its excited and ground state. With similar steps, it is possible to calculate the other matrix elements in Eq. (3.16) related to the intermediate state $|I_2\rangle$, finally obtaining

$$M = \sum_{\lambda=e,m} \int d^3r \int_0^{+\infty} d\omega \sum_{ijk} \left[\frac{\mu^{eg}_{Ai} G_{\lambda ij}(\mathbf{r}_A,\mathbf{r},\omega) G^*_{\lambda kj}(\mathbf{r}_B,\mathbf{r},\omega) \mu^{ge}_{Bk}}{\hbar\omega_0 - \hbar\omega \pm i\eta} - \frac{\mu^{ge}_{Bk} G^*_{\lambda kj}(\mathbf{r}_B,\mathbf{r},\omega) G_{\lambda ij}(\mathbf{r}_A,\mathbf{r},\omega) \mu^{eg}_{Ai}}{\hbar\omega_0 + \hbar\omega \pm i\eta} \right]. \tag{3.18}$$

Now, using the integral relation (3.9), the resonance energy transfer amplitude can be written as

$$M = \frac{1}{\pi\epsilon_0 c^2} \int_0^\infty d\omega \omega^2 \sum_{ij} \left\{ \frac{1}{\omega_0 - \omega \pm i\eta} \left[\mu^{eg}_{Ai}\, \mathrm{Im} G_{ij}(\mathbf{r}_A,\mathbf{r}_B,\omega)\, \mu^{ge}_{Bj} \right] - \frac{1}{\omega_0 + \omega \pm i\eta} \left[\mu^{eg}_{Ai}\, \mathrm{Im} G_{ij}(\mathbf{r}_B,\mathbf{r}_A,\omega)\, \mu^{ge}_{Bj} \right] \right\}. \tag{3.19}$$

Equation (3.19) gives the amplitude probability that the electronic excitation is transferred from one atom to the other one, when they are placed near a generic linear magneto-dielectric medium, whose properties are completely included in the Green's tensor expression [117, 152]. Therefore, if the Green's tensor of a particular physical system is known, it is possible to calculate and investigate the resonance energy transfer between two atoms inside the structured environment, considered.

It is easily shown that Eq. (3.19) reduces to the well-known free-space RET amplitude (see Eq. (1.91)) if the atoms are in the free space, without any external environment. This calculation is discussed in detail in the Appendix A.

3.2 Resonance energy transfer in a conducting cylindrical waveguide

In this section we specify our calculation of the resonance exchange of energy between two identical atoms to the case when the atoms are placed inside a perfectly conducting cylindrical waveguide of radius R, as shown in Fig. 3.2 [152]. The outer layer of the waveguide is made of a perfect conductor, while the inner part is empty; the atoms A and B are considered as two two-level system with eigenstates $|e\rangle$ and $|g\rangle$ for the excited and ground state, with energy E_e and E_g,

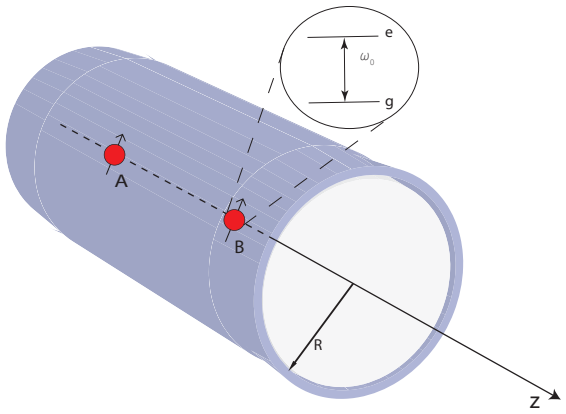

Figure 3.2: The physical system: two identical two-level atoms placed on the axis of a perfectly conducting cylindrical waveguide of radius R [152].

respectively. $\omega_0 = (E_e - E_g)/\hbar$ is the transition frequency for both atoms A and B. We assume they are placed on the waveguide axis, with $z = |\boldsymbol{r}_A - \boldsymbol{r}_B|$ being their distance.

Our purpose is to investigate the effects of the presence of the waveguide on the resonance energy transfer process between the atoms. To achieve this purpose we will use the analytical expression of the energy transfer amplitude (3.19) in terms of the Green's tensor, obtained in the previous section, specifying the specific Green tensor expression describing the conducting cylindrical waveguide, shown in Figures 3.2 and 3.3.

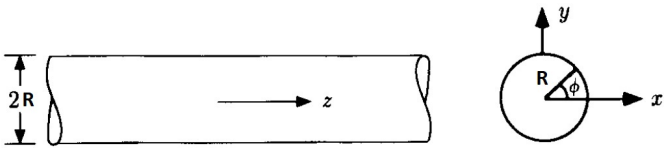

Figure 3.3: A cylindrical waveguide with circular cross section.

The analytical expression of the Green's tensor of a cylindrical waveguide is known in the literature, and it is given by [126] (see also [67, 154])

$$\mathbf{G}(\mathbf{r},\mathbf{r}',\omega) = -\frac{1}{k^2}\delta(\mathbf{r}-\mathbf{r}')\hat{z}\otimes\hat{z} + \sum_{n,m}\Big[c_{\mu n}\mathbf{M}_{\substack{e\\o}n\mu}(\pm k_\mu)\mathbf{M}'_{\substack{e\\o}n\mu}(\mp k_\mu) + c_{\lambda n}\mathbf{N}_{\substack{e\\o}n\lambda}(\pm k_\lambda)\mathbf{N}'_{\substack{e\\o}n\lambda}(\mp k_\lambda)\Big] \qquad (z \gtrless z'), \tag{3.20}$$

where $\mathbf{M}$ and $\mathbf{N}$ are vector cylindrical wave functions given by

$$\mathbf{M}_{\substack{e\\o}mn}(h) = \left[\mp \frac{nJ_n(\mu r)}{r} \begin{matrix}\sin\\\cos\end{matrix}(n\phi)\ \hat{r} - \frac{\partial J_n(\mu r)}{\partial r} \begin{matrix}\cos\\\sin\end{matrix}(n\phi)\ \hat{\phi} \right] e^{ihz}, \tag{3.21}$$

$$\begin{aligned}\mathbf{N}_{\substack{e\\o}mn}(h) = \frac{1}{k}\Bigg[& ih\frac{\partial J_n(\lambda r)}{\partial r} \begin{matrix}\cos\\\sin\end{matrix}(n\phi)\ \hat{r} \mp \frac{ihn}{r} J_n(\lambda r) \begin{matrix}\sin\\\cos\end{matrix}(n\phi)\ \hat{\phi} \\ & + \lambda^2 J_n(\lambda r) \begin{matrix}\cos\\\sin\end{matrix}(n\phi)\ \hat{z} \Bigg] e^{ihz}.\end{aligned} \tag{3.22}$$

Here, $\mu = q_{nm}/R$ and $\lambda = p_{nm}/R$, with p_{nm} being the m-th root of the n-order Bessel function ($J_n(p_{nm}) = 0$), and q_{nm} being the m-th root of the derivative of the n-order Bessel function ($J'_n(q_{nm}) = 0$). λ and μ are the radial components of the wavevector $\mathbf{k}$ ($k = \frac{\omega}{c}$) of the electric field for, respectively, the traverse magnetic (TM) and transverse electric (TE) modes inside the waveguide; likewise, k_λ and k_μ are the axial components of the wavevector, obeying the following relations

$$k_\lambda = \sqrt{k^2 - \lambda^2}, \quad \text{TM modes} \tag{3.23}$$

$$k_\mu = \sqrt{k^2 - \mu^2}, \quad \text{TE modes.} \tag{3.24}$$

The coefficients $c_{\mu n}$ and $c_{\lambda n}$ in Eq. (3.20) are normalization factors, given by

$$c_{\mu n} = i\frac{(2-\delta_{n0})}{4\pi\mu^2 I_{\mu n} k_\mu}, \qquad c_{\lambda n} = i\frac{(2-\delta_{n0})}{4\pi\lambda^2 I_{\lambda n} k_\lambda} \tag{3.25}$$

with the overlap integrals

$$I_{\lambda n} = \int_0^R dr\, r J_n^2(\lambda r) = \frac{R^2}{2} J_n'^2(p_{nm}) \tag{3.26}$$

$$I_{\mu n} = \int_0^R dr\, r J_n^2(\mu r) = \frac{R^2}{2}\left(1 - \frac{n^2}{q_{nm}^2}\right) J_n^2(q_{nm}). \tag{3.27}$$

Since the atoms are placed on the cylinder's axis, the Green's tensor expression (3.20) can be simplified as [67]

$$\mathbf{G}(\mathbf{r}, \mathbf{r}', \omega) = \frac{i}{4\pi} \sum_m \left[\left(\frac{e^{ik_\mu z}}{2I_{\mu 1} k_\mu} + \frac{k_\lambda e^{ik_\lambda z}}{2I_{\lambda 1} k^2} \right) (\hat{r} \otimes \hat{r} + \hat{\phi} \otimes \hat{\phi}) + \frac{\lambda^2 e^{ik_\lambda z}}{I_{\lambda 0} k_\lambda k^2} \hat{z} \otimes \hat{z} \right], \tag{3.28}$$

where the overlap integrals are given by

$$I_{\mu 1} = \frac{R^2}{2}\left(1 - \frac{1}{q_{1m}^2}\right) J_1^2(q_{1m}), \tag{3.29}$$

$$I_{\lambda 1} = \frac{R^2}{4}\Big(J_0(p_{1m}) - J_2(p_{1m})\Big)^2, \tag{3.30}$$

$$I_{\lambda 0} = \frac{R^2}{2} J_1^2(p_{0m}). \tag{3.31}$$

It is important to point out that the presence of the cylindrical waveguide significantly changes the density of states of the electromagnetic field inside of it; owing to the boundary conditions on the perfectly conducting shell, the wavevector radial components assume discrete values and depend on the cylinder radius R,

$$\mu = q_{nm}/R \qquad \text{for TE modes,} \tag{3.32}$$

$$\lambda = p_{nm}/R \qquad \text{for TM modes,} \tag{3.33}$$

which means that only electric field with specific radial components can exist inside the waveguide. Radial field modes also depend on the waveguide radius R, so they can be strongly modified by changing the geometry of the system, in particular its radius. The waveguide determines a lower cut-off frequency for the TE and TM field modes, given by

$$(\omega_{min})_{TM} \simeq \frac{2.4c}{R}, \tag{3.34}$$

$$(\omega_{min})_{TE} \simeq \frac{1.8c}{R}, \tag{3.35}$$

where $p_{01} \simeq 2.4$ and $q_{11} \simeq 1.8$ are the smallest roots of the Bessel function and its derivative, respectively. Therefore only field modes (TE or TM) with frequency $\omega > (\omega_{min})_{TE(TM)}$ can propagate inside the waveguide; since the cut-off frequency depends on R^{-1}, it is possible to change and thus control the density of states and the field modes inside the waveguide, through its radius. This allows to control the transfer of energy between the atoms by means of a macroscopic parameter of the system, that is the guide radius. The presence of a lower cut-off frequency, as we will demonstrate below, has a strong effect on the exchange of energy between the atoms: if $k_0 R \ll 1$, the atomic transition frequency is smaller than the waveguide cut-off frequency, $\omega_0 < \omega_{min}$, and this means that the waveguide suppresses the field modes resonant with the atomic transition frequency. Since they cannot contribute to the exchange of excitation between the atoms, the energy transfer is significantly suppressed in this regime. Otherwise, when $\omega_0 > \omega_{min}$, that is when $k_0 R \gtrsim 1$, the resonant field modes can contribute to the excitation transfer, and

we expect that the energy transfer process is much less influenced by the presence of the waveguide.

It is relevant to point out that in the first regime, $\omega_0 < \omega_{min}$, the waveguide cut-off frequency ω_{min} becomes the lower limit of the frequency integral in the RET amplitude expression (3.19); on the other hand, when $\omega_0 > \omega_{min}$, the lower limit of integration can be set to zero because the contribution from resonant field modes to the energy transfer is much more relevant with respect to any other contribution from non-resonant field modes. For these reasons, in our research work we investigate the resonance energy transfer between the atoms in the case $k_0 R \ll 1$, that is $\omega_0 < \omega_{min}$, for which the presence of the cylindrical guide is expected to be more relevant with respect to the case when $\omega_0 > \omega_{min}$.

On this basis, we start from the generic expression for the RET amplitude obtaining in the previous section, written in terms of the Green's tensor

$$M = \frac{1}{\pi\epsilon_0 c^2}\int_{\omega_{min}}^{\infty} d\omega\, \omega^2 \sum_{ij}\left\{\frac{1}{\omega_0 - \omega \pm i\eta}\left[\mu_{Ai}^{eg}\, \mathrm{Im}G_{ij}(\mathbf{r}_A, \mathbf{r}_B, \omega)\, \mu_{Bj}^{ge}\right] - \frac{1}{\omega_0 + \omega}\left[\mu_{Ai}^{eg}\, \mathrm{Im}G_{ij}(\mathbf{r}_B, \mathbf{r}_A, \omega)\, \mu_{Bj}^{ge}\right]\right\}, \tag{3.36}$$

valid when $k_0 R \ll 1$, as discussed before. In this regime, we wish to point out that there is not a resonant pole at $\omega = \omega_0$, right because $\omega_0 < \omega_{min}$. Since the waveguide Green's tensor (3.28) is symmetric with respect to the exchange of the atomic positions, $\mathrm{Im}\, G_{ij}(\mathbf{r}_A, \mathbf{r}_B, \omega) = \mathrm{Im}\, G_{ij}(\mathbf{r}_B, \mathbf{r}_A, \omega)\ \forall i, j, \omega$, the energy transfer amplitude (3.36) becomes

$$M = \frac{2}{\pi\epsilon_0}\sum_{ij}\mu_{Ai}^{eg}\,\mu_{Bj}^{ge}\int_{k_{min}}^{\infty} dk \frac{k^3}{k_0^2 - k^2}\mathrm{Im}\, G_{ij}(\mathbf{r}_A, \mathbf{r}_B, \omega). \tag{3.37}$$

where $k_{min} = \omega_{min}/c$. Since the cylindrical Green's tensor (3.28) is also diagonal, the energy transfer amplitude (3.37) can be written as a sum of three independent terms

$$M = M_z + M_r + M_\phi, \tag{3.38}$$

where

$$M_z = \frac{(\boldsymbol{\mu}_A^{eg}\cdot\hat{z})(\boldsymbol{\mu}_B^{ge}\cdot\hat{z})}{2\pi^2\epsilon_0}\sum_m \frac{\lambda^2}{I_{\lambda 0}}\int_{k_{min}}^{\infty} dk \frac{k\cos(k_\lambda z)}{(k_0^2 - k^2)k_\lambda}, \tag{3.39}$$

$$M_r = \frac{(\boldsymbol{\mu}_A^{eg}\cdot\hat{r})(\boldsymbol{\mu}_B^{ge}\cdot\hat{r})}{4\pi^2\epsilon_0}\sum_m \int_{k_{min}}^{\infty} dk \frac{k^3}{k_0^2 - k^2}\left(\frac{\cos(k_\mu z)}{I_{\mu 1}k_\mu} + \frac{k_\lambda\cos(k_\lambda z)}{I_{\lambda 1}k^2}\right), \tag{3.40}$$

$$M_\phi = \frac{(\boldsymbol{\mu}_A^{eg}\cdot\hat{\phi})(\boldsymbol{\mu}_B^{ge}\cdot\hat{\phi})}{4\pi^2\epsilon_0}\sum_m \int_{k_{min}}^{\infty} dk \frac{k^3}{k_0^2 - k^2}\left(\frac{\cos(k_\mu z)}{I_{\mu 1}k_\mu} + \frac{k_\lambda\cos(k_\lambda z)}{I_{\lambda 1}k^2}\right), \tag{3.41}$$

and the imaginary part of the cylindrical Green's tensor (3.28) has been written explicitly.

Let us now investigate in detail the behaviour of the resonance exchange of energy between the atoms in the regime $Rk_0 \ll 1$, as a function of the relevant parameters of the system: the interatomic distance $z = \mid \mathbf{r}_A - \mathbf{r}_B \mid$, the waveguide lower cut-off frequency ω_{min}, or equivalently the waveguide radius R, and the orientation of the atomic dipoles relative to the waveguide axis. For symmetry reasons, we need to consider only the two following cases: axial dipoles (M_z contribution) and radial dipoles (M_r contribution), relative to the waveguide axis.

3.2.1 Energy transfer amplitude for axial atomic dipole moments

Les us now first investigate the case when the atoms have electric dipole moments parallel between each other and oriented along the positive z axis, that is along the waveguide axis [152]. In the regime $Rk_0 \ll 1$ we are investigating, the energy transfer amplitude M (3.38) is given only by the M_z term

$$M_z = \frac{\mu_{Az}^{eg}\mu_{Bz}^{ge}}{2\pi^2\epsilon_0}\sum_m \frac{\lambda^2}{I_{\lambda 0}}\int_{k_{min}}^{\infty} dk \frac{k\cos(k_\lambda z)}{(k_0^2-k^2)k_\lambda}, \tag{3.42}$$

because M_r and M_ϕ contributions vanish (see Eqs. 3.40 and 3.41). The integral over the wavevector k in (3.42) can be written as

$$\begin{aligned}\int_{k_{min}}^{\infty} dk \frac{k\cos(k_\lambda z)}{(k_0^2-k^2)k_\lambda} &= \int_{k_{min}}^{\infty} dk \frac{k\cos\left(\sqrt{k^2-\lambda^2}z\right)}{(k_0^2-k^2)\sqrt{k^2-\lambda^2}} \\ = \int_0^{\infty} dk_\lambda \frac{\cos(k_\lambda z)}{k_0^2-\lambda^2-k_\lambda^2}&, \end{aligned} \tag{3.43}$$

where, in the last row, a change of variable has been done using $k_\lambda = \sqrt{k^2-\lambda^2}$, taking into account that λ is constant with respect to the integration variable k_λ. We wish to point out that in the regime $Rk_0 \ll 1$ there is not a resonant pole at $k = k_0$ in the k integral, because $k_0 < k_{min}$. On the other hand the integral in Eq. (3.43) has poles at the imaginary values $k_\lambda = \pm i\sqrt{\lambda^2-k_0^2}$, and using the residue theorem, we obtain

$$\int_0^{\infty} dk_\lambda \frac{\cos(k_\lambda z)}{k_0^2-\lambda^2-k_\lambda^2} = -\frac{\pi e^{-\sqrt{\lambda^2-k_0^2}z}}{2\sqrt{\lambda^2-k_0^2}}. \tag{3.44}$$

Therefore the energy transfer amplitude is

$$M_z = -\frac{\mu_{Az}^{eg}\mu_{Bz}^{ge}}{4\pi\epsilon_0}\sum_m \frac{\lambda^2}{I_{\lambda 0}}\frac{e^{-\sqrt{\lambda^2-k_0^2}z}}{\sqrt{\lambda^2-k_0^2}}, \tag{3.45}$$

where the sum on m is over all allowed radial field modesinside the waveguide.

We now briefly show that this series converges. When $m \to +\infty$ and thus $p_{nm}, q_{nm} \to +\infty$, the asymptotic expansion of the Bessel functions of the first kind for large arguments can be used [26–28]

$$J_n(p_{nm}) \simeq \sqrt{\frac{2}{\pi p_{nm}}} \cos\left(p_{nm} - \frac{n\pi}{2} - \frac{\pi}{4}\right), \tag{3.46}$$

and the expansion for large Bessel zeros is given by the McMahon asymptotic expansion

$$p_{nm} \simeq (m + \frac{n}{2} - \frac{1}{4})\pi - \frac{4n^2 - 1}{8(m + \frac{n}{2} - \frac{1}{4})\pi} + \dots. \tag{3.47}$$

For large m, only the first term of expansion (3.47) can be considered, leading to

$$\begin{aligned} I_{\lambda 0} =& \frac{R^2}{2} J_1^2(p_{0m}) \simeq \frac{R^2}{2} \frac{2}{\pi p_{0m}} \cos^2\left(p_{0m} - \frac{\pi}{2} - \frac{\pi}{4}\right) \\ \simeq& \frac{R^2}{2\pi^2(m - \frac{1}{4})}, \end{aligned} \tag{3.48}$$

and

$$\lambda = \frac{p_{0m}}{R} \simeq \frac{(m - \frac{1}{4})\pi}{R}, \tag{3.49}$$

where, in the last row of Eq. (3.48) the cosine squared has been mediated to 1/2. Thus, for large m, the series becomes

$$\sum_m \frac{\lambda^2}{I_{\lambda 0}} \frac{e^{-\sqrt{\lambda^2 - k_0^2} z}}{\sqrt{\lambda^2 - k_0^2}} \simeq \sum_m \frac{2\pi^4 (m - \frac{1}{4})^3}{R^3 \sqrt{\pi^2 (m - \frac{1}{4})^2 - k_0^2 R^2}} e^{-\sqrt{\pi^2 (m - \frac{1}{4})^2 - k_0^2 R^2} \frac{z}{R}}. \tag{3.50}$$

Since m run from one to infinity, this is a non-negative series and we can exploit the root test to verify its convergence. Performing the root test, we get

$$\begin{aligned} &\lim_{m \to +\infty} \sqrt[m]{\frac{(m - \frac{1}{4})^3}{\sqrt{\pi^2 (m - \frac{1}{4})^2 - k_0^2 R^2}} e^{-\sqrt{\pi^2 (m - \frac{1}{4})^2 - k_0^2 R^2} \frac{z}{R}}} \\ &= \lim_{m \to +\infty} \sqrt[m]{\frac{m^2}{\pi} e^{-\frac{\pi m z}{R}}} = e^{-\frac{\pi z}{R}}, \end{aligned} \tag{3.51}$$

and since the result of the limit is smaller than one, the series converges. Once we have checked the convergence of the expression (3.45), we have numerically verified explicitly that a good estimate for the resonance energy transfer amplitude can be obtained by taking only the first thirty terms of the sum over m. We can now

investigate the RET amplitude between the two atoms with axial dipoles as a function of the interatomic distance z and the waveguide lower cut-off frequency ω_{min}.

Bearing in mind that $Rk_0 \ll 1$, that is $\omega_0 < \omega_{min}$, we have evaluated numerically the energy transfer amplitude (3.45) as a function of the atomic separation z in two different regimes: when the interatomic distance is smaller or larger than the atomic transition wavelength, that is, respectively, the near zone regime, $z < \lambda_0$, and the far zone regime, $z > \lambda_0$. In our numerical evaluation, we have chosen the waveguide radius equal to $R = 10^{-8}$ m, and the atomic transition wavelength $\lambda_0 = 5 \cdot 10^{-7}$ m, a typical wavelength value in the visible range of the electromagnetic spectrum.

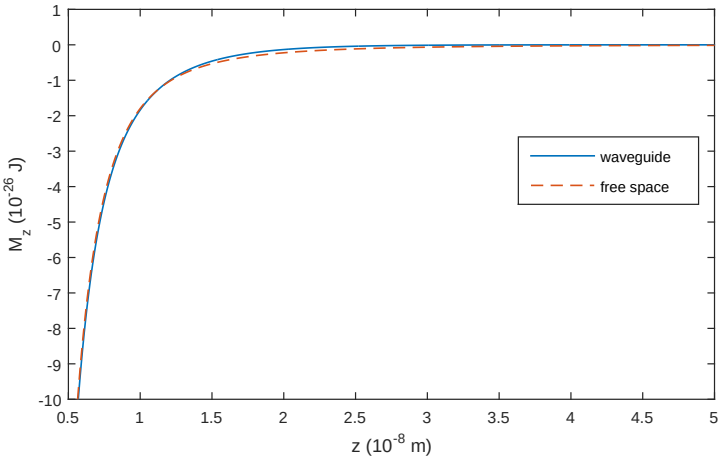

Figure 3.4: Comparison between the energy transfer amplitude $M = M_z$ (axial dipoles) in the free space (orange dashed line) and in the waveguide (blue solid line), as a function of the interatomic distance z, for $z < \lambda_0$ (near-zone). The numerical values of the parameters are chosen such that $\lambda_0 = 5 \cdot 10^{-7}$ m, $R = 10^{-8}$ m, and $\mu^{eg}_{A(B)\,z} = 10^{-30}$ C $\cdot$ m.

Fig. 3.4 shows the energy transfer amplitude between two atoms with axial dipoles, in the near zone, as a function of the interatomic distance z, when they are placed inside the waveguide (Eq. 3.45), depicted as the blue continuous curve. It is compared with the near zone resonance energy transfer amplitude between two axial atomic dipoles in the free space that is given by

$$(M_z)_{fs} \simeq -\frac{\mu^{eg}_{Az}\mu^{ge}_{Bz}}{2\pi\epsilon_0 z^3}\cos(k_0 r), \qquad \text{for } \; k_0 z \ll 1, \tag{3.52}$$

depicted as the orange dashed line in Fig. 3.4. The plot shows that the behaviour of the RET inside the waveguide is very similar to that in the free space case.

In order to better highlight relevant differences, in Fig. 3.5 we plot the ratio between the energy transfer amplitudes in the waveguide and in the free space, as a function of z. The plot shows that for $z \lesssim 1.2 \cdot 10^{-8}$ m the two amplitudes

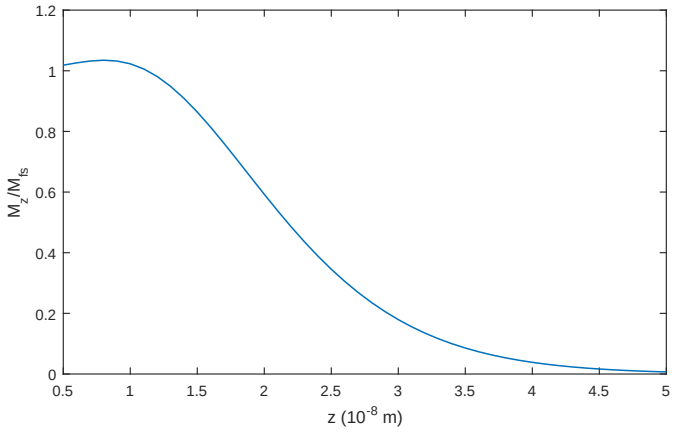

Figure 3.5: Energy transfer amplitude between atoms with axial dipoles, in the near zone, normalised to the free-space energy transfer amplitude, as a function of the interatomic distance z. When z approaches the transition region between near and far zone ($z \sim \lambda_0$), the amplitude in the waveguide becomes more and more suppressed with respect to the free-space case. The parameters used are $\lambda_0 = 5 \cdot 10^{-7}$ m, $R = 10^{-8}$ m and $\mu^{eg}_{A(B)\,z} = 10^{-30}$ C $\cdot$ m.

are essentially the same, while for $z \gtrsim 1.2 \cdot 10^{-8}$ m, when the intermediate region between the near and far zone is approached, the energy transfer amplitude in the waveguide becomes more and more suppressed. This result is related to the fact that in the very near zone range, when $z \ll \lambda_0$, the interaction between the atoms is essentially an electrostatic dipole-dipole interaction, that is not significantly modified by the waveguide. Approaching the intermediate region, $z \sim \lambda_0$, the exchange of energy between the atoms start to become a radiative process and, since $Rk_0 \ll 1$, the effect of the waveguide on the amplitude is relevant, leading to a significant suppression of the resonance energy transfer.

On the contrary, in the far zone limit, for $z \gg \lambda_0$, the plot in Fig. 3.6 shows that the energy transfer in the waveguide is strongly inhibited with respect to the free-space case, given by

$$(M_z)_{fs} \simeq -\frac{\mu^{eg}_{Az}\mu^{ge}_{Bz}}{2\pi\epsilon_0 z^2} k_0 \sin(k_0 r), \qquad \text{for } \; k_0 z \geq 1. \tag{3.53}$$

The energy transfer amplitude inside the waveguide does not show the typical free-space spatial oscillations, and a numerical analysis shows that it is several

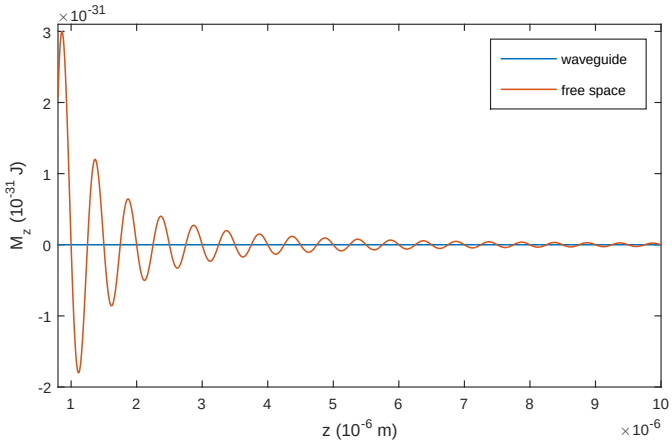

Figure 3.6: Comparison between the energy transfer amplitude $M = M_z$ (axial dipoles) in the free space (orange continuous line) and in the waveguide (blue solid line), as a function of the interatomic distance z, for $z \gg \lambda_0$ (far-zone). The numerical values of the parameters are chosen such that $\lambda_0 = 5 \cdot 10^{-7}$ m, $R = 10^{-8}$ m, and $\mu^{eg}_{A(B)\,z} = 10^{-30}$ C $\cdot$ m.

tens orders of magnitude smaller with respect to the one in the free space:

$$\frac{M_z}{(M_z)_{fs}} \sim 10^{-90} \quad \text{for} \quad k_0 z \geq 1, \tag{3.54}$$

meaning that it is virtually zero, totally inhibited by the waveguide, for $z > \lambda_0$.

The results obtained show that, since in the regime $Rk_0 \ll 1$ the resonant field modes are suppressed by the waveguide ($\omega_0 < \omega_{min}$), the energy transfer between the atoms is slightly modified in the very near zone, more and more suppressed approaching the intermediate region, and totally inhibited (virtually zero) in the far zone. The completely different effect of the waveguide in the near and in the far zone is due to the fact that in the near zone the resonance energy transfer is a radiationless process, mediated by virtual photons, and thus slightly modified by the external environment, the waveguide in our case. On the contrary, when the atoms are in the far zone regime, the RET is a radiative process, and the main contribution is due to the exchange of the resonant real photon between the atoms; since $Rk_0 \ll 1$, the waveguide suppresses the exchange of the real photon, leading to a complete inhibition of the resonance energy transfer process [152].

Let us now investigate the energy transfer amplitude as a function of the waveguide cut-off frequency $\omega_{min} \propto \frac{1}{R}$, which means as a function of the cylinder radius R. By decreasing R, the cut-off frequency ω_{min} increases and thus the gap between ω_0 and ω_{min} increases too, further suppressing more modes near the resonance atomic frequency ω_0. This involves a further reduction of the energy transfer am-

plitude between the atoms owing to the decrease of the waveguide radius. Fig. 3.7 shows the numerical results for the energy transfer amplitude when the atoms are in the near zone, as a function of the waveguide radius R, (blue solid line). The atomic transition wavelength and the atomic separation are now fixed to specific values, $\lambda_0 = 5 \cdot 10^{-7}$ m and $z = 10^{-8}$ m, respectively. In this regime, when the

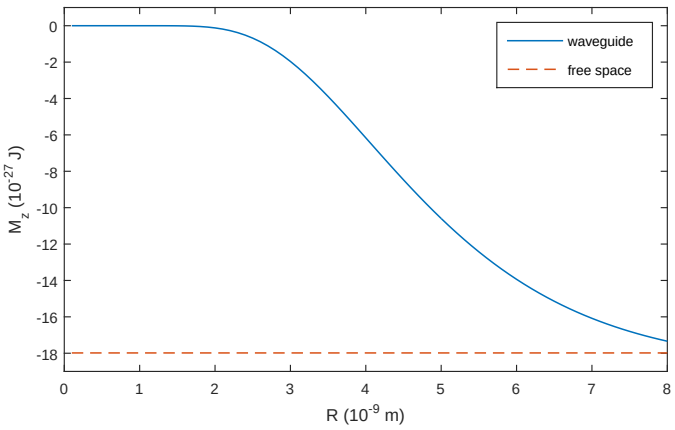

Figure 3.7: The energy transfer amplitude M_z for axial dipoles placed inside the waveguide in the near zone, $z < \lambda_0$, as a function of the waveguide radius R (blue solid line) . The orange horizontal line is the value of the energy transfer amplitude in the free space. The numerical values of the parameters are $z = 10^{-8}$ m, $\lambda_0 = 5 \cdot 10^{-7}$ m and $\mu^{eg}_{A(B)\,z} = 10^{-30}$ C $\cdot$ m.

waveguide radius R is increased, and thus the gap between ω_0 and ω_{min} decreases, the absolute value of the energy transfer amplitude first increases and then settles to an almost constant value. On the contrary, by decreasing R, the energy transfer amplitude quickly tends to vanish, as expected, for the reasons mentioned above. The orange dashed line in the figure is the energy transfer amplitude between the two atoms in the free space (see Eq. 3.53), calculated for $z = 10^{-8}$ m and $\lambda_0 = 5 \cdot 10^{-7}$ m. Here, the RET amplitude in the far zone limit as a function of R is not plotted since, as we have previously highlighted, it is essentially zero when the interatomic distance is larger than the atomic transition wavelength.

These results clearly show that the transfer of energy between the atoms inside the waveguide can be strongly modified and controlled by varying the waveguide's radius R.

3.2.2 Energy transfer amplitude for radial atomic dipole moments

We now consider the case of atomic dipole moments along the radial direction, that is orthogonal to the guide axis, and parallel to each other [152]. In this case, the energy transfer amplitude M is given only by the term M_r, while the contributions M_z and M_ϕ vanish. The analytic expression of the energy transfer amplitude for radial dipoles, when $Rk_0 \ll 1$, can be obtained from Eq. (3.40), after performing the integral over k, yielding

$$M_r = \frac{\mu_{Ar}^{eg}\mu_{Br}^{ge}}{8\pi\epsilon_0}\sum_m\left(-\frac{k_0^2 e^{-\sqrt{\mu^2-k_0^2}z}}{I_{\mu 1}\sqrt{\mu^2-k_0^2}}+\frac{\sqrt{\lambda^2-k_0^2}e^{-\sqrt{\lambda^2-k_0^2}z}}{I_{\lambda 1}}\right). \tag{3.55}$$

As already done for the axial dipoles case, using the root test, we have checked that the sum over radial field modes in (3.55) converges; a numerical analysis shows that the first forty terms of the sum give a good numerical estimate of the energy transfer amplitude, in the range of the parameters we are considering. As in the case of axial dipoles, we investigate M_r as a function of the interatomic distance z and the waveguide cut-off frequency ω_{min}.

Fig. 3.8 shows the energy transfer amplitude as a function of the interatomic distance z, when the atoms are in the near zone limit, using the same values as before for the atomic transition wavelength, $\lambda_0 = 5\cdot 10^{-7}$ m, and for the waveguide radius, $R = 10^{-8}$ m. The orange dashed line is the energy transfer amplitude

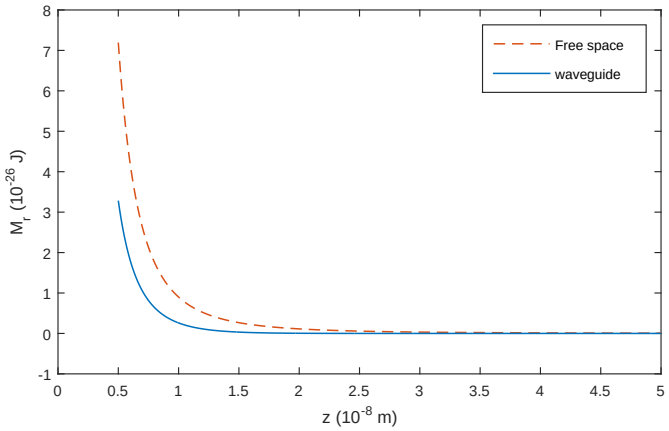

Figure 3.8: The energy transfer amplitude for radial dipoles in the near zone, $z < \lambda_0$, as a function of the interatomic distance z. The blue solid line is for atoms in the waveguide, while the orange dashed line refers to the free-space case. The parameters used are $\lambda_0 = 5\cdot 10^{-7}$ m, $R = 10^{-8}$ m and $\mu_{A(B)\,z}^{eg} = 10^{-30}$ C $\cdot$ m.

when atomic radial dipoles are in the free space and in the near zone, given by the following expression

$$(M_r)_{fs} \simeq \frac{\mu_{Ar}^{eg}\,\mu_{Br}^{ge}}{4\pi\epsilon_0 z^3}\cos(k_0 z). \tag{3.56}$$

In this regime, the energy transfer amplitude inside the waveguide is reduced with respect to the free-space case, and this effect results to be much larger with respect of the previous case of axial dipoles. The reduction of the energy transfer amplitude significantly grows as the transition region between near and far zone is approached: as an example, for $z = 5 \cdot 10^{-8}$ m, M_r is reduced of about three orders of magnitude with respect to $(M_r)_{fs}$. In the far zone limit, which means when $z \gg \lambda_0$, our numerical analysis shows that the behaviour of the energy transfer is very similar to that for axial dipoles case: the waveguide strongly suppresses the energy transfer process, which is virtually zero.

These results confirm that the energy transfer amplitude is significantly affected by the presence of the waveguide, also when the electric dipole moments are orthogonal to the cylinder axis. The amplitude is more and more reduced with respect to the free-space case, when the transition region at $z \sim \lambda_0$ is being reached, and completely suppressed in the far zone. When the atoms are in the very near zone limit, that is for $z \in [5 \cdot 10^{-10}$ m $; 10^{-8}$ m $]$, the suppression of the energy transfer is more relevant for radial atomic dipoles than for the axial dipoles.

We now consider the excitation exchange between the atoms in the near zone, as a function of the waveguide cut-off frequency ω_{min}, or equivalently, of the waveguide radius R. Fig. 3.9 shows that the energy transfer amplitude decreases for decreasing R, as expected because the difference between the atomic transition frequency ω_0 and the waveguide cut-off frequency ω_{min} increases. In the range considered, it is always smaller than the energy transfer amplitude in the free space, given in the figure by the orange dashed line, even if of the same order of magnitude. The plot clearly shows the possibility to control, through the waveguide radius R, also the exchange of energy between two atomic radial dipoles [152].

3.3 Conclusions

In this Chapter we have presented our original work on the resonance exchange of energy between two identical atoms, interacting with the quantum electromagnetic vacuum, placed in a macroscopic environment, such as a perfectly conducting cylindrical waveguide [152].

Firstly, an analytical expression for the energy transfer amplitude between two atoms when they are in the presence of a generic external environment has been introduced: to achieve this purpose the Green's tensor formalism has been

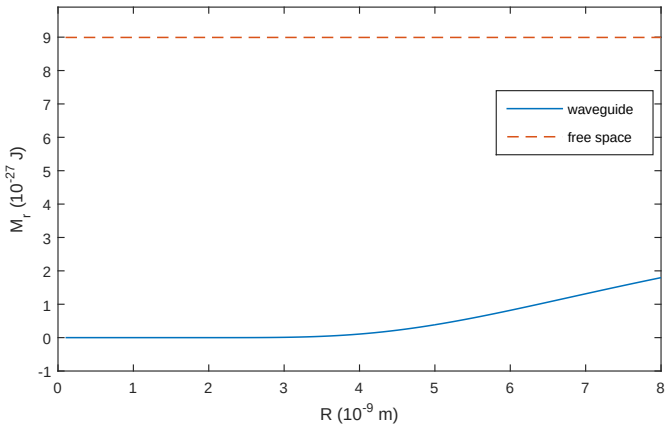

Figure 3.9: The energy transfer amplitude M_r for radial dipoles in the near zone ($z < \lambda_0$), as a function of the waveguide radius R, for atoms inside a cylindrical waveguide (blue continuous line). The orange horizontal line represents the value of the amplitude in the free space. Parameters are $z = 10^{-8}$ m, $\lambda_0 = 5 \cdot 10^{-7}$ m and $\mu^{eg}_{A(B)\,z} = 10^{-30}$ C $\cdot$ m.

used. We have then considered the specific case of the energy transfer between two atoms placed on the axis of a perfectly conducting cylindrical waveguide, which determines a lower cut-off frequency for the electromagnetic modes inside it. Both cases of atomic dipole moments parallel and orthogonal to the axis of the waveguide have been investigated. When the atomic transition frequency is smaller than the cut-off frequency of the waveguide, we have shown that the presence of the waveguide can significantly change the energy transfer amplitude, depending on the distance between the two atoms compared to their transition wavelength (radiationless near zone or radiative far zone). It has been shown that, when the atomic transition frequency is smaller than the waveguide lower cut-off frequency, the energy transfer process is strongly suppressed in the far zone, whereas it is much less influenced in the intermediate and near zone; this latter effect is much larger for radial atomic dipoles than for axial dipoles. A physical interpretation of this result has been given. We have also shown the possibility to strongly manipulate and control the resonant transfer of energy between the atoms through the waveguide radius: decreasing the cylinder radius it is possible to suppress or even totally inhibit the transfer of energy between the atoms. These results show how the presence of the external environment, the cylindrical waveguide in our case, can significantly change the radiation-mediated electronic exchange of energy between the atoms, yielding possibility of controlling it through external actions.

Chapter 4

Resonance interaction between two entangled atoms in non-equilibrium conditions and in an external environment

The resonance dipole-dipole interaction is a quantum interaction between two atoms or molecules, one excited and the other in its ground state, prepared in an entangled state, mediated by the quantum electromagnetic field, as outlined in Chapter 1. From a quantum electrodynamical point of view, is one of the simplest and fundamental intermolecular interactions, arising from the exchange of virtual and real photons between the quantum emitters [11]. In recent years, many investigations have concerned with the resonant forces between atoms or molecules, that occur when one or more atoms are in an excited state [155]. In this case, the interaction can be mediated by the exchange of a real photon and it can be a very long-range interaction, scaling as r^{-1} for atoms in the free space.

If the two atoms, one excited and the other in its ground state, are uncorrelated, the resonant van der Waals/Casimir-Polder force is a fourth-order process in the atom-field coupling, and asymptotically scales as r^{-2}: in this case controversial results exist in the literature concerning with the presence or not of spatial oscillations in the far zone limit[49, 156–158]. A different, albeit related, phenomenon takes place when two identical atoms, one excited and the other in the ground state, are prepared in a symmetric or antisymmetric entangled state [9, 11]. In this case, the excitation is delocalized between them, and the interaction is a second-order effect in the coupling with the transverse field, asymptotically scaling as r^{-1} (far zone limit). Resonance forces are particularly relevant because they are much more intense than dispersion interactions, for example as van der Waals/Casimir-Polder interactions both for ground-state and excited atoms, and

almost comparable with the Casimir-Polder interaction between a ground-state atom and a mirror. From a physical point of view, the resonance interaction is a second-order effect because the correlated state has non-vanishing unperturbed dipole-dipole correlations, whereas, for dispersion interactions, correlated dipole moments must be induced by vacuum field fluctuations [70, 108, 159, 160].
Despite their strength, resonance forces has not been yet observed directly, since this detection requires that the system be prepared in an entangled state and that its coherence be preserved over a sufficiently long time: this makes them extremely difficult to observe. In fact, the correlated state is a very fragile state because the spontaneous emission or the influence of the environment can destroy its coherent superposition, eventually leading the system to a factorized state. In this case, the force between the atoms, one excited and the other in its ground state, becomes the well-known fourth-order Casimir-Polder interaction.

For these reasons, the possibility of manipulating resonance forces between quantum emitters through static or time-modulated external environments experimentally achievable (i.e. reflecting mirrors, cavities, waveguides, photonic crystals), have been recently investigated, becoming a fundamental field of research [115, 116, 145, 152, 161–163]. In fact, exploiting appropriate environments, from one side it could be possible to preserve the correlated atomic state for a longer time, and on the other side to enhance the resonance force between the atoms, allowing to its direct detection. The observation of the resonance force, in particular in the retarded regime, would be an important confirmation of an effect due to the quantum coherence of the system. It could be also relevant in different physical processes and in other fields, such as biology: for example, the possible fundamental role of resonant interactions in bio-molecular systems has been recently argued [164–166]. An analogous interaction, mediated by the exchange of an electron in the continuum band of the wire, has been shown for two impurities (adatoms) embedded in a semiconductor quantum wire [167, 168].

The Chapter introduces our original works on the resonance force between two correlated atoms and is divided in two main parts, considering two different relevant aspects of the resonance interaction, i.e. a non-equilibrium condition, and the presence of an external environment [152, 169].

In the first section of the Chapter, a non-equilibrium condition for the resonance interaction between two atoms is considered. The time-dependent resonance interaction energy between two identical two-level atoms, during the dynamical self-dressing process of the system has been first investigated [169]. The two atoms, one excited state and the other in its ground-state, are initially prepared in a symmetric or antisymmetric entangled state, and are in the empty space, interacting with the electromagnetic field in the vacuum state. Since the initial state of the system is not an eigenstate of the total Hamiltonian, it evolves in time, and we

investigate the time-dependent resonance interaction during the dressing process of the two-atoms-field interacting system. We find that this interaction is equal to zero when the two atoms are outside the light-cone of each other, in agreement with the relativistic causality, while it sharply settles to its stationary value after the causality time $t = R/c$ (R being the interatomic distance). We show that the behaviour of the time-dependent resonance interaction can be related to an interference effect between the contributions from rotating and counterrotating terms, bringing the system to its local equilibrium configuration immediately after the causality time. The time-dependent electric energy density in the space around the two correlated atoms has been also investigated, and its behaviour in both cases of subradiant (symmetrical) and superradiant (antisymmetrical) initial state is discussed. In particular, we show that for points at the same distance from the two atoms, the value of the electric energy density is zero for atoms prepared in the subradiant state, whereas it is doubled with respect to the case of uncorrelated atoms, if the atoms are in the superradiant superposition. Finally, the possibility to probe this result through a measurement of the Casimir-Polder force on a third atom, placed near the two-atom system, is discussed.

In the second section of the Chapter, the possibility to modify and control the resonance interaction energy between two correlated atoms through an external static environment, specifically a cylindrical waveguide, is investigated [152]. The results obtained are mathematically partially based on our results for the resonance energy transfer between two atoms in a cylindrical waveguide, presented in Chapter 3. An analytical expression for the resonance interaction energy between two quantum emitters in the presence of a generic magneto-dielectric medium is first obtained, using the electromagnetic Green's tensor formalism. Then, we consider the particular case of two entangled atoms inside a perfectly conducting cylindrical waveguide, and we study the resonance interaction energy as a function of the atomic distance, the waveguide radius and the atomic dipoles orientation. We evaluate numerically the resonance interaction in the regime in which the field modes resonant with the atomic transition frequency are suppressed by the waveguide, explicitly showing a suppression of the resonance interaction with respect to that in the free space: in the far (radiative) zone, the effect of the waveguide significantly modifies the interaction yielding to a total inhibition of the process; on the other hand, in the near (radiationless) zone the suppression of the interaction is much less relevant. This is analogous to what we obtained in Chapter 3 for the resonant energy transfer process between two atoms. We also show that, for the case of atomic dipole moments orthogonal to the cylinder axis, the waveguide can even change the character of the resonance force, turning it from repulsive to attractive. Finally, the possibility to strongly manipulate and control the resonance interaction and force through the waveguide radius is shown.

The Chapter is structured as follows: in Sec. 4.1 we consider the time-dependent resonance interaction energy between two entangled identical atoms, one in the ground state and the other in its excited state, interacting with the vacuum radiation field, during a non-equilibrium situation, such as the dynamical atomic self-dressing process. We also investigate the time-dependent electric energy density in the space around the two correlated atoms, in both cases of antisymmetric (subradiant) and symmetric (superradiant) states, during the dressing process of the two-atom system. In Sec. 4.2 we first introduce an analytical expression for the resonance interaction energy between two correlated atoms, in the presence of a generic magneto-dielectric medium, in terms of the electromagnetic Green's tensor. We will then consider the resonance interaction energy when the atoms are placed inside a perfectly conducting cylindrical waveguide, studying it as a function of the relevant parameters of the system, that is atomic dipole orientations, the waveguide radius and the interatomic distance. Finally, Sec. 4.3 is devoted to our conclusions and final remarks.

4.1 Time-dependent resonance interaction between two entangled atoms

In this Section, the time-dependent resonance interaction energy between two identical atoms, during the dynamical self-dressing process of the system is investigated. We consider two atoms, labelled A and B and modelled as two-level systems, respectively placed at positions $\boldsymbol{r}_A$ and $\boldsymbol{r}_B$ in the free space, and interacting with the quantum electromagnetic field in its vacuum state [169]. The atomic system, with one atom in the excited state and the other in the ground state, is initially prepared in a correlated symmetric or antisymmetric Dicke state [170],

$$|\phi_\pm\rangle = \frac{1}{\sqrt{2}}\Big(|e_A, g_B\rangle \pm |g_A, e_B\rangle\Big), \tag{4.1}$$

and the radiation field is in the vacuum state $|0\rangle$; the initial state of the system is thus the bare state

$$|\psi_\pm\rangle = |\phi_\pm\rangle\,|0\rangle\,, \tag{4.2}$$

with energy $E_\psi = 0$. Since the initial state (4.2) is not an eigenstate of the total Hamiltonian, it will evolve in time according to

$$|\psi_\pm(t)\rangle = e^{-iHt/\hbar}|\psi_\pm\rangle, \tag{4.3}$$

where H is the total Hamiltonian of the system. The interaction energy will therefore be time-dependent, because the system starts from a dynamical non-equilibrium state, and we shall investigate the dynamical resonance interaction during the dressing process of the atoms-field interacting system.

The Hamiltonian of the system in the multipolar coupling scheme, in the Coulomb gauge and within the dipole approximation, is [6]

$$H = H_0 + H_i \tag{4.4}$$

where

$$H_0 = \hbar\omega_0(S_z^A + S_z^B) + \sum_{\mathbf{k}j} \hbar\omega_k a_{\boldsymbol{k}j}^\dagger a_{\boldsymbol{k}j} \tag{4.5}$$

is the free Hamiltonian, and

$$H_i = -\boldsymbol{\mu}_A \cdot \boldsymbol{E}(\boldsymbol{r}_A) - \boldsymbol{\mu}_B \cdot \boldsymbol{E}(\boldsymbol{r}_B) \tag{4.6}$$

is the interaction Hamiltonian. The unperturbed Hamiltonian H_0 is the sum of the atomic and radiation field Hamiltonians. In the expressions above, $S_z = \frac{1}{2}(|e\rangle\langle e| - |g\rangle\langle g|)$ is the pseudospin atomic operator, $|g\rangle$ and $|e\rangle$ are the ground and the excited atomic states with energies $\mp\hbar\omega_0/2$, respectively, with ω_0 being the atomic transition frequency. $\boldsymbol{\mu}_i = e\boldsymbol{r}_i$ is the atomic dipole moment operator of atom $i = A, B$, that can be conveniently written as

$$\boldsymbol{\mu}_i = \boldsymbol{\mu}_i^{eg}(S_+^i + S_-^i), \tag{4.7}$$

where $\boldsymbol{\mu}_i^{eg} = \langle e \mid \boldsymbol{\mu}_i \mid g\rangle$ is the matrix element of the atomic dipole moment between the states $|e\rangle$ and $|g\rangle$, assumed real, and S_+ and S_- being pseudospin ladder operators. Also, $a_{\mathbf{k}j}$ ($a_{\boldsymbol{k}j}^\dagger$) is the bosonic annihilation (creation) operator for photons with wavevector $\mathbf{k}$ and polarization j. Finally, $\mathbf{E}(\boldsymbol{r}, t)$ is the transverse displacement field operator, that outside the atoms coincides with the total, longitudinal plus transverse, electric field, written, in c.g.s. unit as

$$\mathbf{E}(\mathbf{r}, t) = i\sum_{\boldsymbol{k},j} \sqrt{\frac{2\pi\hbar\omega_k}{V}}\hat{\boldsymbol{e}}_{\boldsymbol{k}j}\left(a_{\mathbf{k}j}(t)e^{i\boldsymbol{k}\cdot\boldsymbol{r}} - a_{\mathbf{k}j}^\dagger(t)e^{-i\boldsymbol{k}\cdot\boldsymbol{r}}\right) \tag{4.8}$$

where $\hat{\boldsymbol{e}}_{\boldsymbol{k}j}$ are the polarisation unit vectors of the electromagnetic field, assumed real. In the case of two-level atoms, the interaction Hamiltonian in (4.6) can be conveniently rewritten as

$$H_i(t) = -i\sum_{i=A,B}\sum_{\boldsymbol{k},j} \sqrt{\frac{2\pi\hbar ck}{V}}(\hat{\boldsymbol{e}}_{\boldsymbol{k}j}\cdot\boldsymbol{\mu}_i^{eg})\left[a_{\mathbf{k}j}e^{i\boldsymbol{k}\cdot\boldsymbol{r}_i}\left(S_+^i + \lambda S_-^i\right) - a_{\mathbf{k}j}^\dagger e^{-i\boldsymbol{k}\cdot\boldsymbol{r}_i}\left(S_-^i + \lambda S_+^i\right)\right], \tag{4.9}$$

where $\lambda = 0, 1$ is a parameter that allows to easily identify the role of counterrotating terms: for $\lambda = 1$ we recover the full Hamiltonian with the counterrotating terms, while for $\lambda = 0$ we get the Hamiltonian in the rotating wave approximation (RWA). Our purpose is to investigate the time-dependent resonance interaction

between the atoms, during the dynamical self-dressing process of the system. The physical situation we are considering is equivalent to switching the atoms-field coupling on at $t = 0$; after that, the system is not longer in an equilibrium situation, and it will unitarily evolve starting from its bare state $|\psi_{\pm}\rangle$.

In order to obtain the time-dependent interaction energy, we can follow the same approach used in [109, 119, 121] for the dynamical atom-surface Casimir-Polder interaction. Specifically, we first write down the Heisenberg equations for field and atomic operators, and solve them iteratively at the lowest significant order; the time-dependent energy shift of the system is then obtained by evaluating the quantity

$$\Delta E(t) = \frac{1}{2}\langle\psi_{\pm}|H_i^{(2)}(t)|\psi_{\pm}\rangle, \tag{4.10}$$

where $H_i^{(2)}(t)$ is the interaction Hamiltonian (4.6) in the Heisenberg representation at the second-order in the coupling with the radiation field, obtained by substitution of the second-order solution of the Heisenberg equations for atom and field operators. This method is a direct generalization to time-dependent situations of the following (time-independent) relation, as obtained by second-order stationary perturbation theory [171],

$$\Delta E = \frac{1}{2}\langle\psi_D|H_i|\psi_D\rangle, \tag{4.11}$$

where $|\psi_D\rangle$ is the second-order interacting (dressed) state of the system, and H_i is the interaction Hamiltonian in the Schrödinger representation. It should be observed that, since time evolution is unitary, the total energy of the system is conserved during the self-dressing process. In particular, this means that the average value of the total Hamiltonian $H^{(2)}(t)$ on the initial bare state $|\psi_{\pm}\rangle$ does not depend on time:

$$\langle\psi_{\pm}|H^{(2)}(t)|\psi_{\pm}\rangle = \langle\psi_{\pm}|H_0^{(2)}(t)|\psi_{\pm}\rangle + \langle\psi_{\pm}|H_i^{(2)}(t)|\psi_{\pm}\rangle = 0, \tag{4.12}$$

for any t. Eq. (4.12) can be easily verified by evaluating, at the second-order in the atom-field coupling, the single contributions to the total energy of the system, that is the average value of atomic, field and interaction Hamiltonian (in the Heisenberg representation) on the initial bare state, similarly to the case of the atom-plate dynamical Casimir-Polder interaction energy investigated in [22]. Nevertheless, the average value of the interaction Hamiltonian $H_i^{(2)}(t)$ on the bare-state $|\psi_{\pm}\rangle$, related to the local interaction energy of the atoms with the field evaluated at their position, is nonvanishing and depends on time; actually, it gives the time-dependent resonance interaction energy of our two-atom system.

Let us first obtain the expressions of field and atomic operators in the Heisenberg representation, at the lowest significant order. Starting from the Heisenberg equation

$$\dot{a_{\mathbf{k}j}} = \frac{i}{\hbar}[H, a_{\mathbf{k}j}] \tag{4.13}$$

$$\dot{S^i_-} = \frac{i}{\hbar}[H, S^i_-] \tag{4.14}$$

$$\dot{S^i_+} = \frac{i}{\hbar}[H, S^i_+] \tag{4.15}$$

and considering that, $\dot{S^i_-} = (\dot{S^i_+})^\dagger$, after some algebra, we obtain

$$\begin{aligned} a_{\mathbf{k}j}(t) &= a_{\mathbf{k}j}(0)e^{-i\omega_k t} + \sum_{i=A,B} e^{-i\boldsymbol{k}\cdot\boldsymbol{r}_i} e^{-i\omega_k t}\sqrt{\frac{2\pi\omega_k}{\hbar V}}[\boldsymbol{\mu}_i^{eg}\cdot\mathbf{e}_{\boldsymbol{k}j}] \\ &\quad\times[S^i_+(0)F(\omega_0+\omega_k,t) + \lambda S^i_-(0)F(\omega_k-\omega_0,t)], \end{aligned} \tag{4.16}$$

$$\begin{aligned} S^i_-(t) &= S^i_-(0)e^{-i\omega_0 t} + 2S^i_z(0)e^{-i\omega_0 t}\sum_{\mathbf{k}j}\sqrt{\frac{2\pi\omega_k}{\hbar V}}[\boldsymbol{\mu}_i^{eg}\cdot\mathbf{e}_{\boldsymbol{k}j}] \\ &\quad\times[a_{\mathbf{k}j}(0)e^{i\boldsymbol{k}\cdot\boldsymbol{r}_i}F(\omega_0-\omega_k,t) - \lambda a^\dagger_{\mathbf{k}j}(0)e^{-i\boldsymbol{k}\cdot\boldsymbol{r}_i}F(\omega_k+\omega_0,t)], \end{aligned} \tag{4.17}$$

$$\begin{aligned} S^i_+(t) &= S^i_+(0)e^{i\omega_0 t} + 2S^i_z(0)e^{i\omega_0 t}\sum_{\mathbf{k}j}\sqrt{\frac{2\pi\omega_k}{\hbar V}}[\boldsymbol{\mu}_i^{eg}\cdot\mathbf{e}_{\boldsymbol{k}j}] \\ &\quad\times[a^\dagger_{\mathbf{k}j}(0)e^{-i\boldsymbol{k}\cdot\boldsymbol{r}_i}F^*(\omega_0-\omega_k,t) - \lambda a_{\mathbf{k}j}(0)e^{i\boldsymbol{k}\cdot\boldsymbol{r}_i}F^*(\omega_k+\omega_0,t)], \end{aligned} \tag{4.18}$$

with $i = (A, B)$ and where we have defined the function

$$F(x,t) = \frac{e^{ixt}-1}{ix}\,. \tag{4.19}$$

These equations represent the expansion of the field and atomic operators up to the first order in the atom-field coupling. Now, using Eqs. (4.16), (4.17) and (4.18) in the expression (4.9) of $H_i(t)$, and taking only terms up to the second-order in the

coupling, we obtain the explicit expression of the interaction Hamiltonian $H_i^{(2)}(t)$

$$
\begin{aligned}
H_i^{(2)}(t) &= -\frac{2\pi i}{V}\sum_{q=A,B}\sum_{s=A,B}\sum_{\mathbf{k}j}\omega_k(\boldsymbol{\mu}_q^{eg}\cdot\mathbf{e}_{\boldsymbol{k}j})(\boldsymbol{\mu}_s^{eg}\cdot\mathbf{e}_{\boldsymbol{k}j})e^{i\boldsymbol{k}\cdot(\boldsymbol{r}_q-\boldsymbol{r}_s)}e^{-i\omega_k t}\\
&\times\Big(S_+^q(0)e^{i\omega_0 t}+\lambda S_-^q(0)e^{-i\omega_0 t}\Big)\Big(S_-^s(0)F(\omega_k-\omega_0,t)+\lambda S_+^s(0)F(\omega_k+\omega_0,t)\Big)\\
&-\frac{4\pi i}{V}\sum_{q=A,B}\sum_{\mathbf{k}j}\sum_{\mathbf{k}'j'}\sqrt{\omega_k\omega_{k'}}(\boldsymbol{\mu}_q^{eg}\cdot\mathbf{e}_{\boldsymbol{k}j})(\boldsymbol{\mu}_q^{ge}\cdot\mathbf{e}_{\boldsymbol{k}'j'})S_z^q(0)a_{\mathbf{k}j}(0)e^{i(\boldsymbol{k}\cdot\boldsymbol{r}_q-\omega_k t)}\\
&\times\Big[a_{\mathbf{k}'j'}^\dagger(0)e^{-i\boldsymbol{k}'\cdot\boldsymbol{r}_q}\Big(F^*(\omega_0-\omega_{k'},t)e^{i\omega_0 t}-\lambda^2F(\omega_0+\omega_{k'},t)e^{-i\omega_0 t}\Big)\\
&-\lambda a_{\mathbf{k}'j'}(0)e^{i\boldsymbol{k}'\cdot\boldsymbol{r}_q}\Big(F^*(\omega_0+\omega_{k'},t)e^{i\omega_0 t}-F(\omega_0-\omega_{k'},t)e^{-i\omega_0 t}\Big)\Big]+h.c. \qquad (4.20)
\end{aligned}
$$

In order to evaluate the time-dependent resonance interaction energy using Eq. (4.10), we must calculate the average value of (4.20) on the correlated states $|\psi_\pm\rangle$. We take into account only terms depending on the interatomic distance $\mathbf{R}=\mathbf{r}_A-\mathbf{r}_B$, which are the only ones relevant for the dynamical interatomic interaction energy, from which, in a quasi-static approach, the resonance force can be obtained by taking the negative derivative with respect to the atomic separation. The distance-independent terms just give single-atom energy shifts that are irrelevant for the interaction energy. After some algebra, the time-dependent resonance interaction energy is obtained

$$
\begin{aligned}
\Delta E(t) &= \frac{1}{2}\langle\psi_\pm|H_i^{(2)}(t)|\psi_\pm\rangle = \mp i\frac{\pi c}{2V}\sum_{\substack{q,s=A,B\\(q\neq s)}}\sum_{\mathbf{k},j}k(\boldsymbol{\mu}_q^{eg}\cdot\mathbf{e}_{\boldsymbol{k}j})(\boldsymbol{\mu}_s^{ge}\cdot\mathbf{e}_{\boldsymbol{k}j})\\
&\times\left[e^{i\boldsymbol{k}\cdot(\boldsymbol{r}_q-\boldsymbol{r}_s)}\Big(F^*(\omega_k-\omega_0,t)+\lambda^2F^*(\omega_k+\omega_0,t)\Big)\right]+c.c.\,, \qquad (4.21)
\end{aligned}
$$

where the upper and lower signs refer to the symmetric and antisymmetric entangled state, respectively, and in the summation over q and s we must take $q\neq s$. In the continuum limit, $\sum_{\boldsymbol{k}}\to V/(2\pi)^3\int d^3k$, performing the polarization sum using $\sum_j(\mathbf{e}_{\boldsymbol{k}j})_l(\mathbf{e}_{\boldsymbol{k}j})_m=\delta_{lm}-\hat{\boldsymbol{k}}_l\hat{\boldsymbol{k}}_m$ (where $l,m=x,y,z$), the angular integration yields

$$
\int d\Omega_k(\delta_{lm}-\hat{\boldsymbol{k}}_l\hat{\boldsymbol{k}}_m)e^{\pm i\boldsymbol{k}\cdot\boldsymbol{R}}=\frac{4\pi}{k^3}(-\delta_{lm}\nabla^2+\nabla_l\nabla_m)^R\frac{\sin(kR)}{R}, \qquad (4.22)
$$

where the differential operators $F_{lm}^R=(-\delta_{\ell m}\nabla^2+\nabla_l\nabla_m)^R$ act on the variable

$R = |\boldsymbol{R}|$. Therefore, the time-dependent resonance interaction becomes

$$\Delta E(t) = \mp \frac{c}{\pi}(\boldsymbol{\mu}_A^{eg})_l(\boldsymbol{\mu}_B^{eg})_m F_{lm}^R \frac{1}{R}\int_0^{+\infty} dk \sin(kR) \times \left(\frac{1-\cos(ck-\omega_0)t}{ck-\omega_0} + \lambda^2 \frac{1-\cos(ck+\omega_0)t}{ck+\omega_0}\right), \tag{4.23}$$

where the Einstein convention for repeated indices has been used [169].

The time-dependent resonance interaction energy (4.23) is given by two different terms: a time-independent contribution, that is the same obtained in the static case [115, 161], and a term explicitly depending on time, related to the time-dependent self-dressing of the entangled two-atom system. We also note that, contrary to the stationary case where a resonant pole at $ck = \omega_0$ appears, related to the emission of a real photon from the excited atom, in the present case there are no poles in (4.23); therefore, there is not ambiguity in circumventing the pole in the frequency integration. This observation could be relevant also in connection with controversial results in the literature concerning with the long-distance behaviour (with space oscillations or not) of the dispersion Casimir-Polder interaction between an excited- and a ground-state atom [122, 156, 158]. We should however point out that the perturbative approach used is valid only for times much smaller than the lifetime of the excited atom, that, for an optical transition of the hydrogen atom, is of the order of 10^{-8} s.

In order to obtain the explicit expression of the dynamical resonance interaction energy, we now evaluate the integral over k in (4.23). Since it is possible to show that the time-dependent integrals diverge on the light-cone, when $R = ct$, we shall perform the calculation of the integral by considering separately two different time regions: for $t < R/c$ and $t > R/c$, that is before and after the causality time. As discussed in [119, 121], these divergences are related to the assumption of point-like field sources, as well as to our bare-state initial condition [107–109]. Similar divergences appear during the time-dependent self-dressing of a single initially bare source [172], as well as in the field energy densities nearby a reflecting mirror [160, 173, 174] or a point-like field source [175, 176].

For $t < R/c$, we obtain

$$\Delta E(t) = \pm \frac{1-\lambda^2}{2\pi}(\boldsymbol{\mu}_A^{eg})_l(\boldsymbol{\mu}_B^{eg})_m F_{lm}^R \frac{1}{R}\Bigg[\sin(k_0R)\Big(2\mathrm{Ci}[k_0R] - \mathrm{Ci}[k_0(R-ct)] - \mathrm{Ci}[k_0(R+ct)]\Big) - \cos(k_0R)\Big(2\mathrm{si}[k_0R] - \mathrm{si}[k_0(R-ct)] - \mathrm{si}[k_0(R+ct)]\Big)\Bigg], \tag{4.24}$$

while for $t > R/c$ we have

$$\Delta E(t) = \mp\,(\boldsymbol{\mu}_A^{eg})_l(\boldsymbol{\mu}_B^{eg})_m F_{lm}^R\,\frac{1}{R}\cos(k_0R) \pm \frac{1-\lambda^2}{2\pi}(\boldsymbol{\mu}_A^{eg})_l(\boldsymbol{\mu}_B^{eg})_m F_{lm}^R\,\frac{1}{R}\Bigg[\sin(k_0R)\Big(2\mathrm{Ci}[k_0R] - \mathrm{Ci}[k_0(ct-R)] - \mathrm{Ci}[k_0(ct+R)]\Big) - \cos(k_0R)\Big(2\mathrm{si}[k_0R] + \mathrm{si}[k_0(ct-R)] - \mathrm{si}[k_0(ct+R)]\Big)\Bigg], \tag{4.25}$$

where the cosine and sine integral functions $\mathrm{Ci}(x)$ and $\mathrm{si}(x) = \mathrm{Si}(x) - \frac{\pi}{2}$ have been introduced [26–28]. Equations (4.24) and (4.25) give the dynamical resonance interaction energy during the self-dressing process of the two-atom system before and after the causality time $t = R/c$, respectively. It is important to point out that for $\lambda = 0$, that is when the RWA is used and only the rotating terms of the Hamiltonian contribute to the dynamical resonance interaction, the time-dependent interaction energy is different from zero even before the causality time $t = R/c$. Therefore in the RWA the causality is violated, since the atoms could interact even before the causality time. On the contrary, if we also include the contribution from virtual photons given by the counterrotating terms in the Hamiltonian, that is if we set $\lambda = 1$, from (4.24) and (4.25) we immediately obtain

$$\Delta E(t) = \mp(\boldsymbol{\mu}_A^{eg})_l(\boldsymbol{\mu}_B^{eg})_m F_{lm}^R\,\frac{\cos(k_0R)}{R}\theta(ct-R), \tag{4.26}$$

where $\theta(x)$ is the Heaviside step function. Therefore the causal behaviour is fully recovered. The Eq. (4.26) clearly shows that the contribution of virtual photons given by the counterrotating terms is essential to ensure the causal behaviour of the dynamical resonance interaction energy, similarly to the case of two ground-state atoms [172] or in the Fermi problem [177]. Applying the differential operator F_{lm}^R, and performing the derivatives with respect to R in (4.26), we get

$$\Delta E(t) = \pm(\boldsymbol{\mu}_A^{eg})_l(\boldsymbol{\mu}_B^{eg})_m V_{lm}(k_0,R)\theta(ct-R), \tag{4.27}$$

where $V_{lm}(k_0,R)$ is the potential tensor

$$V_{lm}(k_0,R) = \frac{1}{R^3}\Big[(\delta_{lm} - 3\hat{R}_l\hat{R}_m)(\cos(k_0R) + k_0R\sin(k_0R)) - (\delta_{lm} - \hat{R}_l\hat{R}_m)k_0^2R^2\cos(k_0R)\Big]. \tag{4.28}$$

From Eq. (4.27) it is clear that there is not interaction between the atoms before time $t = R/c$. After this time, the dynamical resonance interaction instantaneously settles to its stationary value and thus an observer measuring the resonance force on one atom, for example atom A, will detect the full value of the stationary force immediately after the causality time $t = R/c$ [169]. Mathematically, the instantaneous change of the interaction is related to the fact that the time-dependent contributions, related to the dynamical dressing process of the two atoms, cancel with each other, and thus the system approaches to its local equilibrium configuration immediately after the causality time R/c, as we will show later. From a physical point of view, this sharp change of the time-dependent resonance interaction energy at $t = R/c$ is related to the assumption of point-like atoms, inherent in the dipole approximation, and to the bare initial state assumption.

This peculiar behaviour of the resonance interaction energy can be mathematically understood by performing explicitly the calculation of the integrals in (4.23). For $\lambda = 1$, that is taking into account also the counterrotating terms in the Hamiltonian, the two integrals can be easily performed by considering separately time-independent and time-dependent contributions. For the time-independent terms, we have

$$\begin{aligned} I_1 &= \mathcal{P}\int_0^\infty dk \sin(kR)\left(\frac{1}{ck-\omega_0}+\frac{1}{ck+\omega_0}\right) \\ &= \mathcal{P}\int_{-\infty}^\infty dk \frac{\sin(kR)}{ck+\omega_0}\,, \end{aligned} \tag{4.29}$$

where $\mathcal{P}$ denotes the principal value, and in the first integral we have performed the variable change $k \to -k$. This integral has a pole in $k = -k_0 = -\omega_0/c$ and, using the residue theorem, we obtain

$$I_1 = \frac{\pi}{c}\cos(k_0 R). \tag{4.30}$$

The time-dependent integral can be similarly evaluated, obtaining

$$\begin{aligned} I_2(t) &= \mathcal{P}\int_0^\infty dk \sin(kR)\left(\frac{\cos[(ck-\omega_0)t]}{ck-\omega_0}+\frac{\cos[(ck+\omega_0)t]}{ck+\omega_0}\right) \\ &= \mathcal{P}\int_{-\infty}^\infty dk \frac{\sin(kR)}{ck+\omega_0}\cos[(ck+\omega_0)t] = \frac{\pi}{c}\cos(k_0 R)\theta(R-ct). \end{aligned} \tag{4.31}$$

These results clearly show that the time-dependent resonance interaction energy, depending from $I_1 - I_2$, vanishes for $t < R/c$, while it is nonvanishing and time-independent for $t > R/c$. The system thus sharply approaches its equilibrium configuration at the causality time R/c, as we have already pointed out. This behaviour is clearly illustrated in figures (4.1) and (4.2), which show the contributions

to the dynamical resonance interaction energy from the rotating and counterrotating terms in the two time intervals, $t < R/c$ and $t > R/c$, as a function of t.

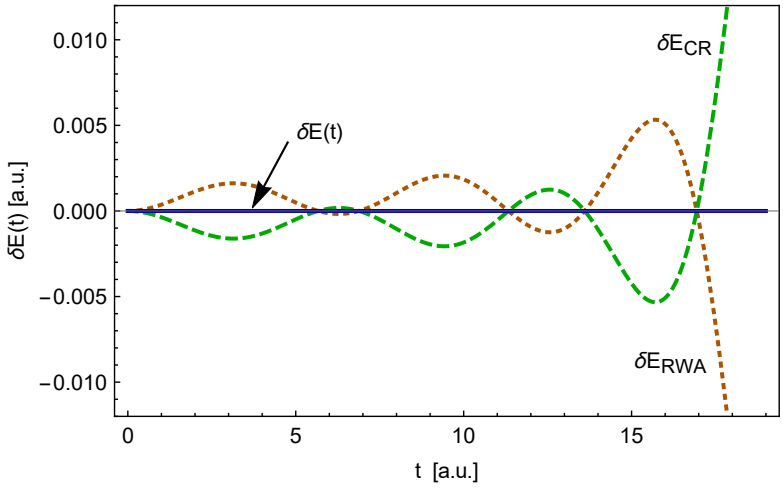

Figure 4.1: Plots of the time-dependent contributions to the dynamical resonance interaction energy as a function of time, for $t < R/c$. Energy and time are in arbitrary units. The interatomic distance is set to $R = 20$, while $c = 1$ and $k_0 = 1$; thus $t < R/c$ means $t < 20$. The orange dotted line and the green dashed line represent the time-dependent contributions from rotating ($\delta E_{RWA}(t)$) and counterrotating ($\delta E_{CR}(t)$) terms, respectively. The blue solid line is the total dynamical resonance interaction energy before the causality time. Both contributions diverge on the light cone $t = R/c$.

Fig. 4.1 shows the time-dependent contributions to the dynamical resonance interaction energy as a function of time, before the causality time. These contributions are related to the rotating and counterrotating terms, labelled respectively by $\delta E_{RWA}(t)$ and $\delta E_{CR}(t)$, and are represented by the orange dotted line and the green dashed line, while the total resonance interaction is given by the blue solid line. This plot points out that the two contributions $\delta E_{RWA}(t)$ and $\delta E_{CR}(t)$ oscillate in time out of phase and that their sum, that is the total resonance interaction, vanishes at all times for $t < R/c$. This means that the two atoms do not interact before the time $t = R/c$, preserving the causality, as expected. On the other hand, Fig. 4.2 shows that, after the causality time, time-dependent contributions cancel out each other, and what remains is time-independent, coinciding with the static value of the resonance interaction energy between two atoms in free space. The two inserts are enlargements showing the presence of time oscillations of both contributions soon after the causality time. These results suggest that the peculiar sharp behaviour of the dynamical resonance interaction is owing to an interference

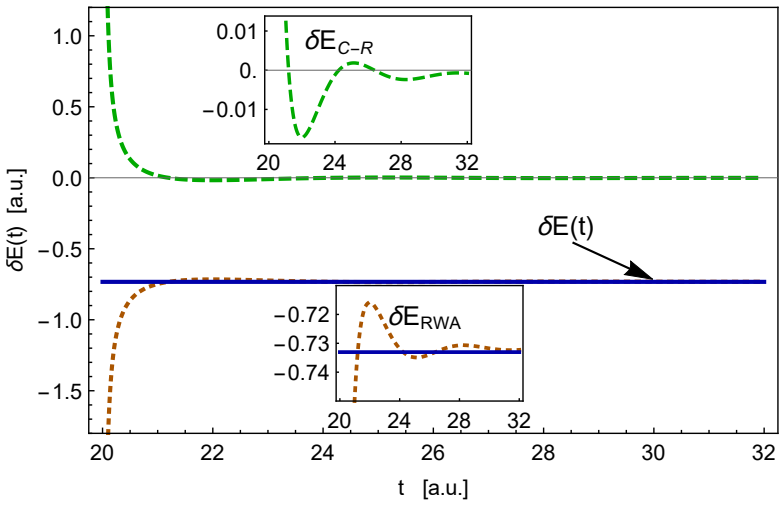

Figure 4.2: Plots of the time-dependent contributions, $\delta E_{RWA}(t)$ and $\delta E_{CR}(t)$, to the dynamical resonance interaction energy as a function of time, for $t > R/c$. Energy and time are in arbitrary units. Parameters are $R = 20$, $c = 1$ and $k_0 = 1$; thus $t > 20$. The orange dotted line and the green dashed line represent the time-dependent contributions from rotating ($\delta E_{RWA}(t)$) and counterrotating ($\delta E_{CR}(t)$) terms, respectively. The blue solid line is the total dynamical resonance interaction energy after the causality time. Both contributions diverge on the light cone $t = R/c$.

effect between the virtual-photon and the real-photon contributions; these photons are generated by the two atoms during their dynamical self-dressing process [169].

As mentioned before, our results are valid for times shorter than the decay time of the atomic excited state, that is typically of the order of 10^{-8} s. For typical values of the atomic parameters $\mu \simeq 10^{-29}$ C m, $k_0 \simeq 10^{7}$ m^{-1}, and for an interatomic distance of $R \simeq 10^{-6}$ m, the resonance force between the two atoms is of the order of $F \simeq 10^{-21}$ N, which is several orders of magnitude larger than the dispersion Casimir-Polder interaction energy between ground-state atoms, that can be measured directly [178], and comparable with the atom-surface Casimir-Polder interaction, for which many measurements exist [179]. But even so, the resonance interaction energy, and the consequent interatomic force, is very difficult to observe directly, since it requires that the system be prepared and maintained in an entangled state for a sufficiently long time, as previously mentioned. The coherent superposition of the entangled state can be easily destroyed by spontaneous emission and interactions with the environment. Very recently, the possibility to control decoherence effects through a structured environment, such as a photonic crystal, has been explored [115, 161], thus suggesting possible experimental setups to observe such interaction for atoms placed inside a structured environment.

In order to gain further physical evidences of the processes involved during the dynamical dressing, in the next section we shall investigate the time-dependent electric field energy density during the self-dressing of the two-atom system.

4.1.1 Time-dependent electric energy density around the two entangled atoms

The time-dependent electric energy density near the two-atom system, for both the symmetric and antisymmetric entangled state, is now evaluated in order to further investigate the time-dependent self-dressing process of the system [169]. It can be written as

$$\langle\psi_\pm|\mathcal{H}_{el}(\boldsymbol{r},t)|\psi_\pm\rangle = \frac{1}{8\pi}\,\langle\psi_\pm|E^2(\boldsymbol{r},t)|\psi_\pm\rangle\,, \tag{4.32}$$

where $\mathcal{H}_{el}(\boldsymbol{r},t)$ is the electric energy density and the electric field operator is in the Heisenberg representation. Up to the second order in the atom-field coupling, the equation (4.32) can be written as

$$\begin{aligned}\frac{1}{8\pi}\,\langle\psi_\pm|E^2(\boldsymbol{r},t)|\psi_\pm\rangle = \frac{1}{8\pi}\,\langle\psi_\pm|\Big(&\boldsymbol{E}^{(0)}(\boldsymbol{r},t)\cdot\boldsymbol{E}^{(0)}(\boldsymbol{r},t)+\boldsymbol{E}^{(1)}(\boldsymbol{r},t)\cdot\boldsymbol{E}^{(1)}(\boldsymbol{r},t)\\&+\boldsymbol{E}^{(0)}(\boldsymbol{r},t)\cdot\boldsymbol{E}^{(2)}(\boldsymbol{r},t)+\boldsymbol{E}^{(2)}(\boldsymbol{r},t)\cdot\boldsymbol{E}^{(0)}(\boldsymbol{r},t)\Big)|\psi_\pm\rangle,\end{aligned} \tag{4.33}$$

where the superscript indicates the perturbative order. In order to calculate the electric energy density (4.33), we need to solve the Heisenberg equation for the field operators; iterative solution for the field annihilation operator at the leading order, gives

$$a^{(0)}_{\mathbf{k}j}(t) = a^{(0)}_{\mathbf{k}j}(0)e^{-i\omega_k t} \tag{4.34}$$

$$\begin{aligned}a^{(1)}_{\mathbf{k}j}(t) =&\sqrt{\frac{2\pi\omega_k}{V\hbar}}\sum_{q=A,B}\Big[(\boldsymbol{\mu}^{eg}_q\cdot\mathbf{e}_{\boldsymbol{k}j})e^{-i(\mathbf{k}\cdot\mathbf{r}_q-\omega_k t)}\Big(S^q_+(0)F(\omega_0+\omega_k,t)\\&+S^q_-(0)F(\omega_k-\omega_0,t)\Big)\Big]\,,\end{aligned} \tag{4.35}$$

$$a^{(2)}_{\mathbf{k}j}(t) = -\frac{4\pi}{\hbar V}\sum_{q=A,B} S^q_z(0)e^{-i(\mathbf{k}\cdot\mathbf{r}_q-\omega_k t)}\sum_{\mathbf{k}'j'}\sqrt{\omega_k\omega_{k'}}(\boldsymbol{\mu}^{eg}_q\cdot\mathbf{e}_{\boldsymbol{k}j})(\boldsymbol{\mu}^{ge}_q\cdot\mathbf{e}_{\boldsymbol{k}'j'})$$
$$\times i\Bigg\{a_{\mathbf{k}'j'}(0)e^{i\mathbf{k}'\cdot\mathbf{r}_q}\Bigg[iF(\omega_k-\omega_{k'},t)\left(\frac{1}{\omega_0+\omega_k}+\frac{1}{\omega_0-\omega_{k'}}\right)-\frac{1}{\omega_0+\omega_{k'}}F(\omega_0+\omega_k,t)$$
$$-\frac{1}{\omega_0-\omega_{k'}}F^*(\omega_0-\omega_k,t)\Bigg]-a^\dagger_{\mathbf{k}'j'}(0)e^{-i\mathbf{k}'\cdot\mathbf{r}_q}\Bigg[F(\omega_k+\omega_{k'},t)\left(\frac{1}{\omega_0-\omega_{k'}}+\frac{1}{\omega_0+\omega_{k'}}\right)$$
$$-\frac{1}{\omega_0-\omega_{k'}}F(\omega_0+\omega_k,t)-\frac{1}{\omega_0+\omega_{k'}}F^*(\omega_0-\omega_k,t)\Bigg]\Bigg\}\,. \tag{4.36}$$

Since second-order field operators, expressed by Eq. (4.36), depend on $S^A_z(0)$ and $S^B_z(0)$, the contribution related to $\langle\psi_\pm|\boldsymbol{E}^{(2)}(\boldsymbol{r},t)\cdot\boldsymbol{E}^{(0)}(\boldsymbol{r},t)|\psi_\pm\rangle$ in (4.33) vanishes, being $\langle\psi_\pm|S^{A,B}_z(0)|\psi_\pm\rangle = 0$. The only nonvanishing term comes from $\langle\psi_\pm|\boldsymbol{E}^{(1)}(\boldsymbol{r},t)\cdot\boldsymbol{E}^{(1)}(\boldsymbol{r},t)|\psi_\pm\rangle$ and, in order to evaluate it, we first substitute (4.35) into the electric field expression (4.8), obtaining

$$\mathbf{E}^{(1)}(\mathbf{r},t) = i\frac{2\pi}{V}\sum_{q=A,B}\sum_{\mathbf{k}j}\omega_k(\boldsymbol{\mu}^{eg}_q\cdot\mathbf{e}_{\boldsymbol{k}j})$$
$$\times\left[e^{i\mathbf{k}\cdot(\mathbf{r}-\mathbf{r}_q)}e^{-i\omega_k t}\Big(S^q_+(0)F(\omega_0+\omega_k,t)+S^q_-(0)F(\omega_k-\omega_0,t)\Big)\right]\mathbf{e}_{\boldsymbol{k}j}+h.c.\,, \tag{4.37}$$

that is the electric field operator expression up to the first order in the coupling with the radiation field.
The time-dependent electric energy density will be obtained by substitution of (4.37) into (4.33), disregarding the bare space-uniform vacuum field contributions coming from the 0-th order term. After some algebra, involving polarization sum and integration over $\mathbf{k}$, we finally obtain that the electric energy density can be written as a sum of three distinct terms

$$\langle\psi_\pm|\mathcal{H}_{el}(\boldsymbol{r},t)|\psi_\pm\rangle = \langle\psi_\pm|\mathcal{H}^A_{el}(\boldsymbol{r},t)|\psi_\pm\rangle + \langle\psi_\pm|\mathcal{H}^B_{el}(\boldsymbol{r},t)|\psi_\pm\rangle + \langle\psi_\pm|\mathcal{H}^{AB}_{el}(\boldsymbol{r},t)|\psi_\pm\rangle, \tag{4.38}$$

where

$$\langle\psi_\pm|\mathcal{H}^A_{el}(\boldsymbol{r},t)|\psi_\pm\rangle = \frac{1}{8\pi}\Re\left((\boldsymbol{\mu}^{eg}_A)_m(\boldsymbol{\mu}^{ge}_A)_n F^{R_A}_{lm}\frac{e^{ik_0R_A}}{R_A}F^{R_A}_{ln}\frac{e^{-ik_0R_A}}{R_A}\right)\theta(ct-R_A)\,, \tag{4.39}$$

$$\langle\psi_\pm|\mathcal{H}^B_{el}(\boldsymbol{r},t)|\psi_\pm\rangle = \langle\psi_\pm|\mathcal{H}^A_{el}(\boldsymbol{r},t)|\psi_\pm\rangle \quad \text{with } A\leftrightarrows B\,, \tag{4.40}$$

$$\langle\psi_\pm|\mathcal{H}_{el}^{AB}(\boldsymbol{r},t)|\psi_\pm\rangle = \pm\frac{1}{8\pi}\Re\left((\boldsymbol{\mu}_A^{eg})_m(\boldsymbol{\mu}_B^{ge})_n F_{lm}^{R_A}\frac{e^{ik_0R_A}}{R_A}F_{ln}^{R_B}\frac{e^{-ik_0R_B}}{R_B}+c.c.\right) \times\theta(ct-R_A)\theta(ct-R_B)\,. \tag{4.41}$$

Here, $\mathbf{R_{A(B)}} = \mathbf{r} - \mathbf{r_{A(B)}}$ is the distance between a generic observation point $\mathbf{r}$, where the electric energy density is evaluated, and the atom $A(B)$, and the $+/-$ sign refers to the superradiant/subradiant correlated state of the system. Therefore, the time-dependent electric energy density emitted by atoms A and B, expressed in Eq. (4.38) is given by the sum of two main contributions. The first contribution, given by equations (4.39) and (4.40), is related to the retarded electric field emitted by each atom, and it is causal, due to the presence of the Heaviside step function. This contribution vanishes if the observation point $\mathbf{r}$ is outside the causality sphere of both atoms A and B, that is if $R_A, R_B > ct$, as expected. On the other hand, the second main contribution, given by Eq. (4.41), is a sort of *interference* term, related to the electric field radiated by the overall two-atom system. Inspection of (4.39)-(4.41) clearly shows that if the observation point $\mathbf{r}$ is outside the light-cone of both atoms, the total electric energy density (4.38) vanishes. On the other hand, if point $\mathbf{r}$ is inside the causality sphere of only one atom, for example if $R_A < ct$ but $R_B > ct$, then the electric energy density in $\mathbf{r}$ is only related to the presence of atom A: this is compatible with relativistic causality, of course. Yet, interesting results are obtained if point $\mathbf{r}$ is inside the causality sphere of both atoms A and B. In this case, all terms in (4.38) contribute to the time-dependent electric energy density. In particular, assuming atoms with identical dipole moments, and for distances such that $R_A = R_B < ct$, we find that the electric energy density emitted by the two-atom system during the self-dressing process is doubled, with respect to the single-atom case, when the atoms are in the superradiant-state, while it vanishes in the subradiant state. This result is due to the presence of the interference term in (4.38), and clearly shows that the superradiant or subradiant behaviour of the two-atom system can be understood, as far as the electric field energy density is concerned with, in terms of an interference effect between the electric energy densities emitted by the atoms [169].

Finally, we wish to point out that these results related to the time-dependent electric energy density could be experimentally investigated by measuring the retarded Casimir-Polder interaction energy on an appropriate polarizable body with static polarizability α. As it is known, in the far-zone limit, that is when the distance is larger than relevant wavelengths associated to the atomic transitions, the Casimir-Polder energy on a body with static polarizability α can be written as

$$\Delta E = -\frac{1}{2}\alpha\langle E^2(\mathbf{r})\rangle, \tag{4.42}$$

where the electric field operator $\mathbf{E}(\mathbf{r})$ is evaluated at the position of the polarizable body; thus the interaction energy is strictly related to the electric energy density. Therefore we could investigate the dispersion force on a third atom C due to the interaction with the two other atoms A and B, located at some distance from C, and prepared in an entangled symmetric or antisymmetric state, as shown in Fig. (4.3). From Eq. (4.42), the atom C feels a force that is directly related to the

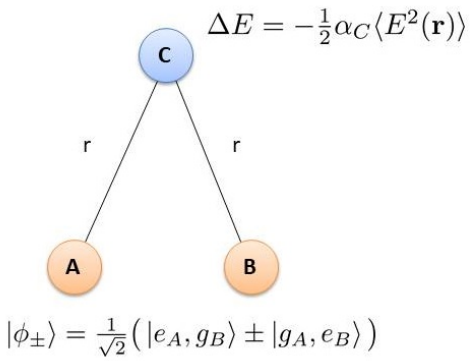

Figure 4.3: Sketch of the hypothetical physical system proposed to investigate the subradiant and superradiant behaviour of the two-atom entangled system. Atoms A and B are prepared in an entangled symmetric or antisymmetric state, and C is an appropriate polarizable body.

local electric field energy density generated at its position by the two entangled atoms A and B. In particular, assuming that the distance of atom C from A and B is such that $\mid \mathbf{r}_C - \mathbf{r}_A \mid = \mid \mathbf{r}_C - \mathbf{r}_B \mid$, the force acting on C will be enhanced if the two atoms are prepared in a correlated symmetric (superradiant) state, while it is zero if the atoms are prepared in a antisymmetric (subradiant) state, even if the atom C is inside the light-cone of both atoms A and B [169]. Thus, the subradiant or superradiant behaviour of the two-atom system is strictly related to the field energy density, and it could be experimentally probed through a measurement of the Casimir-Polder interaction on a third atom.

4.2 Resonance interaction between two atoms in the presence of a generic magneto-dielectric medium

In this Section the resonance interaction energy between two atoms, one excited and the other in its ground state, prepared in an entangled state and in the presence

of an arbitrary magneto-dielectric medium is studied [152]. Our purpose is to investigate whether and how the resonance force can be modified by the presence of the structured environment and, if it is possible to control its strength and its character, exploiting the external parameters of the environment. Manipulate the resonance interaction through external environments could be also experimentally relevant in order to suggest an experimental setup able to detect this interaction : e.g., a suitable macroscopic body could reduce the environment's influences and the atomic spontaneous emission (that destroys the correlation of the entangled atomic state), and even enhance the resonance interaction energy between the atoms, allowing to detect it.

We consider two identical two-levels atoms, one excited and the other in its ground state, labelled A and B, with transition frequency $\omega_0 = ck_0$, interacting with the quantum vacuum. The system is prepared in a correlated symmetric or antisymmetric state, given by

$$|\psi_\pm\rangle = \frac{1}{\sqrt{2}}\Big(|e_A, g_B, 0\rangle \pm |g_A, e_B, 0\rangle \Big), \tag{4.43}$$

where $|e\rangle$ and $|g\rangle$ are the excited and ground atomic state, respectively, and the radiation field is in the vacuum state $|0\rangle$; in this case the excitation is delocalized between the atoms. The Hamiltonian of the system in the multipolar coupling scheme, within the dipole approximation, is [6]

$$H = H_0 + H_i \tag{4.44}$$

where

$$H_0 = \hbar\omega_0(S_z^A + S_z^B) + \sum_{\lambda=e,m} \int d^3r \int_0^{+\infty} d\omega\ \hbar\omega\ \boldsymbol{f}_\lambda^\dagger(\boldsymbol{r},\omega)\cdot\boldsymbol{f}_\lambda(\boldsymbol{r},\omega), \tag{4.45}$$

is the free Hamiltonian, and

$$H_i = -\boldsymbol{\mu}_A\cdot\boldsymbol{E}(\boldsymbol{r}_A) - \boldsymbol{\mu}_B\cdot\boldsymbol{E}(\boldsymbol{r}_B) \tag{4.46}$$

is the interaction Hamiltonian. The unperturbed Hamiltonian is the sum of atomic and radiation field Hamiltonians: the first is written in terms of pseudo-spin operators S_z of the two atoms, whereas the second is given in terms of medium-assisted field operators $\boldsymbol{f}_\lambda^\dagger$ and $\boldsymbol{f}_\lambda$, describing the field inside a generic medium. Here $\boldsymbol{\mu}_{A(B)}$ is the electric dipole moment operator of the atom A(B) placed in $\boldsymbol{r}_{A(B)}$, and $\mathbf{E}(\mathbf{r}_{A(B)})$ is the medium-assisted electric field operator evaluated at atomic positions and given by

$$\begin{aligned}\mathbf{E}(\mathbf{r}) &= \int_0^\infty d\omega \mathbf{E}(\mathbf{r},\omega) + H.c. \\ &= \sum_{\lambda=e,m}\int d^3r' \int_0^\infty d\omega\ \mathbf{G}_\lambda(\mathbf{r},\mathbf{r}',\omega)\cdot\mathbf{f}_\lambda(\mathbf{r}',\omega) + H.c.,\end{aligned} \tag{4.47}$$

where $\mathbf{G}(\mathbf{r},\mathbf{r}',\omega)$ is the electromagnetic Green's tensor, introduced in Chapter 2 (see Eq. (2.62)). The resonance interaction energy between the entangled atoms, owing to the atom-field interaction, is given by [11]

$$\Delta E_{\pm} = \mathcal{P}\sum_{I} \frac{\langle\psi_{\pm}|\, H_i\,|I\rangle\,\langle I|\, H_i\,|\psi_{\pm}\rangle}{\hbar\omega_0 - E_I}, \tag{4.48}$$

where $\mathcal{P}$ indicates the principal value. Here $|I\rangle$ are the intermediate states, with energies E_I that contribute to the resonance interaction; these states are

$$\begin{aligned} |I\rangle_1 &= |g_A, g_B, \mathbf{1}_\lambda(\mathbf{r},\omega)\rangle\,, \\ |I\rangle_2 &= |e_A, e_B, \mathbf{1}_\lambda(\mathbf{r},\omega)\rangle\,, \end{aligned} \tag{4.49}$$

where $\mathbf{1}_\lambda(\mathbf{r},\omega)$ is a medium-assisted excitation of the radiation field.

Following a calculation similar to that done in Chapter 3 for the resonance energy transfer amplitude (3.19), a general expression for the resonance interaction energy between the two entangled atoms in terms of the Green's tensor of a generic environment is obtained,

$$\begin{aligned} \Delta E_{\pm} = \pm\frac{\hbar}{2\pi\epsilon_0 c^2}\mathcal{P}\int_0^\infty d\omega\omega^2 \sum_{ij}\Bigg\{ &\frac{1}{\hbar\omega_0 - \hbar\omega} \\ &\times\left[\mu_{Ai}^{eg}\,\mathrm{Im}\,G_{ij}(\mathbf{r}_A,\mathbf{r}_B,\omega)\,\mu_{Bj}^{ge} + \mu_{Bi}^{eg}\,\mathrm{Im}\,G_{ij}(\mathbf{r}_B,\mathbf{r}_A,\omega)\,\mu_{Aj}^{ge}\right] \\ - \frac{1}{\hbar\omega_0 + \hbar\omega}&\left[\mu_{Bi}^{ge}\,\mathrm{Im}\,G_{ij}(\mathbf{r}_B,\mathbf{r}_A,\omega)\,\mu_{Aj}^{eg} + \mu_{Ai}^{ge}\,\mathrm{Im}\,G_{ij}(\mathbf{r}_A,\mathbf{r}_B,\omega)\,\mu_{Bj}^{eg}\right]\Bigg\}. \end{aligned} \tag{4.50}$$

In this expression we have neglected the single-atom energy terms since, being space independent, do not contribute to the interatomic force. The (+) or (-) sign in Eq. (4.50) is related to the symmetrical or anti-symmetrical entangled state of the system, respectively, and the resulting interatomic force is then obtained by taking the derivative of (4.50) with respect to the interatomic distance $r = |\,\mathbf{r}_A - \mathbf{r}_B\,|$, changed of sign (quasi-static approach). We stress that Eq. (4.50) is an analytical expression of the resonance interaction between the two entangled atoms in the presence of a generic magneto-dielectric medium of arbitrary shape and material: all geometrical and structural properties of the environment are included in the Green's tensor expression [152]. If the atoms are in the free space, Eq. (4.50) reduces to the well-known resonance interaction expression in the free space (Eq. 1.78), as shown in detail in Appendix A.

In the next Section we will use the expression (4.50) to investigate the resonance interaction in the particular case of a cylindrical waveguide made of a perfect conductor.

4.2.1 Resonance interaction between two atoms inside a conducting cylindrical waveguide

The resonance dipole-dipole interaction between two entangled atoms placed on the axis of a perfectly conducting cylindrical waveguide is now investigated. Our purpose is to study how and whether the strength and the character of the resonance force between the atoms is modified by the presence of the cylindrical waveguide, investigating it as a function of the atomic separation z, the waveguide radius R, and as a function of the atomic dipole moments direction [152]. In order to achieve this purpose we use the analytical expression for the resonance interaction (4.50) and the well-known cylindrical Green tensor expression, already used in Chapter 3 to study the resonance energy transfer process inside a cylindrical waveguide. We recall that, if the atoms are placed on the cylinder axis, the Green's tensor is given by

$$\mathbf{G}(\mathbf{r},\mathbf{r}',\omega) \;=\; \frac{i}{4\pi}\sum_{m}\left[\left(\frac{e^{ik_{\mu}z}}{2I_{\mu 1}k_{\mu}}+\frac{k_{\lambda}e^{ik_{\lambda}z}}{2I_{\lambda 1}k^{2}}\right)(\hat{r}\otimes\hat{r}+\hat{\phi}\otimes\hat{\phi})+\frac{\lambda^{2}e^{ik_{\lambda}z}}{I_{\lambda 0}k_{\lambda}k^{2}}\hat{z}\otimes\hat{z}\right], \tag{4.51}$$

with the same notation and remarks done in Chapter 3.

Although we are considering the same physical system discussed in Chapter 3, it is relevant to point out that we are investigating different albeit related physical processes: the resonance interaction energy in this Section and the resonant energy transfer in Chapter 3. The first is a quantum interaction between two correlated atoms, one excited and the other in the ground state, arising from the exchange of a real or virtual photon between them; it eventually yields a force between the atoms that, in a quasi-static approach, is obtained from the derivative of the interaction energy with respect to the interatomic distance, changed of sign. On the other hand, the resonance energy transfer, as widely discussed in Chapter 3, is an exchange of electronic excitation between two atoms mediated by the quantum electromagnetic field; the atomic system, initially prepared in a factorized state $|e_A, g_B\rangle$ evolves to a different final state $|g_A, e_B\rangle$, owing to the exchange of energy.

We now consider the resonance interaction between the two atoms when $Rk_0 \ll 1$, which means that the atomic transition frequency is below the waveguide cut-off frequency $\omega_0 < \omega_{min}$. In this case the radiation field modes resonant with the atomic transition frequency are suppressed by the waveguide, and do not contribute to the resonance interaction energy (similarly to the case of the energy transfer process discussed in Chapter 3). Since the cylindrical electromagnetic Green's tensor (4.51) is symmetric for exchange of the positions of the atoms, the

resonance interaction (4.50) can be written as

$$\Delta E_{\pm} = \pm \frac{2}{\pi \epsilon_0} \sum_{ij} \mu_{Ai}^{eg} \mu_{Bj}^{ge} \mathcal{P} \int_{k_{min}}^{\infty} dk \frac{k^3}{k_0^2 - k^2} \operatorname{Im} G_{ij}(\mathbf{r}_A, \mathbf{r}_B, \omega), \tag{4.52}$$

where (+) and (−) sign refers to the symmetric or antisymmetric atomic entangled state, respectively.

It is now fundamental to note that the resonance interaction expression (4.52) coincides in modulus with the energy transfer amplitude (3.37), obtained in Chapter 3. Since we are assuming that $k_0 < k_{min}$, the resonant pole at $k = k_0$ is absent and thus the principal value in (4.52), and the prescriptions in (3.37) around the pole, do not play any role. For these reasons, all results obtained in the previous Chapter related to the energy transfer amplitude, (3.39), (3.40) and (3.41), when the atomic transition frequency is below the waveguide lower cut-off frequency, can be easily extended to the resonance interaction energy between two correlated atoms.

We investigate the resonance interaction energy as a function of the interatomic distance z and the waveguide cut-off frequency ω_{min}. For the sake of completeness, we show again these plots when both atoms have dipole moments parallel or perpendicular with respect to the waveguide axis. When the atoms are prepared in a symmetrical entangled state and have atomic dipole moments parallel to the guide axis and between each other, the resonance interaction is given by

$$\Delta E_{+} = -\frac{\mu_{Az}^{eg} \mu_{Bz}^{ge}}{4\pi \epsilon_0} \sum_{m} \frac{\lambda^2}{I_{\lambda 0}} \frac{e^{-\sqrt{\lambda^2 - k_0^2} z}}{\sqrt{\lambda^2 - k_0^2}}. \tag{4.53}$$

We have already demonstrated in Chapter 3 that the sum over the radial field modes converges. The plots in Fig. 4.4 show the Eq. (4.53), as a function of the interatomic distance z (Fig. 4.4a) and the waveguide radius R (Fig. 4.4b). The atoms are in the near zone range, $z < \lambda_0$, which means that the interatomic distance is smaller than the atomic transition wavelength, and the cylindrical waveguide radius R is such that $Rk_0 \ll 1$, which means that the waveguide suppresses the field mode resonant with the atomic transition frequency. Fig. 4.4a shows that the interaction has essentially the same dependence from the distance as in the free space case. Approaching the transition region between near and far zone, the resonance interaction becomes more and more suppressed with respect to the free space case. Fig. 4.4b shows that the resonance interaction quickly tends to vanish by decreasing R, whereas when R is increased, first increases (in absolute value) and then settles to an almost constant value.

In the far zone limit, $z > \lambda_0$, a numerical analysis shows that the resonance interaction is totally inhibited by the waveguide with respect to the free space

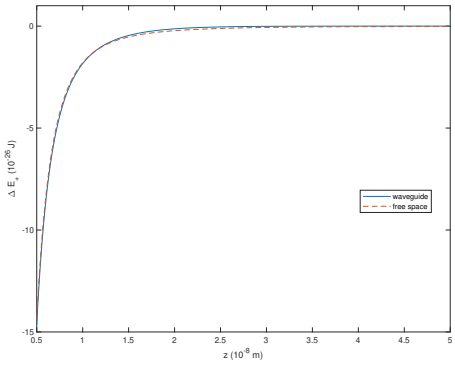

(a) Resonance interaction as a function of the interatomic distance z, with fixed radius $R = 10^{-8}$ m.

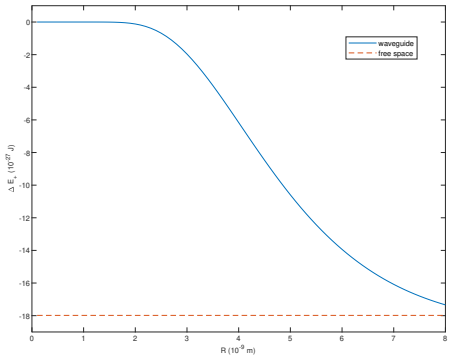

(b) Resonance interaction as a function of the waveguide radius R, with fixed distance $z = 10^{-8}$ m.

Figure 4.4: Resonance interaction between two atoms with axial dipole moments when $z < \lambda_0$ (near-zone limit), as a function of the interatomic distance z (4.4a), and as a function of the waveguide radius R (4.4b), when $Rk_0 \ll 1$, that is when $\omega_0 < \omega_{min}$. The blue solid line is the resonance interaction inside the cylindrical waveguide, whereas the orange dashed line is that in the free space. The numerical values of the parameters are $\lambda_0 = 5 \cdot 10^{-7}$ m, and $\mu^{eg}_{A/B\,z} = 10^{-30}$ C $\cdot$ m.

case by several orders of magnitude; e.g. when $z = 10^{-6}$ m the ratio between the resonance interaction in the waveguide and in the free space is $\Delta E_+/\Delta E_0 \sim 10^{-84}$, that is virtually zero. This emphasizes a completely different effect of the waveguide in the near and in the far zone.

The results obtained above show that, since in the regime $Rk_0 \ll 1$ the field modes resonant with the atomic transition frequency ω_0 are suppressed by the waveguide, the resonance interaction shall be suppressed too. In the very near zone, being essentially an electrostatic interaction between two correlated dipoles, the resonance interaction is slightly affected by the waveguide; whereas, approaching the intermediate region, it becomes an interaction dominated by radiative processes, and becoming more and more suppressed by the waveguide, and leading to a totally inhibition in the far zone. We have also shown that it is possible to modify and control the resonance interaction energy between the atoms through the waveguide's radius R. This result can be explained by taking into account that the lower cut-off frequency of the waveguide is strictly related to the waveguide radius R, $\omega_{min} \propto R^{-1}$; therefore by decreasing R, the cut-off frequency ω_{min} increases and the gap between ω_0 and ω_{min} increases too. This involves a further reduction of the number of field modes near the resonant frequency ω_0 that can contribute to the resonance interaction energy, thus leading to further reduction of

the interaction itself. In the limiting case, when the waveguide radius approaches zero, the resonance interaction vanishes, as expected.

We now consider the case of atoms having dipole moments along the radial direction, that is orthogonal to the waveguide axis, and parallel to each other. As before, the atomic system is prepared in the symmetrical entangled state. Likewise the case of axial dipoles, the resonance interaction expression, when $Rk_0 \ll 1$, coincides with that of the resonance energy transfer amplitude (3.55), given by

$$\Delta E_+ = \frac{\mu_{Ar}^{eg}\mu_{Br}^{ge}}{8\pi\epsilon_0}\sum_m \left(-\frac{k_0^2 e^{-\sqrt{\mu^2-k_0^2}z}}{I_{\mu 1}\sqrt{\mu^2-k_0^2}} + \frac{\sqrt{\lambda^2-k_0^2}e^{-\sqrt{\lambda^2-k_0^2}z}}{I_{\lambda 1}} \right). \tag{4.54}$$

For this reason, the same remarks and results previously obtained can be easily extended to the resonance interaction energy between two correlated atoms inside the waveguide.

Nevertheless, a brand-new, interesting aspect emerges when we investigate the resonance interaction between two radial dipoles inside the waveguide as a function of the interatomic distance z, in the near zone limit. Fig. (4.5) shows the ratio

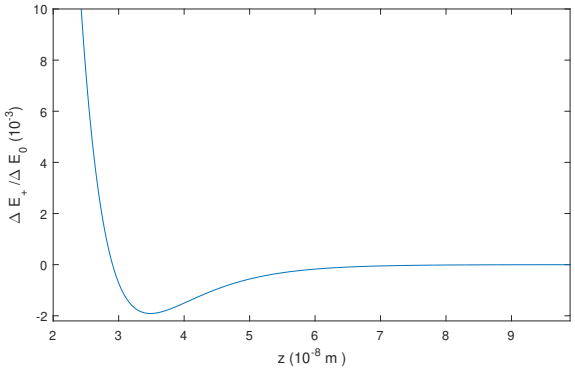

Figure 4.5: Resonance interaction energy between atoms with radial dipoles as a function of the interatomic distance z, normalised to the free space interaction ΔE_0. The atoms are in a symmetric entangled state and in the near zone. When z approaches the transition region between the near and the far zone ($z \sim \lambda_0$), the resonance interaction becomes more and more suppressed with respect to the free-space interaction. We also point out that the resonance interaction changes its character, from repulsive to attractive for interatomic separation larger than $z \gtrsim 2.9 \cdot 10^{-8}$m. The parameters used are $\lambda_0 = 5 \cdot 10^{-7}$ m, $R = 10^{-8}$ m and $d_{A/B\,z}^{eg} = 10^{-30}$ C $\cdot$ m.

between the resonance interaction energy between two radial dipoles inside the waveguide (ΔE_+) and in the free space (ΔE_0) as a function of the interatomic

distance z. The resonance interaction energy ΔE_0, in the free space and in the near zone limit, is

$$\Delta E_0 = \frac{\mu_{Ar}^{eg}\mu_{br}^{eg}}{4\pi\epsilon_0 z^3}\cos(k_0 z). \tag{4.55}$$

One of the most relevant effects to highlight is that the waveguide changes the character of the resonance interaction, from repulsive to attractive, for interatomic distance larger than $z \gtrsim 2.9 \cdot 10^{-8}$ m. We point out that the resonance interaction between radial dipoles in the free space and in the near zone regime (4.55) is always repulsive but, if the atoms are inside the cylindrical waveguide, the resonance interaction changes its character, becoming attractive [152]. Furthermore, in this range the interaction is reduced by a factor of the order of 10^{-3}, compared to the free-space case. We stress that this reduction is much more significant in the present configuration of the system, compared to the axial dipoles case. Therefore, these results show that when the atoms have atomic dipole moments orthogonal to the cylinder axis, the presence of the conducting waveguide influences the resonance interaction more deeply; in addition to a suppression of its strength, a change of its character, from repulsive to attractive, is obtained. In the far zone limit, analogously to the case for which the atoms have axial dipole moments, the resonance interaction is strongly suppressed by the waveguide and it is virtually zero.

Similar considerations hold for the case of atoms prepared in the antisymmetric entangled state; in this situation the resonance interaction energy is the same obtained for the symmetric entangled state, except for a change of sign (see Eq. (4.52)).

4.3 Conclusions

In this Chapter we have presented our original results on the resonance interaction energy between two identical correlated atoms, prepared in a symmetrical or antisymmetrical Bell-type state: two different physical situations have been considered in detail, highlighting different and interesting aspects of the resonance force.

In the first Section, the time-dependent resonance interaction energy during the dynamical self-dressing process of the two atoms has been considered, starting from a nonequilibrium configuration (bare state). We have shown that the resonance interaction vanishes when the two atoms are outside the light-cone of each other, while it settles to its stationary value immediately after the causality time $t = R/c$. We have related these findings to a sort of interference between the contributions of real and virtual processes occurring during the time evolution of the system. We have also discussed the time-dependent electric energy density in the space around

the two entangled atoms, both for subradiant (antisymmetrical) and superradiant (symmetrical) states, and pointed out that its behaviour is due to interference effects of the field emitted by the two atoms. Finally, we have also suggested that our results concerning the time-dependent electric energy density for the two entangled atoms, can be experimentally probed through a measure of the Casimir-Polder force on a third atom located in the vicinity of the two entangled atoms.

In the second Section, the effect of a perfectly conducting cylindrical waveguide on the resonance interaction between two entangled atoms has been investigated. We have first introduced an analytical expression for the resonance interaction energy between two correlated atoms in the presence of a generic magneto-dielectric medium, using the electromagnetic Green tensor formalism. We have then considered the resonance interaction in the specific case of two entangled atoms placed on the axis of a perfectly conducting cylindrical waveguide, which determines a lower cut-off frequency for the radiation field modes inside it. We have shown that, when the atomic transition frequency is smaller than the waveguide cut-off frequency, the resonance interaction between the atoms is strongly modified by the presence of the waveguide. We have investigated the interaction both for atomic dipole moments parallel and orthogonal to the cylinder axis; in both cases the resonance interaction is deeply suppressed if the atoms are in the radiative far zone, while it is much less modified if they are in the radiationless near zone. We have also stressed that it is possible to modify and control the strength of the interaction through external actions, specifically by changing the cylinder radius. Finally, we have shown that in the near zone, for radial atomic dipole moments, it is possible to change even the character of the resonance force, turning it from repulsive to attractive (symmetric state). These results point out how the presence of a structured environment, such as the conducting waveguide, allows to manipulate and control the strength and even the character of the resonance interaction energy between two entangled atoms.

Chapter 5

Dispersion interaction between two hydrogen atoms in a static electric field

The van der Waals/Casimir-Polder force is a dispersion interaction between neutral, unpolarised and unmagnetised atoms, molecules or any quantum emitters, mediated by the quantum electromagnetic field [9, 11, 12], as discussed in Chapter 1. In the absence of any external electromagnetic field applied on the atomic system, the Casimir-Polder interaction between two ground-state atoms is a fourth-order effect in the coupling with the quantum radiation field [5, 6, 8]. This is equivalent to the exchange of a pair of virtual photons between them. For this reason, the Casimir-Polder force is an ubiquitous interaction between any pair of quantum emitters, existing even between neutral atoms, and it is usually a very weak interaction, several orders of magnitude smaller than Coulomb interactions. When the atoms are in their ground-state, the interaction is always attractive, behaves as r^{-6} in the nonretarded near zone [13] and as r^{-7} in the retarded far zone regime [14], being r the interatomic distance. This behaviour is related to the fact that in the near zone regime the dispersion interaction is essentially a radiationless process, whereas, in the far zone limit, the process becomes radiative, taking into account the finite speed of light propagation [1, 5, 18]. Although its small strength, the dispersion interactions have great relevance in many areas of physics, and also several applications in biology [52, 166], chemistry [180] and nano-technologies [79, 181, 182].

A striking property of the Casimir-Polder interaction, and related effects, is that it can be strongly modified by an external environment [65], such as for example a cavity or a conducting wall [25, 66, 183], a waveguide [67, 116, 184, 185], or a photonic band-gap material.

In recent years, the possibility of manipulating van der Waals interactions

between atoms through external optical fields has been investigated in the literature, specifically modifications of the dispersion interaction due to the applied field, and changes of its distance dependence [106, 186, 187]. Modifications of the atom-surface Casimir-Polder force have been recently considered too. In [188], for example, it is shown that near-resonant light can significantly modify atom-surface van der Waals/Casimir-Polder interactions in the nonretarded regime; in particular, near-resonant laser light with an intensity of 5 W/cm^2 is predicted to double the interaction strength for sodium atoms, and possible experiments to detect this effect are discussed. Very recently, it has been also shown that the Casimir-Polder interaction between a ground-state atom and a non-dispersive surface, in the presence of an external quantum field, has similar features of the Casimir-Polder potential between excited atoms [189], leading to the possibility of a repulsive Casimir-Polder force [190];

In this Chapter we present our original work on the van der Waals/Casimir-Polder interaction between two ground-state hydrogen atoms in the free space and at zero temperature, subjected to an external static electric field. Our purpose is to investigate whether and how the dispersion interaction is modified by the external field and if it should be exploited to tailor and control the interatomic force [191]. Main point is that, due to the presence of the external field, the atoms become polarized, with correlated dipole moments; we find that the dispersion interaction between the atoms is strongly modified by the external field, even for a reasonable field strength experimentally achievable in the laboratory. We investigate both cases when the atoms are in the nonretarded and in the retarded Casimir-Polder regime. We consider in detail different configurations of the system, according to the relative direction of the homogeneous electric fields acting on the two atoms, specifically parallel and antiparallel between each other, as well as parallel and orthogonal orientation of the interatomic distance with respect to the direction of the external field. We find that the space dependence of the dispersion interaction between the atoms changes, decreasing slower with the distance: the field-modified Casimir-Polder interaction behaves as r^{-3} and r^{-4} in the near and far zone respectively, rather than the well-known r^{-6} and r^{-7} behaviour for unperturbed atoms. We also show that it is possible to significantly modify and control its magnitude and even its character, turning it from attractive to repulsive and vice versa, through external fields with a strength that can be easily reached in current experiments. We also find that, given a specific distance between the atoms, choosing external fields with an appropriate strength and direction, the dispersion force between the atoms can be totally cancelled. These new findings show the possibility to deeply control the strength, the spatial dependence and even the character of the dispersion interaction between the atoms or molecules through an external static electric field. A clear physical interpretation of these results is

discussed, as well a numerical estimate of the effect and its observability for values of the electric field that can be currently obtained in the laboratory. These results could be relevant also for a possible direct measurement of dispersion interactions between atoms, in particular in the retarded Casimir-Polder regime, as well as for macroscopic properties of gases of neutral atoms or molecules interacting through long-range van der Waals dispersion interactions.

This Chapter is organized as follows: in Sec. 5.1 the theory is developed within the framework of quantum electrodynamics and a general expression for the dispersion interaction between two hydrogen atoms in the presence of static external electric fields is obtained. In Sec. 5.2, we consider two specific geometric configurations of the atomic system with respect to the external fields: interatomic distance orthogonal and parallel with respect to the external field directions. We show the possibility to modify the magnitude, the spatial dependence and even the character of the dispersion interaction through external electric fields. Finally, Sec. 5.3 is devoted to our conclusions and final remarks.

5.1 The field-modified dispersion interaction

We consider the dispersion interaction between two hydrogen atoms, labelled A and B, interacting with the quantum electromagnetic field in the vacuum state, in the presence of external static and uniform electric fields [191]. $\boldsymbol{\mathcal{E}}$ and $\boldsymbol{\mathcal{E}}'$ are respectively the external classical fields acting on atoms A and B, and they are assumed uniform over the atomic dimensions. We assume that atom A is placed at the origin $\mathbf{r} = 0$, and $\mathbf{r}$ is the distance between the two atoms. The system is prepared in its unperturbed ground state,

$$|\psi_0\rangle = \mid \phi^A_{100}, \phi^B_{100}\rangle \mid 0_{\boldsymbol{k}\lambda}\rangle, \tag{5.1}$$

where $\mid \phi_{n\ell m}\rangle$ is an hydrogen states with the quantum numbers n, ℓ, m (principal quantum number, orbital quantum number, and magnetic quantum number). The electromagnetic field is in its vacuum state $\mid 0_{\boldsymbol{k}\lambda}\rangle$. The energy of the state (5.1) is $E_0 = 2E_1$, where $E_1 = -\hbar^2/2ma_0^2$ is the unperturbed energy of the ground state of the hydrogen atom, and $a_0 = 0.53$ Å is the Bohr's radius.

The Hamiltonian of the system is

$$H = H_0 + V_A + V_B + H_i^A + H_i^B, \tag{5.2}$$

where $H_0 = H_A + H_B + H_F$ is the unperturbed Hamiltonian, sum of the atomic Hamiltonians, H_A and H_B, and the transverse field Hamiltonian H_F; $V_{A(B)}$ and $H_i^{A(B)}$ are, respectively, the interaction Hamiltonians of atom $A(B)$ related to the

external classical field and to the radiation field. In the multipolar coupling scheme and within the dipole approximation, they are given by

$$V_A = -\boldsymbol{\mu}_A \cdot \boldsymbol{\mathcal{E}} \qquad V_B = -\boldsymbol{\mu}_B \cdot \boldsymbol{\mathcal{E}}', \tag{5.3}$$

$$H_i^A = -\boldsymbol{\mu}_A \cdot \mathbf{E}(\mathbf{0}) \quad H_i^B = -\boldsymbol{\mu}_B \cdot \mathbf{E}(\mathbf{r}), \tag{5.4}$$

where $\boldsymbol{\mu}_{A(B)}$ is the dipole moment operator of atom A(B), and

$$\mathbf{E}(\boldsymbol{r}) = i \sum_{\boldsymbol{k}\lambda} \sqrt{\frac{\hbar c k}{2V\epsilon_0}} \hat{e}_{\boldsymbol{k}\lambda} \left(a_{\boldsymbol{k}\lambda} e^{i\boldsymbol{k}\cdot\boldsymbol{r}} - a_{\boldsymbol{k}\lambda}^\dagger e^{-i\boldsymbol{k}\cdot\boldsymbol{r}} \right) \tag{5.5}$$

is the transverse displacement field operator, that, outside the atomic positions, coincides with the total (transverse plus longitudinal) electric field operator [5, 11].

In the absence of the external static classical electric field, the dispersion interaction between the two atoms is due to the exchange of two virtual photons between them, and it is a fourth-order effect in the coupling with the quantum radiation field [5, 6, 8]. From a physical point of view, this is because vacuum field fluctuations must induce and correlate dipole moments in the atoms (this accounts two orders in the atom-field coupling), and, afterwards, the correlated induced dipoles yield a nonvanishing interaction energy (accounting two more orders in the coupling constant) [192]. In the present case, where the atoms are embedded in a static electric field, the situation for the component of the dispersion interaction related to the external field, changes: i) the external electric fields polarize both atoms, that acquire a permanent electric dipole moment and also correlate them: this is a first order process in the coupling with the external field, for each atom; ii) then, the induced permanent dipole moments interact through the transverse field, exchanging one virtual photon, thus a second-order process in the coupling with the transverse field; iii) so, even though the interaction energy is still a fourth-order effect, proportional to the fourth power of the electron charge q, a factor q^2 is related to the interaction with the external classical field and proportional to their intensity, while another factor q^2 is related to the interaction with the quantum transverse field. Therefore, the interatomic potential is due to the exchange of just one virtual photon, similarly to the atom-wall Casimir-Polder interaction [15] or the resonance interaction between identical entangled atoms, one excited and the other in the ground state, discussed in Chapter 4 [11, 161].

We assume that external classical fields can be treated as a small perturbation of the system, thereby leading to a correction of the unperturbed ground state (5.1), and a Stark energy shift, that can be obtained through time-independent perturbation theory. Now, we first obtain the corrected ground state at second order in the coupling with the external field, and then, in order to obtain the interatomic dispersion interaction, we evaluate the distance-dependent part of the

energy shift due to the interaction with the quantum transverse field. As previously mentioned, we will find that this energy shift starts from the second order in the coupling with the transverse radiation field. We assume that both fields $\boldsymbol{\mathcal{E}}$ and $\boldsymbol{\mathcal{E}}'$ are along the z axis, directed in the positive or negative direction. For simplicity, in our evaluation we include only the contribution from atomic intermediate states with principal quantum number $n = 2$. Using the time-independent perturbation theory, the perturbed ground state, at the second order in the coupling with the external static field, is

$$\begin{aligned} \mid \psi\rangle &= \left\{ \left[1-\gamma^2(\mathcal{E}^2+\mathcal{E}'^2)\right] \mid \phi^A_{100},\phi^B_{100}\rangle \right. \\ &- \sqrt{2}\gamma\left(\mathcal{E} \mid \phi^A_{210},\phi^B_{100}\rangle + \mathcal{E}' \mid \phi^A_{100},\phi^B_{210}\rangle\right) \\ &+ \gamma^2\left[2\mathcal{E}\mathcal{E}' \mid \phi^A_{210},\phi^B_{210}\rangle - \frac{1}{\sqrt{2}}\left(\frac{3}{2}\right)^6\right. \\ &\times \left.\left.\left(\mathcal{E}^2 \mid \phi^A_{200},\phi^B_{100}\rangle + \mathcal{E}'^2 \mid \phi^A_{100},\phi^B_{200}\rangle\right)\right]\right\} \mid 0_{\boldsymbol{k}\lambda}\rangle, \end{aligned} \tag{5.6}$$

where $\gamma = 2^9 q a_0/(3^6 E_1)$, E_1 is the unperturbed energy of the ground state of the hydrogen atom, a_0 the Bohr's radius, and $\mid 0_{\boldsymbol{k}\lambda}\rangle$ the photon vacuum. The state (5.6) is the ground state of the system corrected up to the second-order in the coupling between atoms and the external fields $\boldsymbol{\mathcal{E}}$ and $\boldsymbol{\mathcal{E}}'$. The second-order Stark energy shift, owing to the external fields, is given by

$$\begin{aligned} E^{(2)} =& \sum_I \frac{\langle\psi_0|\left(V_A+V_B\right)|I\rangle\langle I|\left(V_A+V_B\right)|\psi_0\rangle}{E_0-E_I} \\ =& \frac{3}{2}\gamma^2 E_1(\mathcal{E}^2+\mathcal{E}'^2) \end{aligned} \tag{5.7}$$

where E_0 is the energy of the unperturbed state (5.1) and $|I\rangle$ are intermediate states, $|\phi^A_{100},\phi^B_{210},0_{\boldsymbol{k}\lambda}\rangle$ and $|\phi^A_{210},\phi^B_{100},0_{\boldsymbol{k}\lambda}\rangle$, that contribute to the energy shift (5.7). Therefore the energy of the perturbed state (5.6), corrected up to the second order in the coupling with external fields, is

$$E_\psi = 2E_1 + \frac{3}{2}\gamma^2 E_1(\mathcal{E}^2+\mathcal{E}'^2). \tag{5.8}$$

This quantity is negative since $E_1 < 0$. Since we have assumed that the external fields can be treated perturbatively with respect to the atomic energies of the system, their intensities must be such that the second order energy correction in Eq. (5.8), should be much smaller than the unperturbed energy of the system; that is

$$\frac{3}{2}\gamma^2 E_1(\mathcal{E}^2+\mathcal{E}'^2) \ll 2E_1. \tag{5.9}$$

Assuming external fields with the same intensities $\mathcal{E} = \mathcal{E}'$, a numerical estimation of (5.9) relation yields

$$\mathcal{E} \ll 3 \cdot 10^{11} \text{ V/m}. \tag{5.10}$$

The relation (5.10) establishes possible external electric field intensities that can be exploited in our system, in order to calculate the field-assisted dispersion interaction between the hydrogen atoms using a perturbative approach.

Les us now consider the energy correction to the state (5.6) due to the interaction between the atoms and the quantum transverse radiation field given by (5.4). The second-order energy correction is

$$\Delta E = \sum_I \frac{\langle\psi| \left(H_i^A + H_i^B\right) |I\rangle \langle I| \left(H_i^A + H_i^B\right) |\psi\rangle}{E_\psi - E_I}, \tag{5.11}$$

where E_ψ is the energy of the perturbed state (5.8). Since we are interested to the dispersion force between the two atoms, we need to evaluate only the part of the shift (5.11) that depends on the interatomic distance, and thus only terms of ΔE containing both H_I^A and H_I^B are relevant [191]. Thus, neglecting atomic self-interaction terms, that do not contribute to the interatomic potential, we obtain

$$\begin{aligned}\Delta E &= \sum_I \frac{\langle\psi| H_i^A |I\rangle \langle I| H_i^B |\psi\rangle}{E_\psi - E_I} + \sum_I \frac{\langle\psi| H_i^B |I\rangle \langle I| H_i^A |\psi\rangle}{E_\psi - E_I} \\ &= 2\sum_I \frac{\langle\psi| H_i^A |I\rangle \langle I| H_i^B |\psi\rangle}{E_\psi - E_I}\end{aligned} \tag{5.12}$$

where $|I\rangle$ are all possible intermediate states, with energy E_I, that contribute to the energy shift (5.12). These states are eigenstates of $H_0 + V_A + V_B$ and, in our approximation that takes into account only atomic excited states with principal quantum number $n = 2$, with a fourfold degeneracy and a unperturbed energy $E_2 = E_1/4$, we must consider that these states are degenerate. Thus, using degenerate-state perturbation theory, the intermediate states at zeroth-order in the coupling with the external static fields, are

$$|I\rangle = \frac{1}{2}\Big(|\phi_{210}^A\rangle \pm |\phi_{200}^A\rangle \Big)\Big(|\phi_{210}^B\rangle \pm |\phi_{200}^B\rangle \Big) \mid 1_{\boldsymbol{k}\lambda}\rangle \tag{5.13}$$

where $\mid 1_{\boldsymbol{k}\lambda}\rangle$ represents a one-photon state with wavevector $\boldsymbol{k}$ and polarization $\lambda = 1, 2$. From intermediate states (5.13), considering only fourth-order terms in the electron charge that lead to a distance-dependent energy shift, we easily find that the only relevant intermediate states are in the form $\mid \phi_{210}^A, \phi_{210}^B, 1_{\boldsymbol{k}\lambda}\rangle$, with energy $E_I = 2E_2 + \hbar\omega_k$. It can be easily shown that first or higher-order corrections of the intermediate states $|I\rangle$ lead to the distance-dependent contributions to the energy shift contributions that are at an order higher than the fourth in the electron

charge, and thus we can neglect them. Also, we point out that, since the energy shift (5.12) is an overall fourth-order effect, two orders in the quantum transverse fields and two orders in the external static fields, the energies E_ψ and E_I in the denominator of (5.12) are given just by the unperturbed energies, without the second-order Stark-shift correction (5.7).

The distance-dependent energy shift can be then written as

$$\begin{aligned}\Delta E(r) &= \sum_{\boldsymbol{k}\lambda} \frac{4}{2E_1 - (E_2 + \hbar\omega_k)} 2\gamma^2 \mathcal{E}\mathcal{E}' \\ &\times \langle \phi^A_{210}, \phi^B_{100}, 0_{\boldsymbol{k}\lambda} |\, H_i^B \,| \phi^A_{210}, \phi^B_{210}, 1_{\boldsymbol{k}\lambda} \rangle \, \langle \phi^A_{210}, \phi^B_{210}, 1_{\boldsymbol{k}\lambda} |\, H_i^A \,| \phi^A_{100}, \phi^B_{210}, 0_{\boldsymbol{k}\lambda} \rangle \\ &= -\sum_{\boldsymbol{k}\lambda} \frac{8\gamma^2 \mathcal{E}\mathcal{E}'}{2(E_2 - E_1) + \hbar\omega_k} \, \langle \phi^B_{100}, 0_{\boldsymbol{k}\lambda} |\, H_i^B \,| \phi^B_{210}, 1_{\boldsymbol{k}\lambda} \rangle \, \langle \phi^A_{210}, 1_{\boldsymbol{k}\lambda} |\, H_i^A \,| \phi^A_{100}, 0_{\boldsymbol{k}\lambda} \rangle \\ &= -\frac{4\gamma^2 \, \mathcal{E}\mathcal{E}'}{V\epsilon_0} \sum_{\boldsymbol{k}\lambda} \frac{k}{k_0 + k} (\boldsymbol{\mu}_A^{eg} \cdot \boldsymbol{e}_{\boldsymbol{k}\lambda}) \, (\boldsymbol{\mu}_B^{ge} \cdot \boldsymbol{e}_{\boldsymbol{k}\lambda}) \, e^{i\boldsymbol{k}\cdot\boldsymbol{r}} \,, \end{aligned} \tag{5.14}$$

where in the last row, the relations

$$\langle \phi^B_{100}, 0_{\boldsymbol{k}\lambda} |\, H_i^B \,| \phi^B_{210}, 1_{\boldsymbol{k}\lambda} \rangle = i \sqrt{\frac{\hbar c k}{2V\epsilon_0}} (\boldsymbol{\mu}_B^{ge} \cdot \boldsymbol{e}_{\boldsymbol{k}\lambda}) \, e^{i\boldsymbol{k}\cdot\boldsymbol{r}_B} \,, \tag{5.15}$$

$$\langle \phi^A_{210}, 1_{\boldsymbol{k}\lambda} |\, H_i^A \,| \phi^A_{100}, 0_{\boldsymbol{k}\lambda} \rangle = -\, i \sqrt{\frac{\hbar c k}{2V\epsilon_0}} (\boldsymbol{\mu}_A^{eg} \cdot \boldsymbol{e}_{\boldsymbol{k}\lambda}) \, e^{-i\boldsymbol{k}\cdot\boldsymbol{r}_A} \tag{5.16}$$

have been used. Here $\boldsymbol{r} = \boldsymbol{r}_B - \boldsymbol{r}_A$ is the interatomic distance and $k_0 = 2 \mid E_2 - E_1 \mid /(\hbar c) = 3 \mid E_1 \mid /(2\hbar c)$ is related to the wavevector associated to the transition between the ground and the first excited level of the hydrogen atom. The quantities $\boldsymbol{\mu}^{eg}_{A(B)}$ are matrix elements of the atomic dipole moment operator between states $\mid e\rangle = \mid \phi_{210}\rangle$ and $\mid g\rangle = \mid \phi_{100}\rangle$; these vectors are induced by the external electric fields and are oriented along the z axis, that is the same direction of the static fields acting on the atoms.

Performing the polarization sum, $\sum_\lambda (\hat{e}_{\boldsymbol{k}\lambda})_i (\hat{e}^*_{\boldsymbol{k}\lambda})_j = \delta_{ij} - \hat{k}_i \hat{k}_j$, the continuum limit, $\sum_{\boldsymbol{k}} \to V/(2\pi)^3 \int dk k^2 \int d\Omega$, and using the relation

$$\int d\Omega \, (\delta_{ij} - \hat{k}_i \hat{k}_j) \, e^{i\boldsymbol{k}\cdot\boldsymbol{r}} = 4\pi \, \mathrm{Im} \left[\frac{1}{k^3} \Big(-\nabla^2 \delta_{ij} + \nabla_i \nabla_j \Big) \frac{e^{ikr}}{r} \right] , \tag{5.17}$$

after some algebraic calculations involving angular and frequency integrations, equation (5.14) becomes

$$\Delta E = -\frac{2\gamma^2}{\pi^2 \epsilon_0} \mathcal{E}\mathcal{E}' (\mu_A^{eg})_i (\mu_B^{ge})_j \Big(-\nabla^2 \delta_{ij} + \nabla_i \nabla_j \Big) \frac{f(k_0 r)}{r} . \tag{5.18}$$

where the Einstein convention of repeated indices has been used. Here, the differential operators act on the variable r, and we introduce the auxiliary functions

$$f(x) = \mathrm{Ci(x)}\sin(\mathrm{x}) + \left(\frac{\pi}{2} - \mathrm{Si(x)}\right)\cos(\mathrm{x}), \tag{5.19}$$

$$g(x) = -\mathrm{Ci(x)}\cos(\mathrm{x}) + \left(\frac{\pi}{2} - \mathrm{Si(x)}\right)\sin(\mathrm{x}), \tag{5.20}$$

with Si(x) and Ci(x) being the sine and cosine integral functions [26–28]. Applying the differential operators, knowing that

$$\frac{df(x)}{dx} = -g(x) \quad , \quad \frac{dg(x)}{dx} = f(x) - \frac{1}{x}\,, \tag{5.21}$$

the expression (5.18) becomes

$$\Delta E = -\frac{2\gamma^2}{\pi^2\epsilon_0}\mathcal{E}\mathcal{E}'(\mu_A^{eg})_i(\mu_B^{ge})_j\frac{1}{r}\Bigg\{(\delta_{ij} - 3\hat{r}_i\hat{r}_j)\left[\frac{f(k_0r)}{(k_0r)^2} + \frac{g(k_0r)}{k_0r}\right] - (\delta_{ij} - \hat{r}_i\hat{r}_j)\left[f(k_0r) - \frac{1}{k_0r}\right]\Bigg\}. \tag{5.22}$$

The expression (5.22) gives the field-assisted dispersion interaction between the two atoms, for a general configuration of the atoms with respect to the external electric fields, directed along z-axis [191]. Contrarily to the dispersion interaction between nonpolarized atoms or molecules in the vacuum, that is a fourth-order process in the coupling with the radiation field, involving the exchange of two virtual photons, the dispersion interaction (5.22) is a second-order quantity in the coupling with the radiation field, involving the exchange of one virtual photon between the atoms. However, it contains also a second-order coupling with the external fields, and thus it is an overall fourth-order process in the electron charge q. We wish also to point out that this interaction is proportional to the external fields intensities $\mathcal{E}$ and $\mathcal{E}'$ applied to the atoms; this is a relevant result because it is possible to modify and control the strength of the dispersion interaction between the atoms, and even its attractive/repulsive character through external fields, as we will discuss in great detail in the next Section.

It should also be noted that the field-assisted contribution obtained in Eq. (5.22) must of course be added up to the usual, unperturbed van der Waals/Casimir-Polder interaction energy between ground-state nonpolar atoms or molecules. In the next Section we compare these two contribution to the dispersion force, investigating for which geometrical configurations and external field strength, the field-assisted dispersion force becomes comparable, or even larger, than the unperturbed van der Waals interaction.

We will now investigate the total dispersion interaction between two hydrogen atoms, focusing on two specific and relevant geometrical configurations of the system: interatomic distance aligned perpendicularly or parallel to the direction of the external field.

5.2 Atoms aligned perpendicularly and parallel to the external field

We now consider two different geometrical configurations of the atoms with respect to the external static fields: in the first case the interatomic distance is perpendicular to the external fields, and in the second case the atomic separation is parallel to the external fields. These two specific geometrical configurations of the system are shown in Fig. 5.1, where we have assumed for simplicity that the atoms are subjected to the same external fields $\boldsymbol{\mathcal{E}} = \boldsymbol{\mathcal{E}}'$ [191]. The induced atomic dipoles, depicted in Fig. 5.1 by the red arrows on the atoms, have clearly the same direction of the external field.

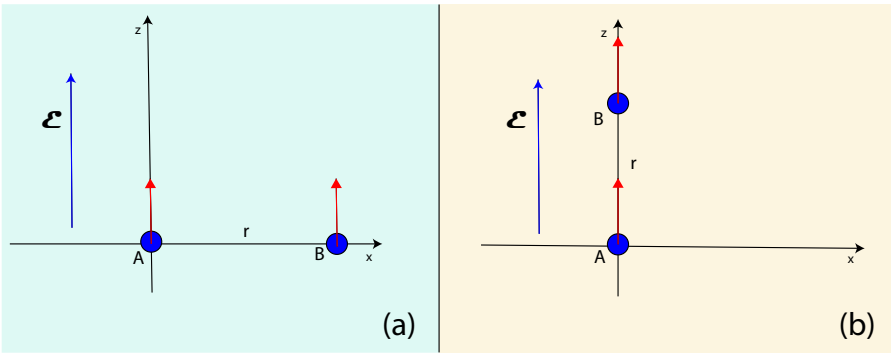

Figure 5.1: Two hydrogen atoms in free space in the presence of an external static electric field $\mathcal{E}$ along the z-direction, acting on the atoms: (a) atoms aligned perpendicularly to the direction of the external field; (b) atoms aligned in the same direction of the external field. In the case shown in the Figure, the fields acting on atoms A and B have the same direction, and the red arrows at the position of the atoms indicate the direction of the induced dipole moments [191].

For convenience, we have defined the quantity

$$\beta = \frac{2\gamma^2 k_0^2}{\pi^2\epsilon_0}\,\mu_A^{eg}\mu_B^{ge} = \frac{2^{32}q^4a_0^4}{3^{20}\pi^2\epsilon_0\hbar^2c^2} = \frac{9k_0^2}{4\pi^2\epsilon_0}\alpha^2, \tag{5.23}$$

where, in the first equality, we have used the fact that the two atoms are identical and that $\boldsymbol{\mu}_{A(B)}^{eg} = \langle\phi_{210} \mid q\boldsymbol{r} \mid \phi_{100}\rangle = 2^{15/2}3^{-5}qa_0\hat{z}$. $\alpha = 2\mu^2/[3(E_2 - E_1)]$ is the

static polarizability of the atoms, k_0 is double the wavevector associated to the atomic transition between the ground and the first excited level of the hydrogen atom, and it was defined in the previous section as $k_0 = 3 \mid E_1 \mid /(2\hbar c)$.

When the atoms are aligned perpendicularly with respect to the direction of the external field, panel *a*) in Fig. 5.1, the dispersion interaction (5.22) becomes

$$\Delta E_{\perp}(r) = \beta \mathcal{E}\mathcal{E}' \frac{1}{r}\left[f(k_0 r)\left(\frac{1}{(k_0 r)^2} - 1\right) + \frac{g(k_0 r)}{k_0 r} + \frac{1}{k_0 r}\right]. \tag{5.24}$$

In order to investigate the near and far zone limits of the field-assisted dispersion interaction (5.24), we use the expansions of the auxiliary function $f(x)$ and $g(x)$ for small and large arguments [26, 27]. For $x \ll 1$, we have

$$f(x) \sim \frac{\pi}{2} + \Big(\gamma + \ln(x) - 1\Big)x - \cdots, \tag{5.25}$$

$$g(x) \sim -\gamma - \ln(x) + \frac{\pi x}{2} + \cdots, \tag{5.26}$$

where γ is the Euler-Mascheroni constant. On the other hand, the asymptotic expansions for $x \gg 1$, are

$$f(x) \sim \frac{1}{x}\left(1 - \frac{2!}{x^2} + \frac{4!}{x^4} - \frac{6!}{x^6} + \cdots\right), \tag{5.27}$$

$$g(x) \sim \frac{1}{x^2}\left(1 - \frac{3!}{x^2} + \frac{5!}{x^4} - \frac{7!}{x^6} + \cdots\right). \tag{5.28}$$

Therefore, the dispersion interaction (5.24) can be conveniently approximated when the atoms are in the near zone, that is when $k_0 r \ll 1$, and when they are in the far zone, $k_0 r \gg 1$, yielding

$$\Delta E_{\perp}(r) = \beta \mathcal{E}\mathcal{E}' \frac{1}{k_0^2} \times \begin{cases} \frac{\pi}{2r^3} & \text{for } \; k_0 r \ll 1 \\ \\ \frac{4}{k_0 r^4} & \text{for } \; k_0 r \gg 1. \end{cases} \tag{5.29}$$

Similarly, in panel *b*) of Fig. 5.1, when the atoms are aligned in the same direction of the external field, we have

$$\Delta E_{\parallel}(r) = -2\beta \mathcal{E}\mathcal{E}' \frac{1}{r}\left[\frac{f(k_0 r)}{(k_0 r)^2} + \frac{g(k_0 r)}{k_0 r}\right], \tag{5.30}$$

and the near and far zone approximations are

$$\Delta E_{\parallel}(r) = -\beta \mathcal{E}\mathcal{E}' \frac{1}{k_0^2} \times \begin{cases} \frac{\pi}{r^3} & \text{for } k_0 r \ll 1 \\ \\ \frac{4}{k_0 r^4} & \text{for } k_0 r \gg 1. \end{cases} \tag{5.31}$$

Equations (5.29) and (5.31) represent the field-assisted dispersion interaction contributions in the near- and in the far-zone regime, respectively when the atoms are aligned perpendicularly and parallel to the external field [191]. As mentioned before, when the external electric fields are present, the total interaction energy between the atoms is the sum of two contributions: the unperturbed van der Waals/Casimir-Polder interaction ΔE_{vdW} and the field-assisted dispersion interaction ΔE, as

$$\Delta E_t = \Delta E_{vdW} + \Delta E. \tag{5.32}$$

The unperturbed van der Waals/Casimir-Polder dispersion interaction energy scales as r^{-6} in the near zone and as r^{-7} in the far zone, and it is given by [9, 11, 12, 15, 193]

$$\Delta E_{vdW}(r) = \begin{cases} -\frac{3}{64\pi^2\epsilon_0^2}\bar{E}\alpha^2\frac{1}{r^6} & \text{for } k_0 r \ll 1 \\ \\ -\frac{23\hbar c}{64\pi^3\epsilon_0^2}\alpha^2\frac{1}{r^7} & \text{for } k_0 r \gg 1, \end{cases} \tag{5.33}$$

where $\bar{E}$ is an average excitation energy of the atoms, and α their static polarizability. Both equations (5.29) and (5.31) show that the component of the dispersion interaction dependent from the external field decreases as r^{-3} in the near zone, and as r^{-4} in the far zone. Thus it decreases with the distance between the atoms quite slower than the unperturbed van der Waals interaction: as r^{-3} in the near zone, and r^{-4} in the far zone, rather than r^{-6} and r^{-7} of the usual dispersion interaction. It should be also noted that its space dependence is the same of the Casimir-Polder interaction between a ground state atom and a perfectly reflecting wall [18, 25]. The same distance scaling of the two processes is related to the fact that they are both due to the exchange of just one virtual photon.

It should be noted that the sign of the field-dependent interaction contribution, determining its attractive or repulsive character, can be different with respect to the unperturbed one, and is related to the geometric configuration and the relative orientation of the electric fields acting on the two atoms. Our results (5.24),(5.29),(5.30),(5.31) show that the change due to external fields, when $\mathcal{E}$ and $\mathcal{E}'$ are parallel between each other, is positive in the perpendicular configuration (a), thus yielding a repulsive contribution, while it is negative in the parallel configuration (b), thus yielding an attractive contribution. All these noteworthy features can be understood on a simple physical basis in terms of the interaction between the dipole moments induced in the atoms: as it is evident from Fig. 5.1, in the perpendicular case (panel (a)) the dipole-dipole interaction yields a repulsive force on the dipoles, while in the parallel case (panel (b)) it yields an attractive force. The situation is reversed if the the electric fields acting on the two atoms have an opposite direction, of course: in such a case $\mathcal{E}$ and $\mathcal{E}'$ have opposite sign, and the field-assisted interaction is attractive in the perpendicular configuration

and repulsive in the parallel case. This can be physically understood in terms of the dipole moments that the external fields induce in both atoms (see Fig. 5.1). On the other hand, the van der Waals/Casimir-Polder interaction between two ground-state atoms, in the absence of an external field, as given by Eq. (5.33), is always attractive. Thus our findings show that we can even modify the character of the dispersion interaction between the atoms, turning it from attractive to repulsive, exploiting external static electric fields.

We only mention that a similar physical picture explains the atom-surface Casimir-Polder dispersion interaction for a ground-state atom near a perfectly reflecting plate, in terms of the interaction of the instantaneous atomic dipole with its image dipole, reflected by the surface. Also in this case, the two instantaneous dipole moments (of the atom and of the image atom) are correlated: the components parallel to the surface point in opposite directions, while the perpendicular components point to the same direction. This eventually yields, for isotropic atoms, the attractive atom-surface Casimir-Polder potential, due to exchange of one virtual photon, scaling as r^{-3} in the near zone and as r^{-4} in the far zone [102, 194]. Also, in the resonance interaction between two entangled atoms, one excited and the other in the ground state, too, the system has correlated dipole moments in the unperturbed state [5, 161], and the interaction energy is due to the exchange of just one photon. Apparently, this interaction also could have some analogy with the field-assisted dispersion interaction here investigated; however, we wish to point out that the resonance interaction has a different scaling with the distance, r^{-3} in the near zone and r^{-1} in the far zone, essentially due to the possibility of exchange of a real photon between the atoms (in the present case the exchanged photons are always virtual).

We now discuss in more detail the relevant aspects concerning the possibility to modify and control the field-assisted dispersion force, in particular its magnitude and its attractive/repulsive character, with respect to the unperturbed van der Waals interaction. We compare numerically the field-dependent contribution to the dispersion interaction with the usual dispersion interaction for unperturbed atoms, when they are placed at a typical distance from each other, choosing $r = 10^{-6}\,\mathrm{m}$. Taking into account that the transition wavevector between the ground and the first excited level of the hydrogen atom is $k_0 \simeq 5 \cdot 10^7\,\mathrm{m}^{-1}$, we have that $k_0 r \gg 1$, thus the atoms are in the far zone regime. From the second row of (5.29) and (5.31), we then obtain

$$\begin{aligned} \delta E_\perp &\simeq 1.67 \cdot 10^{-36}\ \mathcal{E}\mathcal{E}'\ \mathrm{eV}/(\mathrm{V/m})^2, \\ \delta E_\parallel &\simeq -1.67 \cdot 10^{-36}\ \mathcal{E}\mathcal{E}'\ \mathrm{eV}/(\mathrm{V/m})^2. \end{aligned} \tag{5.34}$$

These numerical values should be compared with the usual dispersion interaction between two unperturbed ground-state hydrogen atoms, given in Eq. (5.33).

For consistency, in the numerical evaluation of ΔE_{vdW}, we have included only contributions involving the $n = 2$ states of the hydrogen atoms. At the same interatomic distance used above, $r = 10^{-6}\,\mathrm{m}$, we have

$$\Delta E_{vdW} \simeq -7.4 \cdot 10^{-27}\,\mathrm{eV} \tag{5.35}$$

A direct comparison of (5.34) with (5.35) shows that, at the distance considered, the component of the dispersion interaction due to the external electric field is of the same order of the usual dispersion interaction for field strengths of the order of $\mathcal{E} = \mathcal{E}' \simeq 10^5\,\mathrm{V/m}$. Such an intensity is well within the reach of static electric fields that can currently be obtained in the laboratory [195–200], and within, by several orders of magnitude, the strength limit imposed by our perturbative treatment of the external fields, given in Eq. (5.10). At larger interatomic distances, and with the same strength of the electric field, the field-modified interaction can outmatch the unperturbed interaction energy by several orders of magnitude. On the contrary, at shorter interatomic distances, our results (5.24), (5.29), (5.30), (5.31) show that higher external field intensities are required in order to make the field-assisted interaction comparable with the unperturbed one: of the order of $10^6\,\mathrm{V/m}$ for $r \sim 100\,\mathrm{nm}$, and of the order of $10^8\,\mathrm{V/m}$ for $r \sim 10\,\mathrm{nm}$ (both in near zone regime). Submicrometrical distances, as those we are considering, are a typical distance between the parts of MEMS and NEMS, where Casimir dispersion interactions become relevant [79]. All these remarks indicate a realistic possibility to observe the new effects we have discussed [191].

We also point out that, in the configurations yielding a repulsive field-assisted component of the dispersion force, choosing specific distances between the two atoms, it is possible to "turn off" the total dispersion interaction between the atoms. In fact, the external fields can be appropriately calibrated in order to make the total dispersion interatomic force vanishing, even if the equilibrium interatomic distance turns out to be an unstable point. In principal, this could in principle have also some relevance in applications where Casimir forces are important, for example to contrast stiction in micro-electromechanical systems.

Our new results clearly show how an external static electric field can significantly affect the dispersion interaction between two ground-state atoms, allowing to change its space-dependence, and its attractive/repulsive character. They show that, for reasonable intensities of the external field and a typical interatomic distance, the field-modified interaction can become even larger than the unperturbed van der Waals/Casimir-Polder interaction, and this could be a striking help for a direct detection of such interactions, in particular in the retarded Casimir-Polder regime. Moreover, for appropriate geometric configurations of the atoms with respect to the field, and/or appropriate relative direction (parallel or antiparallel) of the external fields acting on the two atoms, the overall dispersion interaction, usually attractive, can be turned to become repulsive. As shown by Eqs. (5.29) and

(5.31), this can be achieved when the external electric fields acting on the atoms are parallel to each other and the atoms are aligned in a direction perpendicular to the external field, or when the external electric fields are antiparallel to each other and the atoms are aligned parallel to the field.

5.3 Conclusions

In this Chapter we have considered the dispersion interaction (van der Waals and Casimir-Polder) between two ground-state hydrogen atoms subjected to an external static electric field, and shown that the external field can be exploited to strongly modify the intensity, the distance dependence, and the character (attractive/repulsive) of the force. We have considered in detail two specific relevant geometrical configurations of the two atoms with respect to the direction of the external field: in the first case the interatomic distance is aligned perpendicularly with respect to the external field, whereas in the second case it is parallel with respect to the field.

We have found that the field-assisted dispersion interaction decreases slower with the distance (as r^{-3} and r^{-4} in the near and far zone, respectively) compared to the unperturbed dispersion interaction. We have also shown that, for appropriate geometrical configurations of the atoms with respect to the field, and/or appropriate relative direction (parallel or antiparallel) of the external fields acting on the two atoms, it is possible to change the character of the overall dispersion force, usually attractive, to become repulsive. We have also estimated numerically the intensity of the field-modified component of the force, and compared it with the van der Waals/Casimir-Polder force for unperturbed atoms, both in the nonretarded and in the Casimir-Polder retarded regime.

Our new findings show that, with a strength of the external field currently achieved in the laboratory, and sufficiently weak that can be taken into account perturbatively, the force can be controlled and tailored through external fields; the possibility of obtaining a significant increase, or reversing it from attractive to repulsive, or even making it to vanish, according to the geometrical configuration and/or the relative orientation of the electric fields acting on the two atoms, has been shown. We have also stressed possible relevance of these effects for applications where Casimir interactions are relevant.

Conclusions

The main subject of this thesis has been the study of the radiation-mediated processes between quantum emitters, such as atoms or molecules, when they are in the presence of an external environment, in the framework of quantum electrodynamics. In particular, we have investigated the dispersion and the resonance interaction between atoms, and the intermolecular resonance energy transfer process. The presence of the external environment changes the dispersion relation for the field modes, as well as the photon density of states: this determines a change of all radiative processes with respect to the free-space case. Radiation-mediated processes have been widely investigated in the recent literature when the quantum emitters, interacting with the electromagnetic field in the vacuum state, are in the presence of structured/external environments, such as a cavity, a reflecting mirror or a dielectric slab, a waveguide or a photonic crystal. The radiation-mediated processes are in general significantly affected by the geometry of the system, the boundary conditions, external optical fields, and the magneto-dielectric properties of the objects involved. The resulting possibility to manipulate and control such processes through external actions has a great relevance from both a theoretical and experimental points of view, as well as applications to nanotechnologies, and has significantly inspired the original research project reported in this thesis.

The first two Chapters of the thesis contain introductory material and results, that have been used in the next three Chapters, that contain the original results of our work. The first Chapter gives an introduction to the dispersion and resonance interactions between atoms, and to the resonance energy transfer process between atoms or molecules. The second Chapter introduces the formalism of macroscopic quantum electrodynamics, where all properties of the environment are embedded in the electromagnetic Green's tensor.

In Chapter 3, we have investigated the resonance exchange of energy between two atoms or molecules, one excited and the other in its ground state, interacting with the quantum electromagnetic field in the vacuum state, and in the presence of an external environment. Specifically, we have investigated the resonance energy transfer process for two atoms placed on the axis of a perfectly conducting cylindrical waveguide, when the atomic transition frequency is below the waveg-

uide lower cut-off frequency. We have considered the transfer of energy both for atomic dipoles parallel and orthogonal to the guide axis; we show that it is slightly modified if the atoms are in the very near zone of each other, becoming more and more suppressed approaching the intermediate zone, and totally inhibited in the far-zone limit. Our original results show that it is possible to modify and control the resonance energy transfer rate by changing the waveguide radius: when it increases, the amplitude of the process increases too, while, on the contrary, decreasing the radius, the energy transfer is reduced, and this effect is much more evident in the far (radiative) zone. A clear physical interpretation of these findings has been also discussed.

In Chapter 4, we have presented our original work on the resonance interaction between two atoms, one excited and the other in its ground state, prepared in a symmetrical or antisymmetrical entangled state, interacting with the electromagnetic field in its vacuum state. We have considered the resonance force in two different physical cases: i)a dynamical non-equilibrium situation; ii) in the presence of a structured environment. In the first case, the time-dependent resonance interaction energy between two entangled atoms, during the atomic dynamical self-dressing process, has been investigated. We have shown that the interaction energy vanishes when the atoms are outside the light-cone of each other, while it settles instantaneously to its stationary value after the causality time, in agreement with the relativistic causality. We have shown that this behaviour is due to a sort of interference between real and virtual processes. We have also investigated the time-dependent electric energy density around the two atoms. We have found that, for points inside the light-cone of both atoms, the electric energy density can be enhanced or reduced, depending if the system is initially prepared in a symmetrical or antisymmetrical entangled state, respectively. This behaviour is due to the interference effects of the field emitted by the two atoms, and we have also suggested an experimental setup to probe this result. In the second case, the effect of a structured environment on the resonance interaction between two entangled atoms has been investigated. We have considered the resonance force between two entangled atoms inside a cylindrical waveguide made of a perfect conductor, when the atomic transition frequency is below the waveguide cut-off frequency. We have considered two relevant geometrical configurations of the system: atomic dipole moments parallel and orthogonal to the guide axis. In both configurations, we have shown that the interaction is deeply modified and suppressed in the far-zone limit, while it is much less influenced by the waveguide if the atoms are in the near zone. This is coherent with our results for the energy transfer between atoms in a waveguide, presented in Chapter 3. When the atoms have radial dipole moments, we have also found that the waveguide, not only reduces the interaction energy with respect to that in the free space, but also changes the character of

the resonance force, turning it from repulsive to attractive (symmetrical entangled state). Finally, we have shown that it is possible to control the resonance interaction between the atoms by changing the waveguide radius: the interaction can be strongly suppressed by reducing the guide's radius. The physical meaning of all these results has been discussed in detail.

Finally, in Chapter 5, we have reported our original work on the dispersion interaction between two ground-state hydrogen atoms, interacting with the quantum vacuum and subjected to external static electric fields. We have shown that the presence of the external field strongly modifies the dispersion interaction between the atoms, changing its space dependence and its magnitude, both in the nonretarded and in the retarded Casimir-Polder regime. We have found that the field-assisted dispersion interaction, in both near and far zone, decreases with the interatomic distance slower than the dispersion interaction of unperturbed atoms. Also, we have found that, for specific geometrical configurations of the two atoms with respect to the external field and/or the relative orientation of the fields acting on the two atoms, it is possible to change the character of the dispersion force, turning it from attractive to repulsive, or even make it vanishing. We have also pointed out that these new findings can be obtained with a strength of the external fields currently achieved in the laboratory: this is a crucial point, making possible an experimental verification of our theoretical predictions. Thus, it is possible to significantly control the magnitude, the space dependence and even the character of the dispersion interaction between two hydrogen atoms through external fields with a reasonable strength, easily attainable experimentally, and that can be treated perturbatively.

Our results, for the physical systems considered, clearly show the possibility to modify and control radiation-mediated processes, such as the dispersion and the resonance interaction, as well as the resonance energy transfer process, exploiting an appropriate external environment.

Appendix A: Resonance energy transfer and resonance interaction in the free-space limit

In Chapters 3 and 4 we have obtained analytical expressions for the resonance energy transfer amplitude and for the resonance interaction between two identical two-level atoms, using the Green's tensor formalism [15]. We recall these expressions, given by

$$M = \frac{1}{\pi\epsilon_0 c^2}\int_0^\infty d\omega\omega^2 \sum_{ij}\left\{\frac{1}{\omega_0-\omega\pm i\eta}\left[d_{Ai}^{eg}\mathrm{Im}G_{ij}(\mathbf{r}_A,\mathbf{r}_B,\omega)d_{Bj}^{ge}\right]\right.$$
$$\left.-\frac{1}{\omega_0+\omega\pm i\eta}\left[d_{Ai}^{eg}\mathrm{Im}G_{ij}(\mathbf{r}_B,\mathbf{r}_A,\omega)d_{Bj}^{ge}\right]\right\}, \tag{5.36}$$

and

$$\Delta E_\pm = \pm\frac{\hbar}{2\pi\epsilon_0 c^2}\mathcal{P}\int_0^\infty d\omega\omega^2\sum_{ij}\left\{\frac{1}{\hbar\omega_0-\hbar\omega}\right.$$
$$\times\left[d_{Ai}^{eg}\mathrm{Im}G_{ij}(\mathbf{r}_A,\mathbf{r}_B,\omega)d_{Bj}^{ge}+d_{Bi}^{eg}\mathrm{Im}G_{ij}(\mathbf{r}_B,\mathbf{r}_A,\omega)d_{Aj}^{ge}\right]$$
$$\left.-\frac{1}{\hbar\omega_0+\hbar\omega}\left[d_{Bi}^{ge}\mathrm{Im}G_{ij}(\mathbf{r}_B,\mathbf{r}_A,\omega)d_{Aj}^{eg}+d_{Ai}^{ge}\mathrm{Im}G_{ij}(\mathbf{r}_A,\mathbf{r}_B,\omega)d_{Bj}^{eg}\right]\right\}. \tag{5.37}$$

Eqs. (5.36) and (5.37) are, respectively, the resonance energy transfer amplitude M and the resonance interaction energy $\Delta E_\pm$, when the atoms are in the presence of a generic linear magneto-dielectric environment, whose properties are included in the electromagnetic Green's tensor expression [117].

The purpose of this Appendix is to demonstrate that Eqs. (5.36) and (5.37) reduce to the corresponding well-known free-space expressions when the atoms

are placed in an empty space, without any external environments. To achieve this purpose, the free-space electromagnetic Green's tensor will be used. The free-space Green's tensor, solution of the homogeneous Helmholtz equation,

$$\Big[\nabla\times\nabla\times -k^2\Big]\boldsymbol{G}^0(\boldsymbol{r},\boldsymbol{r}',\omega)=\boldsymbol{\delta}(\boldsymbol{r}-\boldsymbol{r}'), \tag{5.38}$$

is

$$\boldsymbol{G}^0(\boldsymbol{r},\boldsymbol{r}',\omega)=-\frac{c^2}{3\omega^2}\boldsymbol{\delta}(\boldsymbol{\rho})-\frac{c^2e^{i\omega\rho/c}}{4\pi\omega^2\rho^3}\Bigg\{\left[1-i\frac{\omega\rho}{c}-\left(\frac{\omega\rho}{c}\right)^2\right]\boldsymbol{I} - \left[3-3i\frac{\omega\rho}{c}-\left(\frac{\omega\rho}{c}\right)^2\right]\boldsymbol{e}_\rho\otimes\boldsymbol{e}_\rho\Bigg\}, \tag{5.39}$$

where

$$k^2=\frac{\omega^2}{c^2}. \tag{5.40}$$

Here $\boldsymbol{\rho}=\boldsymbol{r}-\boldsymbol{r}'$ is the distance between the two points $\boldsymbol{r}$ and $\boldsymbol{r}'$, with modulus $\rho=|\boldsymbol{\rho}|$ and unit vector $\boldsymbol{e}_\rho=\boldsymbol{\rho}/\rho$. The Green's tensor (5.39) is symmetric with respect to the exchange of positions $\boldsymbol{r}\longleftrightarrow\boldsymbol{r}'$, that is

$$\boldsymbol{G}^0(\boldsymbol{r},\boldsymbol{r}',\omega)=\boldsymbol{G}^0(\boldsymbol{r}',\boldsymbol{r},\omega). \tag{5.41}$$

This means that, in the cases we are considering, the Green tensor expression is symmetric with respect to the exchange of the atomic positions. Therefore Eqs. (5.36) and (5.37) can be written as

$$M=\frac{1}{\pi\epsilon_0}\sum_{ij}d_{Ai}^{eg}d_{Bj}^{ge}\int_0^\infty dk\;k^2\left(\frac{1}{k_0-k+i\eta}-\frac{1}{k_0+k+i\eta}\right)\mathrm{Im}\,G_{ij}^0(\mathbf{r}_A,\mathbf{r}_B,\omega), \tag{5.42}$$

and

$$\Delta E_\pm=\pm\frac{2}{\pi\epsilon_0}\sum_{ij}d_{Ai}^{eg}d_{Bj}^{ge}\mathcal{P}\int_0^\infty dk\frac{k^3}{k_0^2-k^2}\mathrm{Im}G_{ij}^0(\mathbf{r}_A,\mathbf{r}_B,\omega). \tag{5.43}$$

The imaginary part of the free-space Green's tensor (5.39) is

$$\mathrm{Im}\boldsymbol{G}_{ij}^0(\mathbf{r},\mathbf{r}',\omega)=-\frac{1}{4\pi k^2\rho^3}\Big[(\delta_{ij}-3\hat\rho_i\hat\rho_i)(\sin k\rho-k\rho\cos k\rho) -(\delta_{ij}-\hat\rho_i\hat\rho_i)k^2\rho^2\sin k\rho\Big]. \tag{5.44}$$

Therefore, the energy transfer amplitude and the resonance interaction between two atoms in the free space, can be obtained substituting Eq. (5.44) into Eqs. (5.42) and (5.43).

Firstly, the energy transfer amplitude (5.42), becomes

$$M = -\frac{1}{4\pi^2\epsilon_0\rho^3}\sum_{ij} d_{Ai}^{eg} d_{Bj}^{ge} \int_0^\infty dk \left(\frac{1}{k_0 - k + i\eta} - \frac{1}{k_0 + k + i\eta}\right) \times \Big[(\delta_{ij} - 3\hat{\rho}_i\hat{\rho}_i)(\sin k\rho - k\rho\cos k\rho) - (\delta_{ij} - \hat{\rho}_i\hat{\rho}_i)k^2\rho^2 \sin k\rho\Big], \tag{5.45}$$

where $\rho = |\boldsymbol{r}_A - \boldsymbol{r}_B|$ represents the interatomic distance. The first integral over k can be conveniently rewritten as

$$\begin{aligned}
&\int_0^\infty dk \left(\frac{1}{k_0 - k + i\eta} - \frac{1}{k_0 + k + i\eta}\right)(\delta_{ij} - 3\hat{\rho}_i\hat{\rho}_i)\sin k\rho \\
&= (\delta_{ij} - 3\hat{\rho}_i\hat{\rho}_i)\left[\int_0^\infty dk\, \frac{\sin k\rho}{k_0 - k + i\eta} - \int_0^\infty dk\, \frac{\sin k\rho}{k_0 + k + i\eta}\right] \\
&= (\delta_{ij} - 3\hat{\rho}_i\hat{\rho}_i)\left[\int_0^\infty dk\, \frac{\sin k\rho}{k_0 - k + i\eta} + \int_{-\infty}^0 dk\, \frac{\sin k\rho}{k_0 - k + i\eta}\right] \\
&= (\delta_{ij} - 3\hat{\rho}_i\hat{\rho}_i)\int_{-\infty}^\infty dk\, \frac{\sin k\rho}{k_0 - k + i\eta},
\end{aligned} \tag{5.46}$$

where in the third row we have done a change of variable $k \longrightarrow -k$ in the second integral. The final integral over k in (5.46) can be performed using the residue theorem, leading to

$$(\delta_{ij} - 3\hat{\rho}_i\hat{\rho}_i)\int_{-\infty}^\infty dk\, \frac{\sin k\rho}{k_0 - k + i\eta} = -(\delta_{ij} - 3\hat{\rho}_i\hat{\rho}_i)\,\pi\, e^{ik_0\rho}. \tag{5.47}$$

The others integrals in (5.45) are done with similar calculations, leading to

$$M = \sum_{ij} \frac{d_{Ai}^{eg} d_{Bj}^{ge}}{4\pi\epsilon_0\rho^3}\Big[(\delta_{ij} - 3\hat{\rho}_i\hat{\rho}_j)(1 - ik_0\rho) - (\delta_{ij} - \hat{\rho}_i\hat{\rho}_j)k_0^2\rho^2\Big]e^{i\mathbf{k}_0\cdot\boldsymbol{\rho}}, \tag{5.48}$$

that is the well-known resonance energy transfer amplitude when the atoms are in the free space (1.91), as expected [9, 50].

Let us now consider the resonance interaction expression (5.43) that, substituting the imaginary part of the free-space Green's tensor (5.44), becomes

$$\Delta E_\pm = \mp\frac{1}{2\pi^2\epsilon_0\rho^3}\sum_{ij} d_{Ai}^{eg} d_{Bj}^{ge}\mathcal{P}\int_0^\infty dk \frac{k}{k_0^2 - k^2} \Big[(\delta_{ij} - 3\hat{\rho}_i\hat{\rho}_i)(\sin k\rho - k\rho\cos k\rho) - (\delta_{ij} - \hat{\rho}_i\hat{\rho}_i)k^2\rho^2\sin k\rho\Big]. \tag{5.49}$$

In Eq. (5.49), the first integral over k, can be conveniently rewritten as

$$\begin{aligned}&(\delta_{ij}-3\hat{\rho}_i\hat{\rho}_i)\mathcal{P}\int_0^\infty dk\frac{k}{k_0^2-k^2}\sin k\rho\\&=\frac{1}{2i}(\delta_{ij}-3\hat{\rho}_i\hat{\rho}_i)\mathcal{P}\int_{-\infty}^\infty dk\frac{k\,e^{ik\rho}}{k_0^2-k^2},\end{aligned}\tag{5.50}$$

where in the second row the fact that integrand functions are even has been used. By the residue theorem, the integral becomes

$$\frac{1}{2i}(\delta_{ij}-3\hat{\rho}_i\hat{\rho}_i)\mathcal{P}\int_{-\infty}^\infty dk\frac{k\,e^{ik\rho}}{k_0^2-k^2}=-(\delta_{ij}-3\hat{\rho}_i\hat{\rho}_i)\frac{\pi\cos k\rho}{2}.\tag{5.51}$$

In a similar manner, the others two integrals arising from (5.49) may be evaluated, so that

$$\Delta E=\pm\sum_{ij}\frac{d_{Ai}^{eg}\,d_{Bj}^{ge}}{4\pi\epsilon_0\rho^3}\left[(\delta_{ij}-3\hat{\rho}_i\hat{\rho}_j)(\cos k\rho+k\rho\sin k\rho)-(\delta_{ij}-\hat{\rho}_i\hat{\rho}_j)k^2\rho^2\cos k\rho\right],\tag{5.52}$$

that is the resonance interaction between two correlated atoms in the free space, obtained in Chapter 1.

Thus, analytical expressions (5.36) and (5.37), written in terms of the electromagnetic Green's tensor, reduce to the well-known resonance energy transfer amplitude (5.48) and resonance interaction (5.52) in the free space, when there are no external environments in the physical system.

Bibliography

[1] P.W. Milonni, *The Quantum Vacuum: An Introduction to Quantum Electrodynamics*, Academic Press (San Diego, 1994).

[2] W. Greiner and J. Reinhardt, *Quantum Electrodynamics*, Springer-Verlag, Berlin Heidelberg, New York (2003).

[3] C. Cohen-Tannoudji, J. Dupont-Roc, G. Grynberg, *Atom-Photon Interactions: Basic Processes and Applications*, Wiley-VCH, (1998).

[4] C. Cohen-Tannoudji, J. Dupont-Roc, G. Grynberg, *Photons and Atoms: Introduction to Quantum Electrodynamics*, Wiley:New York, NY, USA (1989).

[5] R.Passante, Symmetry, **10**, 735 (2018).

[6] G. Compagno, R. Passante, and F. Persico *Atom-field interactions and dressed atoms* (Cambridge University Press, Cambridge, UK, 1995).

[7] P.W. Milonni, Phys. Scr. **76** C167-C171 (2007).

[8] H. B. G. Casimir, Proc. K. Ned. Akad. Wet., Ser. B **51**, 793 (1948).

[9] A. Salam, *Molecular Quantum Electrodynamics: Long-Range Intermolecular Interactions* Wiley, Hoboken, NJ, 2010.

[10] E. A. Power and S. Zienau, Philosophical Transactions of the Royal Society of London. Series A, Mathematical and Physical Sciences, **251**, (1959).

[11] D.P.Craig, T.Thirunamachandran *Molecular quantum electrodynamics: an introduction to radiation-molecule interactions*, Academic Press (1984).

[12] A. Salam, *Non-relativistic QED theory of the van der Waals dispersion interaction*, Springer, (2016).

[13] F. London, Z. Physik **63**, 245 (1930).

[14] H.B.G. Casimir, D. Polder, Phys. Rev. A **73**, 360 (1948).

[15] S.Y.Buhmann, *Dispersion forces I: macroscopic quantum electrodynamics and ground-state Casimir, Casimir-Polder and Van der Waals forces* , Springer (2012).

[16] H. B. G. Casimir, Proc. Kon. Ned. Akad. Wetenschap **51**, 793 (1948).

[17] D. A. R. Dalvit, P.W. Milonni, D. C. Roberts, F. S. S. Rosa, *Casimir Physics*, edited by D. Dalvit, P. Milonni, D. Roberts, F. Rosa, Springer, Berlin (2011).

[18] W.M.R. Simpson, U. Leonhardt, *Forces of the quantum vacuum: an introduction to Casimir physics*, World scientific publishing (2015).

[19] V. Sandoghdar, C.I. Sukenik, E.A. Hinds and S. Haroche, Phys. Rev. Lett. **68**, 3432 (1992).

[20] C.I. Sukenik, M.G. Boshier, D. Cho, V. Sandoghdar and E.A. Hinds, Phys. Rev. Lett. **70**, 560 (1993).

[21] J. Bardeen, Phys. Rev. **58**, 727 (1940).

[22] F. Armata, M. S. Kim, S. Butera, L. Rizzuto, R. Passante, Phys. Rev. D **96**, 045007 (2017).

[23] P. Barcellona, R. Passante, L. Rizzuto, S. Y. Buhmann, Phys. Rev. A **93**, 032508 (2016).

[24] R. Messina, R. Passante, L. Rizzuto, S. Spagnolo, R. Vasile, Phys. Scr. **T160**, 014032 (2014).

[25] E. A. Power and T. Thirunamachandran, Phys. Rev A **25**, 2473 (1982).

[26] M.Abramowitz, I.A.Stegun *Handbook of mathematical functions with formulas, graphs and mathematical tables*, Dover (1972).

[27] F.W.J. Olver, D.W. Lozier, R.F. Boisvert, C.W. Clark *NIST Handbook of Mathematical Functions*, Cambridge University Press (2010).

[28] I.S. Gradshteyn, L.M. Ryzhik, *Tables of Integrals, Series, and Products*, (Academic Press 2000).

[29] E.M. Lifshitz, Sov. Phys. JETP **2**(1), 73 (1956).

[30] W. Jhe, J.W. Kim, Phys. Lett. A **197**(3), 192 (1995).

[31] T.L. Ferrell, R.H. Ritchie, Phys. Rev. A **21**(4), 1305 (1980).

[32] M.M. Taddei, T.N.C. Mendes, C. Farina, Eur. J. Phys. **31**, 89 (2010).

[33] M.J. Sparnaay, Physica **24**, 751 (1958).

[34] P.H.G.M. van Blokland, J.T.G. Overbeek, J. Chem. Soc. Faraday Trans. **74**, 2637 (1978).

[35] S.K. Lamoreaux, Phys. Rev. Lett. **78**, 5 (1997).

[36] U.Mohideen, A. Roy, Phys. Rev. Lett. **81**, 4549 (1998).

[37] G. Bressi, G. Carugno, R. Onofrio, and G. Ruoso, Phys. Rev. Lett. **88**, 041804 (2002).

[38] J.D. van der Waals, (Over de Continuiteit van den Gas- en Vloeistoftoestand (on the continuity of the gas and liquid state). Ph.D. thesis, Universiteit Leiden, (1873).

[39] P. Dehmer and L. Wharton, J. Chem. Phys. **57**, 4821 (1972).

[40] V. Aquilanti, G. Liuti, F. Pirani, F. Vecchiocattivi and G.G. Volpi, J. Chem. Phys. **65**, 4751 (1976).

[41] B. Brunetti, G. Luiti, E. Luzzatti, F. Pirani and G.G. Volpi, J. Chem. Phys. **79**, 273 (1983).

[42] D. Beck, H.J. Loesch, Z. Phys. **195**, 444 (1966).

[43] C.H. Chen, P.E. Siska, Y.T. Lee, J. Chem. Phys. **59**, 601 (1973).

[44] D. Raskin, P. Kusch, Phys. Rev. **179**(3), 712 (1969).

[45] A. Shih, D. Raskin, P. Kusch, Phys. Rev. A **9**(2), 652 (1974).

[46] A. Shih, V.A. Parsegian, Phys. Rev. A **12**(3), 835 (1975).

[47] E. A. Power, T. Thirunamachandran, Phys. Rev. A **47**, 2539 (1993).

[48] E. A. Power, T. Thirunamachandran, Chem. Phys. **171**, 1 (1993).

[49] P. Barcellona, R. Passante, L. Rizzuto, and S.Y. Buhmann, Phys. Rev. A **94**, 012705 (2016).

[50] G. Juzeliūnas and D. L. Andrews, Unified theory of radiative and radiationless energy transfer, in *Resonant Energy Transfer*, edited by D. L. Andrews and A. A. Demidov (Wiley, Chichester, UK, 1999), p. 65.

[51] A. Olaya-Castro, A. Nazir, and G. R. Fleming, Philos. Trans. R. Soc. London Sect. A **370**, 3613 (2012).

[52] A. Chenu and G. D. Scholes, Annu. Rev. Phys. Chem. **66**, 69 (2014).

[53] V. May, O. Kühn, *Charge and energy transfer dynamics in molecular systems*, Wiley-VCH (Weinheim), (2011).

[54] R. M. Clegg, M. Sener and Govindjee, Proc. SPIE 7561, Optical Biopsy VII, 75610C (22 February 2010).

[55] G. D. Scholes, Annu. Rev. Phys. Chem., **54**, p. 57-87 (2003).

[56] D.L. Andrews and B.S. Sherborne, J. Chem. Phys. **86**, 4011 (1987).

[57] D.L. Andrews, Chem. Phys. **135**, 195-201 (1989).

[58] G. Juzeliūnas and D. L. Andrews, Adv. in Chem Phys. **112**. Edited by I. Prigogine and S. A. Rice, John Wiley and Sons (2000).

[59] G.A. Jones, D.S. Bradshaw, Front. Phys. **7**, 100 (2019).

[60] A. Salam, Atoms **6**, 56, (2018).

[61] D.L. Andrews, *Resonance energy transfer: Theoretical foundations and developing applications*, Tutorials in Complex Photonic Media. editor / M.A. Noginov, M.W. McCall, G Dewar, N.I. Zheludev, Bellingham, WA : SPIE Press, pp. 439-478 (2009).

[62] D.L. Andrews and G. Juzeliūnas, J. Chem. Phys. **96**, 6606 (1992).

[63] R.D. Jenkins, G.J. Daniels, and D.L. Andrews, J. Chem. Phys. **120**, 11442 (2004).

[64] E.M. Purcell, Phys. Rev. **69**, 681 (1946).

[65] F. Armata, S. Butera, G. Fiscelli, R. Incardone, V. Notararigo, R. Palacino, R. Passante, L. Rizzuto, and S. Spagnolo, J. Phys. Conf. Series **880**, 012064 (2017).

[66] S. Spagnolo, R. Passante, and L. Rizzuto, Phys. Rev. A **73**, 062117 (2006).

[67] H.R. Haakh and S. Scheel, Phys. Rev. A **91**, 052707 (2015).

[68] C. Schafer, M. Ruggenthaler, H. Appel, A. Rubio, P.N.A.S., **116**, 4883-4892 (2019).

[69] D. L. Andrews, J. Phys. Chem. B, **123**, 5015-5023 (2019).

[70] L. Rizzuto, R. Passante, and F. Persico, Phys. Rev. Lett. **98**, 240404 (2007).

[71] A. Salam, J. Phys. Chem. A, **123**, 2853-2860 (2019).

[72] D.L. Andrews, J.S. Ford, J. Chem. Phys., **139**, 014107 (2013).

[73] A. Noto and R. Passante, Phys. Rev. D **88**, 025041 (2013).

[74] J. Marino, A. Noto, and R. Passante, Phys. Rev. Lett. **113**, 020403 (2014).

[75] H. Bender, C. Stehle, C. Zimmermann, S. Slama, J. Fiedler, S. Scheel, S.Y. Buhmann, and V.N. Marachevsky, Phys. Rev. X **4**, 011029 (2014).

[76] V.A. Parsegian, *Van der Waals Forces: A Handbook for Biologists, Chemists, Engineers, and Physicists*, (Cambridge University Press, Cambridge, UK, 2006).

[77] D.K. Chang, S.F. Cheng, Int. J. Biol. Macromol, **4**, 279 (1996).

[78] F. Capasso, J.M. Munday, D. Iannuzzi, H.B. Chan, IEEE J. of selected topics in Quant. Electr., **13**, 400 (2007).

[79] H. Chan, V.A. Aksyuk, R.N. Kleiman, D.J. Bishop, F. Capasso, Science **291**, 1941 (2001).

[80] M. Mohseni, P. Rebentrost, S. Lloyd, A. Aspuru-Guzik, J. Chem. Phys. **129**, 174106 (2008).

[81] B. Valeur, M. Berberan-Santos, *Molecular Fluorescence*, (Wiley, Hoboken, NJ, 2012).

[82] R. v. Grondelle, V. I. Novoderezhkin, Nature (London) **463**, 614 (2010).

[83] C. Elisabetta, W. Cathy, W. Krystyna, P. M. G. Curmi, P. Brumer, G. D. Scholes, Nature (London) **463**, 644 (2010).

[84] M. P. E. Lock, D. L. Andrews, G. A. Jones, J. Chem. Phys. **140**, 044103 (2014).

[85] D. Sikdar, W. Cheng, M. Premaratne, J. Appl. Phys. **117**, 083101 (2015).

[86] H. T. Hattori, Z. Li, D. Liu, I. D. Rukhlenko, M. Premaratne, Opt. Express **17**, 20878 (2009).

[87] D. Sikdar, I. D. R. W. Cheng, M. Premaratne, J. Opt. Soc. Am. B **30**, 2066 (2013).

[88] D. Sikdar, I. D. Rukhlenko, W. Cheng, M. Premaratne, Plasmonics **9**, 659 (2014).

[89] C. Rupasinghe, I. D. Rukhlenko, M. Premaratne, ACS Nano **8**, 2431 (2014).

[90] A.R. Clapp, I.L. Medintz, H. Mattoussi, Chem. Phys. Chem. **7**, 47-57, (2006).

[91] I.L Medintz, H. Mattoussi, Phys Chem. Chem. Phys. **11**, 17-45 (2009).

[92] W.R. Algar, M.G. Ancona, A.P. Malanoski, K. Susumu, I.L. Medintz, ACS Nano **6**, 11044-58 (2012).

[93] K.F. Chou, A.M. Dennis, Sensors **15**, 13288-325 (2015).

[94] X. Qiu, N. Hildebrandt, ACS Nano **9**, 8449-57 (2015).

[95] M. Stanisavljevic, S. Krizkova, M. Vaculovicova, R. Kizek, V. Adam, Biosens. Bioelectron. **74**, 562-74 (2015).

[96] J. Shi, F. Tian, J. Lyu, M. Yang, J. Mater. Chem. B. **3**, 6989-7005 (2015).

[97] N. Hildebrandt, C.M. Spillmann, W.R. Algar, T. Pons T, M.H. Stewart, E. Oh et al, Chem. Rev. **117**, 536-711 (2017).

[98] A.C.S. Samia, S. Dayal, C. Burda, Photochem. Photobiol. **82**, 617-25 (2006).

[99] L. Li, J.F. Zhao, N. Won, H. Jin, S. Kim, J.Y. Chen, Nanoscale Res. Lett. **7**, 386 (2012).

[100] G. Calajo', L. Rizzuto, and R. Passante, Phys. Rev. A **96**, 023802 (2017).

[101] F. Bagarello, M. Lattuca, R. Passante, L. Rizzuto, and S. Spagnolo, Phys. Rev. A **91**, 042134 (2015).

[102] M. Antezza, C. Braggio, G. Carugno, A. Noto, R. Passante, L. Rizzuto, G. Ruoso, and S. Spagnolo, Phys. Rev. Lett. **113**, 023601 (2014).

[103] V. V. Dodonov, A.B. Klimov, and D.E. Nikonov, Phys. Rev. A **47**, 4422 (1993).

[104] M. Crocce, D.A.R. Dalvit, and F.D. Mazzitelli, Phys. Rev. A **64**, 013808 (2001).

[105] A.E. Cohen, and S. Mukamel, Phys. Rev. Lett. **91**, 233202 (2003).

[106] Y. Sherkunov, J. Phys. Conf. Ser. **161**, 012041 (2009).

[107] R. Passante and N. Vinci, Phys. Lett. A **213**, 119 (1996).

[108] R. Passante and F. Persico, Phys. Lett. A **312**, 319 (2003).

[109] R. Messina, R. Vasile, and R. Passante, Phys. Rev. A **82**, 062501 (2010).

[110] S. John and J. Wang, Phys. Rev. B **43**, 12772 (1991).

[111] R. El-Ganainy and S. John, New J. Phys. **15**, 083033 (2013).

[112] J.D. Hood, A. Goban, A. Asenjo-Garcia, M. Lu, S.-P. Yu, D.E. Chang, and H.J. Kimble, PNAS **113**, 10507 (2016).

[113] T. Sproll, Ch. Martens, M.P. Schneider, F. Intravaia, and K. Busch, arXiv: 1804.01703 (2018).

[114] E. Shahmoon and G. Kurizki, Phys. Rev. A **87**, 033831 (2013).

[115] V. Notararigo, R. Passante, and L. Rizzuto, Sci. Rep. **8**, 5193 (2018).

[116] E. Shahmoon, G.Kurizki , Phys. Rev. A **87**, 062105 (2013).

[117] H.T. Dung, L. Knöll, and D.G. Welsch, Phys. Rev. A **65**, 043813 (2002).

[118] V.V. Dodonov, Phys. Scr. **82**, 038105 (2010).

[119] R. Vasile and R. Passante, Phys. Rev. A **78**, 032108 (2008).

[120] H. R. Haakh, C. Henkel, S. Spagnolo, L. Rizzuto, and R. Passante, Phys. Rev. A **89**, 022509 (2014).

[121] F. Armata, R. Vasile, P. Barcellona, S.Y. Buhmann, L. Rizzuto, and R. Passante, Phys. Rev. A **94**, 042511 (2016).

[122] L. Rizzuto, R. Passante, and F. Persico, Phys. Rev A, **70**, 012107 (2004).

[123] J.D. Jackson, *Classical electrodynamics*, 3rd edn. (Wiley, New York, 1998).

[124] S.Y.Buhmann *Dispersion forces II: Many-body effects, excited atoms, finite temperature and quantum friction*, Springer (2012).

[125] D.G. Welsch, S.Y. Buhmann, Prog. Quantum Electron, **31**, 51 (2007).

[126] Chen-to Tai, *Dyadic Green functions in electromagnetic theory (second edition)*, IEEE series on electromagnetic waves Donald G. Dudley, Series editor (1993).

[127] L. Knöll, S.Scheel, D.G.Welsch, *Coherence and Statistics of Photons and Atoms*, ed. by J. Perina (Wiley, New York, 2001), p. 1.

[128] S. Scheel, S.Y. Buhmann, Acta Phys. Slovaca, **58**, 675 (2008).

[129] B. Huttner, S.M. Barnett, Phys. Rev. A **46**, 4306 (1992).

[130] B. Huttner, S.M. Barnett, Europhys. Lett. **18**, 487 (1992).

[131] H. T. Dung, S. Y. Buhmann, L. Knöll, D.G. Welsch, S. Scheel, J. Kästel, Phys. Rev. A **68**, 043816, (2003).

[132] A. A. Demidov, A. Yu. Borisov, Biophys. J. **64**, 1375 (1993).

[133] R. van Grondelle, J. Dekker, T. Gillbro, V. Sundström, Biochim. Biophys. Acta **1187**, 1 (1994).

[134] H. Qian, C. Georgi, N. Anderson, A.A. Green, M.C. Hersam, L. Novotny, A. Hartschuh, Nano Lett. **8**, 1363-7 (2008).

[135] J. Lefebvre, P. Finnie, J. Phys. Chem. C., **113**, 7536-40 (2009).

[136] R.D. Mehlenbacher, T.J. McDonough, M. Grechko, M.Y. Wu, M.S. Arnold, Nat. Commun. **6**, 6732 (2015).

[137] A.H. Davoody, F. Karimi, M.S. Arnold, I. Knezevic, J. Phys. Chem. C., **120**, 16354-66 (2016).

[138] C.R. Kagan, C.B. Murray, M. Nirmal, M.G. Bawendi, Phys. Rev. Lett. **76**, 1517-20 (1996).

[139] R. Koole, P. Liljeroth, C. de Mello Donegá, D. Vanmaekelbergh, A. Meijerink, J. Am. Chem. Soc. **128**, 10436-41 (2006).

[140] S.W. Clark, J.M. Harbold, F.W. Wise, J. Phys. Chem. C. **111**, 7302-5 (2007).

[141] X. Liu, J. Qiu, Chem. Soc. Rev. **44**, 8714-46 (2015).

[142] S. Buhbut, S. Itzhakov, E. Tauber, M. Shalom, I. Hod, T. Geiger, Y. Garini, D. Oron, A. Zaban, ACS Nano **4**, 1293-1298 (2010).

[143] G. D. Scholes, G. R. Fleming, A. Olaya-Castro, R. van Grondelle, Nat. Chem. **3**, 763-774 (2011).

[144] I. L. Medintz, A. R. Clapp, H. Mattoussi, E. R. Goldman, B. Fisher, J. M. Mauro, Nat. Mater. **2**, 630-638 (2003).

[145] D. Weeraddana, M. Premaratne, S.D. Gunapala, and D.L. Andrews, J. Chem. Phys. **147**, 074117 (2017).

[146] R. Jones, J.A. Needham, I. Lesanovsky, F. Intravaia, and B. Olmos, Phys. Rev. A **97**, 053841 (2018).

[147] P. Allcock, R. D. Jenkins, D.L. Andrews, Chem. Phys. Lett., **301**, 228-234 (1999).

[148] G. Juzeliunas, D. L. Andrews, Phys. Rev. B **49**, 8751 (1994); **50**, 13 371 (1994).

[149] V.V. Klimov, V.S. Letokhov, Phys. Rev. A **58**, 3235 (1998).

[150] T. Kobayashi, Q. Zheng, T. Sekiguchi, Phys. Rev. A **52**, 2835 (1995), Phys. Lett. A **199**, 21 (1995).

[151] M. Cho, R.J.Silbey, Chem. Phys. Lett. **242**, 291 (1995).

[152] G. Fiscelli, L. Rizzuto, R. Passante, Phys. Rev. A **98**, 013849 (2018).

[153] T. Gruner and D.-G. Welsch, Phys. Rev. A **53**, 1818 (1996).

[154] L.-W. Li, M.-S. Leong, T.-S. Yeo, and P.-S. Kooi, J. Electromagn. Waves Appl. **14**, 961 (2000).

[155] E.A. Power, and T. Thirunamachandran, Phys. Rev. A **51**, 3660 (1995).

[156] P. R. Berman, Phys. Rev. A, **91**, 042127 (2015).

[157] M. Donaire, R. Guerout, and A. Lambrecht, Phys. Rev. Lett., **115**, 033201 (2015).

[158] P.W. Milonni and S.M.H. Rafsanjani, Phys. Rev. A **92**, 062711 (2015).

[159] R. Passante, F. Persico, L. Rizzuto, J. Phys. B: At. Mol. Opt. Phys. **39**, S685 (2006)

[160] N. Bartolo and R. Passante. Phys. Rev. A **86**, 012122 (2012).

[161] R. Incardone, T. Fukuta, S. Tanaka, T. Petrosky, L. Rizzuto, and R. Passante, Phys. Rev. A **89**, 062117 (2014).

[162] D. Weeraddana, M. Premaratne, and D.L. Andrews, Phys. Rev. B **92**, 035128 (2015).

[163] G. Kurizki, A. G. Kofman, and V. Yudson, Phys. Rev. A **53**, R35(R) (1996).

[164] O. Berg and P. von Hippel, Ann. Rev. Biophys. Biophys. Chem. **14**, 131 (1985).

[165] J. Preto and M. Pettini, Phys. Lett. A **377**, 587 (2013).

[166] J. Preto, M. Pettini, J. A. Tuszynski, Phys. Rev. E **91**, 052710 (2015).

[167] S. Tanaka, R. Passante, T. Fukuta, T. Petrosky, Phys. Rev. A **88**, 022518 (2013).

[168] H. Yang, L.-P. Yang, T.-Y. Zheng, Comm. Theor. Phys. **66**, 541 (2016).

[169] G. Fiscelli, R. Palacino, R. Passante, L. Rizzuto, S. Spagnolo, W. Zhou, Phys. Rev. A **98**, 042506 (2018).

[170] R.H. Dicke, Phys. Rev. **93**, 99 (1954).

[171] G. Compagno, R. Passante, and F. Persico, Phys. Lett. A **98**, 253 (1983).

[172] A.K. Biswas, G. Compagno, G.M. Palma, R. Passante, and F. Persico, Phys. Rev. A **42**, 4291 (1990).

[173] L.H. Ford and N.F. Svaiter, Phys. Rev. D **58**, 067007 (1998).

[174] N. Bartolo, S. Butera, M. Lattuca, R. Passante, L. Rizzuto, and S. Spagnolo, J. Phys. Condens. Matter **27**, 214015 (2015).

[175] R. Passante, L. Rizzuto, and S. Spagnolo, Eur. Phys. J. C **73**, 2419 (2013).

[176] G. Compagno, R. Passante, and F. Persico, Europhys. Lett. **7**, 399 (1988).

[177] G. Compagno, G.M. Palma, R. Passante, and F. Persico, Chem. Phys. **198**, 19 (1995).

[178] L. Bèguin, A Vernier, R. Chicireanu, T.Lahaye, and A. Browaeys, Phys. Rev. Lett. **110**, 263201, (2013).

[179] M. Bordag, G.L. Klimchitskaya, U. Mohideen, and V.M. Mostepanenko, *Advances in the Casimir effect*, Oxford Science Publications, Oxford 2009.

[180] J. Galego, C. Climent, F.J. Garcia-Vidal, and Johannes Feist, Phys. Rev X **9**, 021057 (2019).

[181] F. Capasso, J.N. Munday, and H.B. Chan, *Attractive and repulsive Casimir-Lifshitz forces, QED torques, and applications to nanomachines*, in *Casimir Physics*, edited by D. Dalvit, P. Milonni, D. Roberts, and F. Rosa, Springer, Heidelberg, (2011), p. 249.

[182] R. Decca, V. Aksyuk, and D. López, *Casimir force in micro and nano electro mechanical systems*, in *Casimir Physics*, edited by D. Dalvit, P. Milonni, D. Roberts, and F. Rosa, Springer, Heidelberg, (2011), p. 287.

[183] H. Safari, S.Y. Buhmann, D.-G. Welsch, and H. T. Dung, Phys. Rev. A **74**, 042101 (2006).

[184] S.A. Ellingsen, S.Y. Buhmann, and S. Scheel, Phys. Rev. A **82**, 032516 (2010).

[185] E. Shahmoon, I. Mazets, and G. Kurizki, PNAS **111**, 10485 (2014).

[186] T.Thirunamachandran, Mol. Phys., **40**, 393 (1980).

[187] P.W. Milonni and A. Smith, Phys. Rev. A **53**, 3484 (1996).

[188] J.D. Perreault, M. Bhattacharya, V.P.A. Lonij, and A.D. Cronin, Phys. Rev. A **77**, 043406 (2008).

[189] T. Haug, R. Bennett and S.Y. Buhmann, Phys. Rev. A **99**, 012508 (2019).

[190] S. Fuchs, R. Bennett, and S.Y. Buhmann, Phys. Rev. A **98**, 022514 (2018).

[191] G. Fiscelli, L. Rizzuto, and R. Passante, Phys. Rev. Lett. **124**, 013604 (2020).

[192] E.A. Power, T. Thirunamachandran, Phys. Rev. A **48**, 4761 (1993).

[193] A. Salam, Int. Rev. Phys. Chem. **27**, 405 (2008).

[194] S.M. Barnett, A. Aspect, and P.W. Milonni, J. Phys. B **33**, L143 (2000).

[195] H. Jäger, Phys. Scrip. **T26**, p. 74-83, (1989).

[196] E. Stambulchik and Y. Maron, Phys. Rev. A **56**, Iss 4, (1997).

[197] S. Tani, F. Blanchard and K. Tanaka, Phys. Rev. Lett. **109**, 166603 (2012)

[198] J. Bailey *et al*, Phys. Rev. Lett. **74**, 1771 (1995).

[199] Y. Maron, M. D. Coleman, D. A. Hammer, and H.S. Peng, Phys. Rev. Lett. **57**, 699 (1986).

[200] R. González-Férez and P. Schmelcher, New J. Phys. **11**, 055013 (2009).

List of publications

This thesis is based upon the following publications and pre-prints.

- F. Armata, S. Butera, **G. Fiscelli**, R. Incardone, V. Notararigo. R. Passante, L. Rizzuto, S. Spagnolo, *Effect of boundaries on vacuum field fluctuations and radiation-mediated interactions between atoms*, J. Phys. Conf. Ser. **880**, 012064 (2017).
- **G. Fiscelli**, L. Rizzuto, R. Passante, *Resonance energy transfer between two atoms in a conducting cylindrical waveguide*, Phys. Rev. A **98**, 013849 (2018).
- **G. Fiscelli**, R. Palacino, R. Passante, L. Rizzuto, S. Spagnolo, W. Zhou, *Time-dependent resonance interaction energy between two entangled atoms under non-equilibrium conditions*, Phys. Rev. A **98**, 042506 (2018).
- **G. Fiscelli**, L. Rizzuto, and R. Passante, *Dispersion interaction between two hydrogen atoms in a static electric field*, Phys. Rev. Lett. **124**, 013604 (2020).

Other works carried out during the PhD (not directly included in the thesis):

- L. Rizzuto, A. Noto, **G. Fiscelli**, R.Passante, *Atom-surface Casimir-polder interaction in external field*, in preparation (2020).
- C. Braggio, G. Carugno, **G. Fiscelli**, M. Guarise, R. Passante, L. Rizzuto, G. Ruoso, in preparation (2020).